

TKK Dissertations 35
Espoo 2006

**REALISTIC ARTIFICIAL FLAWS FOR NDE
QUALIFICATION - A NOVEL MANUFACTURING
METHOD BASED ON THERMAL FATIGUE**

Mika Kemppainen



**Helsinki University of Technology
Department of Mechanical Engineering
Laboratory of Engineering Materials**

TKK Dissertations 35
Espoo 2006

**REALISTIC ARTIFICIAL FLAWS FOR NDE
QUALIFICATION - A NOVEL MANUFACTURING
METHOD BASED ON THERMAL FATIGUE**

Doctoral Dissertation

Mika Kemppainen

Dissertation for the degree of Doctor of Science in Technology to be presented with due permission of the Department of Mechanical Engineering for public examination and debate in Auditorium K216 at Helsinki University of Technology (Espoo, Finland) on the 14th of July, 2006, at 12 noon.

**Helsinki University of Technology
Department of Mechanical Engineering
Laboratory of Engineering Materials**

**Teknillinen korkeakoulu
Konetekniikan osasto
Materiaalitekniikan laboratorio**

Distribution:

Helsinki University of Technology
Department of Mechanical Engineering
Laboratory of Engineering Materials
P.O.Box 4200
FI - 02015 TKK
FINLAND
URL: <http://dislokaatio.hut.fi/>
Tel. +358-9-451 3538
Fax. +358-9-451 3537
E-mail: mika.kemppainen@trueflaw.com

© 2006 Mika Kemppainen

ISBN 951-22-8262-3
ISBN 951-22-8263-1 (PDF)
ISSN 1795-2239
ISSN 1795-4584 (PDF)
URL: <http://lib.tkk.fi/Diss/2006/isbn9512282631/>

TKK-DISS-2157

Gummerus
Vaajakoski 2006



HELSINKI UNIVERSITY OF TECHNOLOGY		ABSTRACT OF DOCTORAL DISSERTATION	
P. O. BOX 1000, FI-02015 TKK			
http://www.tkk.fi			
Author	Kempainen Mika		
Name of the dissertation	Realistic artificial flaws for NDE qualification – a novel manufacturing method based on thermal fatigue		
Date of manuscript	11.6.2006	Date of the dissertation	14.7.2006
<input type="checkbox"/> Monograph	<input checked="" type="checkbox"/> Article dissertation (summary + original articles)		
Department	Department of Mechanical Engineering		
Laboratory	Laboratory of Engineering Materials		
Field of research	Material Science and Engineering		
Opponent(s)	Dr. William H. Cullen, Jr. and Dr. Sc. (Tech.) Pentti Kauppinen		
Supervisor	Professor Hänninen Hannu		
(Instructor)	Dr. Sc. (Tech.) Virkkunen Iikka		
Abstract	<p>Part of regular maintenance of power plants is periodically performed non-destructive in-service inspections (ISIs). The reliability of the ISI is based on the performance of the applied non-destructive inspection procedures and capability of the inspection personnel verified by qualification procedures. In qualification representative flaws are used for simulating postulated or actual service-induced flaws. However, different artificial flaw manufacturing procedures used so far have shown certain limitations in producing representative flaws including variations in reproducibility, introduction of artefacts and non-representative flaw characteristics. Consequently, better artificial flaw manufacturing methods are needed.</p> <p>The aim of this study was to fulfil the need by developing an artificial flaw manufacturing method. The method would allow production of realistic flaws with controllable size, location and characteristics and without additional disturbances, hence, avoiding the current problems.</p> <p>A controlled flaw manufacturing method based on the thermal fatigue damage mechanism was developed. The produced flaws and their characteristics were extensively examined to evaluate their representativeness by means of non-destructive and destructive testing methods. The developed method produces natural thermal fatigue cracks with realistic characteristics, e.g., opening, tortuous propagation, condition of residual stresses, and roughness of the fracture surface.</p> <p>The method is applicable for different materials and components. The produced flaws were compared to service-induced flaws by experimental measurements and by referring the open literature. Produced flaws are judged to be realistic flaws simulating essential characteristics of service-induced flaws and giving realistic NDE response. The developed method overcomes problems related to previous flaw manufacturing methods including, among others, non-representative flaw characteristics, difficulties in applicability to ready-made components and induced artifacts or disturbances.</p>		
Keywords	Thermal fatigue, artificial flaw, flaw manufacturing method, non-destructive evaluation qualification, performance demonstration, ultrasonic testing		
ISBN (printed)	951-22-8262-3	ISSN (printed)	1795-2239
ISBN (pdf)	951-22-8263-1	ISSN (pdf)	1795-4584
ISBN (others)		Number of pages	93 p. + app. 83 p.
Publisher	Helsinki University of Technology, Laboratory of Engineering Materials		
Print distribution	Helsinki University of Technology, Laboratory of Engineering Materials		
<input checked="" type="checkbox"/> The dissertation can be read at http://lib.tkk.fi/Diss/2006/isbn9512282631			



TEKNILLINEN KORKEAKOULU PL 1000, 02015 TKK http://www.tkk.fi		VÄITÖSKIRJAN TIIVISTELMÄ	
Tekijä Kempainen Mika			
Väitöskirjan nimi Realistic artificial flaws for NDE qualification – a novel manufacturing method based on thermal fatigue			
Käsikirjoituksen jättämispäivämäärä 11.6.2006		Väitöstilaisuuden ajankohta 14.7.2006	
<input type="checkbox"/> Monografia		<input checked="" type="checkbox"/> Yhdistelmäväitöskirja (yhteenveto + erillisartikkelit)	
Osasto	Konetekniikan osasto		
Laboratorio	Materiaalitekniikan laboratorio		
Tutkimusala	Materiaalitekniikka		
Vastaväittäjä(t)	Dr. William H. Cullen, Jr. ja TkT Pentti Kauppinen		
Työn valvoja	Professori Hänninen Hannu		
Työn ohjaaja	TkT Virkkunen Iikka		
Tiivistelmä Ainetta rikkomattomat tarkastukset ovat osa säännöllistä voimalaitosten ylläpitoa. Tarkastusten luotettavuus perustuu käytössä olevien menetelmien suorituskykyyn ja tarkastajien kyvykkyyteen. Ennen tarkastusten käyttöä määräaikaistarkastuksissa niiden suorituskyky osoitetaan menettelyllä, jota kutsutaan päteväinniksi. Päteväinnissä menetelmien ja tarkastajien suorituskyky osoitetaan käyttämällä teknisiä perusteluita ja/tai käytännön kokeita, joissa tarvitaan vikoja sisältäviä koekappaleita. Pätevointikappaleissa käytetään mahdollisimman edustavia, tähän tarkoitukseen valmistettuja vikoja, joilla simuloidaan oletettuja tai havaittuja käytön aikana syntyneitä vikoja. Käytössä olleilla vianvalmistusmenetelmillä ei kuitenkaan voida valmistaa kaikissa tapauksissa edustavia vikoja. Menetelmien käyttöä rajoittavat mm. vaihtelu vikojen valmistuksessa ja huono toistettavuus, valmistusprosessin tuottamat ylimääräiset muutokset materiaaliin ja epäedustavat vikojen ominaisuudet. Niinmuodoin tarvitaan parempia vianvalmistusmenetelmiä. Tämän työn tavoitteena oli kehittää uusi keinovikojen valmistusmenetelmä, jolla ei ole edellä mainittuja rajoituksia. Työssä kehitettiin hallittu keinotekoisien vikojen valmistusmenetelmä, joka perustuu termisen väsymisen vaurioitumismekanismin hyödyntämiseen. Kehitetty menetelmä mahdollistaa todellisten kaltaisten vikojen valmistamisen siten, että niiden koko, sijainti ja ominaisuudet hallitaan ilman, että tuotetaan ylimääräisiä, tarkastusta haittaavia tai helpottavia muutoksia materiaaliin. Työssä valmistettuja vikoja tutkittiin sekä ainetta rikkomattomin että rikkovin menetelmin vikojen edustavuuden arvioimiseksi. Menetelmä tuottaa luonnollisia termisen väsymisen säröjä, jotka ovat ominaisuuksiltaan todellisia, laitoksilla käytön aikana syntyviä vikoja vastaavia. Kehitettyä menetelmää voidaan käyttää erilaisille materiaaleille ja komponenteille. Tuotettuja säröjä verrattiin laitosten käytön aikana syntyneisiin säröihin kokeellisesti sekä kirjallisuuden perusteella. Tuotetut säröt todettiin todellisten, käytössä syntyneiden säröjen kaltaisiksi, ja ne simuloivat hyvin todellisten vikojen olennaisia ominaisuuksia ja antavat todellisen kaltaisen NDE-vasteen. Kehitettyllä menetelmällä ei ole aikaisempien vianvalmistusmenetelmien rajoituksia.			
Asiasanat terminen väsyminen, keinotekoinen vika, vian valmistusmenetelmä, ainetta rikkomattoman tarkastuksen päteväinti, tarkastuksen suorituskykyyn osoittaminen, käytännön koe, ultraäänitarkastus			
ISBN (painettu)	951-22-8262-3	ISSN (painettu)	1795-2239
ISBN (pdf)	951-22-8263-1	ISSN (pdf)	1795-4584
ISBN (muut)		Sivumäärä	93 s. + liit. 83 s.
Julkaisija Teknillinen korkeakoulu, Materiaalitekniikan laboratorio			
Painetun väitöskirjan jakelu Teknillinen korkeakoulu, Materiaalitekniikan laboratorio			
<input checked="" type="checkbox"/> Luettavissa verkossa osoitteessa http://lib.tkk.fi/Diss/2006/isbn9512282631			

ABSTRACT

Regular maintenance is conducted to secure reliable operation of power plants. Part of the maintenance is periodically performed non-destructive in-service inspections (ISIs). Reliability of the ISI is based on the performance of the applied non-destructive inspection procedures and capability of the inspection personnel. The performance is verified by qualification procedures.

Qualification requires specimens with representative flaws simulating postulated or actual service-induced flaws in power plant components. However, artificial flaw manufacturing procedures used so far have shown certain limitations in producing representative flaws including variations in reproducibility, restricted application of procedures, introduction of artefacts or additional disturbances, and non-representative flaw characteristics. Consequently, better artificial flaw manufacturing methods are needed.

The aim of this study was to fulfil the need by developing an artificial flaw manufacturing method, which would produce realistic flaws. The method would allow production of flaws with controllable size, location and flaw characteristics, accurate production tolerances, reliable reproducibility, and without any additional disturbances. Hence the developed method would avoid the problems encountered with present flaw manufacturing methods.

A controlled flaw production method based on the natural thermal fatigue damage mechanism was developed. The produced flaws and their characteristics were extensively examined to evaluate their representativeness. This was done by means of several well-known non-destructive and destructive testing methods. Experiments were performed with innovative exploitation of a unique thermal fatigue test installation modified for the intended use. Development of the equipment and methods was needed, as there were neither any standardised nor any best practice methods available.

The results show that the developed method produces realistic flaws. Produced flaws are natural thermal fatigue cracks with realistic opening (at the crack mouth, middle of the crack and crack tip), tortuous propagation following the weakest path through the material, realistic branching, condition of residual stresses and roughness of the fracture surface.

The applicability of the method was verified with different materials and components. The produced flaws were compared to service-induced thermal fatigue, mechanical fatigue and stress corrosion flaws partly by performing experimental measurements and partly by referring to the results given in the open literature. Produced flaws are judged to be realistic flaws simulating essential characteristics of service-induced flaws and giving realistic NDE response. The method was proven to have good reproducibility in flaw manufacturing and not to be restricted by the component size, shape or weight but it is applicable to practically any component. The developed method overcomes problems related to previous flaw manufacturing methods including, among others, non-representative flaw characteristics, difficulties in applicability to ready-made components and induced artefacts or disturbances.

PREFACE

This work was carried out in the Laboratory of Engineering Materials, at the Helsinki University of Technology during the years 1997-2006. Foundation of Walter Ahlström, Foundation of Runar Bäckström, Technology Development Foundation (TES), Foundation of Fortum, and Helsinki University of Technology (postgraduate scholarship) financially supported the work. Their support is gratefully acknowledged. Technology Agency Finland (Tekes), VTT Industrial Systems, Radiation and Nuclear Safety Authority Finland (STUK, Olavi Valkeajärvi and Kai Elfving) Trueflaw Ltd, Pacific Northwest National Laboratories (PNNL, USA, Dr. Steven Doctor), Teollisuuden Voima Oy (Mr. Kari Hukkanen), and Fortum Nuclear Services Ltd (Mr. Raimo Paussu) are gratefully acknowledged for their support and application of the results of this work.

The background of the author, and this work, is in the thermal fatigue research done at the Helsinki University of Technology starting from 1994. The thermal fatigue research group and all the industrial partners connected to my research during these years, their technical support and information brought through their projects are gratefully acknowledged.

This thesis was supervised by professor Hannu Hänninen, to whom I would like to express my gratitude for his valuable advice, comments and support, as well as his encouragement to meet the challenges during this work in bridging different materials science research fields.

I would like to express my deepest gratitude to my colleague and instructor of this work, Dr. Iikka Virkkunen, for the guidance, most valuable advice, fruitful and profound technical discussions, rewarding co-operation, and friendship. I am indebted for all the knowledge and intelligence he has shared, as well as the FE-modeling he has performed to advance this work and my efforts to finalise it. I would like to express my most sincere gratitude to MSc. Martta Martola for her perceptive comments on my thesis and the help with the grammar. Furthermore, her valuable support in the finalisation stage of the work, fruitful conversations, and friendship are warmest respected.

I am grateful for the NDE work done by Lic. Jorma Pitkänen, valuable comments and conversations with Dr. Yuriy Yagodzinskyy and comments on my thesis from MSc. Pasi Mäntysaari. For the researcher colleagues and personnel of the Laboratory of Engineering Materials I would like to express my gratitude for the cooperation and creating the most productive working atmosphere that enabled the successful performance and completion of this work.

Most of all, I would like to express my warmest gratitude to the people closest to me, my siblings and my always loving parents for the support and love they have expressed throughout my work.

June 2006

Mika Kemppainen

CONTENTS

Abstract.....	7
Preface.....	8
Contents.....	9
Nomenclature	11
List of publications.....	12
Author’s contribution	14
Original features	15
1 Introduction.....	16
1.1 Damage and flaws	19
1.1.1 Thermal fatigue	19
1.1.2 Thermal fatigue flaws in base material.....	21
1.1.3 Thermal fatigue flaws in welds.....	23
1.1.4 Characteristics of service-induced thermal fatigue flaws	25
1.1.5 Characteristics of service-induced mechanical fatigue and stress corrosion flaws.....	27
1.2 NDE of flaws.....	29
1.2.1 Physical aspects of UT in relation to the flaw characteristics	30
1.2.2 Ultrasonic inspection techniques.....	32
1.2.3 Detection and sizing of flaws by UT	34
1.3 Flaw properties affecting ultrasonic detection and sizing	35
1.3.1 Effect of fracture surface roughness on detection and sizing.....	36
1.3.2 Effect of opening and residual stresses on detection and sizing	39
1.3.3 Effect of crack orientation on detection and sizing	48
1.3.4 Effect of oxide film on detection and sizing	49
1.3.5 Comparison of ultrasonic responses of an EDM notch and a fatigue crack..	50
1.4 Essential properties of artificially produced flaws	53
1.5 Artificial flaw manufacturing in relation to qualification procedures	55
1.6 Flaw manufacturing techniques.....	56
1.6.1 Implanted flaws.....	59
1.6.2 Natural flaws.....	61
1.6.2.1 Weld-induced cracks	61
1.6.2.2 Thermal fatigue	62
1.6.2.3 Mechanical fatigue	63
1.6.2.4 Stress corrosion.....	63
2 Aims of the work	64
3 Materials and methods.....	65
3.1 Test materials	65
3.2 Thermal fatigue.....	65
3.3 Test methods.....	66
3.3.1 Sample geometry.....	66
3.3.2 Thermal fatigue loading facility.....	66
3.3.3 Temperature measurement.....	68
3.3.4 Finite Element Modelling.....	69
3.3.5 Residual stress measurements	69
3.3.6 Microscopy and replication method	70
3.3.7 Ultrasonic examination	71
3.3.8 Eddy current testing	71
3.3.9 Calculation of fracture surface roughness.....	71
3.3.10 Thermal fatigue loading vs. UT measurements.....	72

4 Results.....	73
4.1 Metallographic representativeness	73
4.2 Metallographic comparison to service-induced MF, TF and SC cracks.....	76
4.3 NDE representativeness.....	77
4.3.1 Ultrasonic inspection.....	77
4.3.2 Eddy current inspection.....	77
4.4 Residual stresses.....	78
4.5 Ultrasonic response during dynamic thermal fatigue loading.....	78
4.6 Real components	79
5 Discussion	80
5.1 Metallographic representativeness	80
5.2 Metallographic comparison to service-induced MF, TF and SC cracks.....	80
5.3 NDE representativeness.....	81
5.4 Residual stresses.....	82
5.5 Response during dynamic thermal fatigue loading.....	82
5.6 Real components	83
5.7 Representativeness of the produced flaws.....	83
5.8 Further studies	85
6 Conclusions.....	86
References	87

NOMENCLATURE

λ	wave length
BMI	bottom mounted instrumentation
BWR	boiling water reactor
CPT	crevised pipe testing
DAC	distance amplitude correction
DGS	distance gain size
EC	eddy current testing
EDM	electrical discharge machining/electro-discharge machining
EDM-notch	electrical discharge machined notch
ENIQ	European Network for Inspection and Qualification
FE	finite element
FEM	finite element modelling
GTA	gas tungsten arc
GTAW	gas tungsten arc welding
HAZ	heat affected zone
ISI	in-service inspection
NDE	non-destructive evaluation
NDT	non-destructive testing
NPP	nuclear power plant
PISC	Program for the Inspection of Steel Components
PT	penetrant testing
PVRC	Pressure Vessel Research Council
PWR	pressurized water reactor
R_y	maximum surface roughness value
R_z	mean/average surface roughness value
RT	radiographic testing
SCC	stress corrosion cracking
SC	stress corrosion
S/N-ratio	signal to noise ratio
TOFD	time-of-flight diffraction
UT	ultrasonic testing
VT	visual testing
VVER	Russian version of the PWR
WS	weld solidification

LIST OF PUBLICATIONS

- Publication I Elfving, K., Hänninen, H., Kemppainen, M., Saarinen, P. and Virkkunen, I., 2004. Method for Producing Defects and Residual Stresses. United States Patent, US6723185 (B1), April 20, 2004.
- Publication II Kemppainen, M., Virkkunen, I., Pitkänen, J., Paussu, R. and Hänninen, H., 2003. Realistic Cracks for In-Service Inspection Qualification Mock-ups. The e-Journal of Nondestructive Testing & Ultrasonics, ISSN: 1435-4934. Vol. 8, no. 3, March 2003. pp. 1-8.
- Publication III Kemppainen, M., Virkkunen, I., Pitkänen, J., Paussu, R. and Hänninen, H., 2003. Comparison of Realistic Artificial Cracks and In-Service Cracks. The e-Journal of Nondestructive Testing & Ultrasonics, ISSN: 1435-4934. Vol. 8, no. 3, March 2003. pp. 1-6.
- Publication IV Kemppainen, M., Virkkunen, I., Pitkänen, J., Paussu, R. and Hänninen, H., 2003. Advanced Flaw Production Method for In-Service Inspection Qualification Mock-ups. Journal of Nuclear Engineering and Design, 224. pp. 105-117.
- Publication V Pitkänen, J., Kemppainen, M. and Virkkunen, I., 2003. Ultrasonic Study of Crack under a Dynamic Thermal Load. Proceedings of the Review of Progress in Quantitative Nondestructive Evaluation Conference, Vol. 23, 27 July – 1 August 2003, Greenbay, Wisconsin, USA. Thompson, D.O. and Chimenti, D.E., eds., American Institute of Physics Conference Proceedings, Vol. 700, 2004. pp. 1582-1586. 0-7354-0173-X/04.
- Publication VI Kemppainen, M., Pitkänen, J., Virkkunen, I. and Hänninen, H., 2003. Advanced Flaw Manufacturing and Crack Growth Control. Proceedings of the Review of Progress in Quantitative Nondestructive Evaluation Conference, Vol 23, 27 July – 1 August 2003, Greenbay, Wisconsin, USA. Thompson, D.O. and Chimenti, D.E., eds., American Institute of Physics Conference Proceedings Vol. 700, 2004. pp. 1272-1279. 0-7354-0173-X/04.
- Publication VII Virkkunen, I., Kemppainen, M., Pitkänen, J. and Hänninen, H., 2003. Effect of Thermal Stresses along Crack Surface on Ultrasonic Response. Proceedings of the Review of Progress in Quantitative Nondestructive Evaluation Conference, Vol. 23, 27 July – 1 August 2003, Greenbay, Wisconsin, USA. Thompson, D.O. and Chimenti, D.E., eds., American Institute of Physics Conference Proceedings, Vol. 700, 2004. pp. 1224-1231. 0-7354-0173-X/04.
- Publication VIII Kemppainen, M., Virkkunen, I., Pitkänen, J., Hukkanen, K. and Hänninen, H., 2003. Production of Realistic Flaw in Inconel 600. Proceedings of the Conference on Vessel Penetration

Inspection, Crack Growth and Repair, sponsored by USNRC and Argonne National Laboratory, Sept. 29th – Oct. 2nd. Washington D.C., Gaithersburg, USA. NUREG/CP-0191, Vol. 1, pp. 51-60 and Vol. 2, pp. 181-196 (presentation slides).

AUTHOR'S CONTRIBUTION

- Publication I Principal developer of the novel method. Formulation of the task, planning of the experiments, design of the equipment and tooling, performing the experiments, analysing results, principal writer.
- Publication II Formulation of the task, planning of the experiments, preparation of the samples, performing most of the experiments (excluding ultrasonic and eddy current testing), evaluation of the results, principal writer.
- Publication III Formulation of the task, planning of the experiments, preparation of the samples, performing most of the experiments (excluding ultrasonic testing), evaluation of the results, principal writer.
- Publication IV Formulation of the task, planning of the experiments, preparation of the samples, performing most of the experiments (excluding ultrasonic and eddy current testing), evaluation of the results, principal writer.
- Publication V Partial formulation of the task, planning of the thermal fatigue loading experiments, preparation of the samples and most of the unique NDE probe holding fixtures, performing the experiments (excluding ultrasonic testing), co-writer.
- Publication VI Formulation of the task, planning of the experiments, preparation of the samples and most of the unique NDE probe holding fixtures, performing most of the experiments (excluding ultrasonic testing), evaluation of the results, principal writer, oral presentation at the conference.
- Publication VII Partial formulation of the task, planning of the experiments, preparation of the samples, performing most of the experiments (excluding ultrasonic testing and FE-analysis), partial evaluation of the results, co-writer, oral presentation at the conference.
- Publication VIII Partial formulation of the task, planning of the experiments, preparation of the samples, performing most of the experiments (excluding ultrasonic testing and FE-analysis), evaluation of the results, principal writer, oral presentation at the conference.

ORIGINAL FEATURES

The thesis describes the development of a new artificial flaw manufacturing method and essential characteristics of the flaws produced with it. Produced flaws can be used for non-destructive evaluation qualification and training purposes. The following observations and features are believed to be original in this thesis:

1. An original controlled flaw manufacturing method based on natural thermal fatigue damage mechanism was developed.
2. The developed method provides a better artificial flaw manufacturing method to simulate real, service-induced flaws in NDE.
3. The method enables production of flaws with controllable location, orientation and size.
4. The developed method enables production of single and separate real flaws reproducibly with accurate tolerances.
5. Different flaw characteristics are controlled during the production of flaws including flaw opening, propagation path, flaw tip tightness, branching and state of residual stresses in the vicinity of the flaw. Furthermore, some of these characteristics can be modified after the production by post-treatment of the flaws with the same production process.
6. The manufactured flaws are identical to actual, service-induced thermal fatigue flaws and very good simulation of service-induced mechanical fatigue and stress corrosion flaws from the destructive metallographic and non-destructive testing points of views.
7. The flaw production method is applicable to a wide variety of specimen geometries.
8. When used in NDE personnel qualification and training, the produced flaws give a realistic challenge to the inspector.

1 INTRODUCTION

Regular maintenance program of a nuclear power plant (NPP) is initially set in the design stage of the plant. One important part of proactive maintenance is in-service inspection (ISI) of critical plant components performed with different non-destructive evaluation (NDE) methods. The most important methods are visual testing (VT), dye penetrant testing (PT), ultrasonic testing (UT), eddy current testing (EC), and radiographic testing (RT). With these methods the gradual material damage, e.g., mechanical fatigue, thermal fatigue and stress corrosion cracking, occurring under service conditions is detected and evaluated. With reliable NDE unanticipated shutdowns and severe damage can be avoided.

Reliability and performance of the used NDE methods is prerequisite for successful ISI. In an ideal situation every inspector using the same equipment and following the same procedure would attain equally reliable results. However, this is not the case and marked differences appear in inspection results between different inspectors. Consequently, it is necessary to quantify the ability of the NDE inspectors and methods to detect and characterise flaws.

Ultrasonic testing is the most important volumetric NDE method used during ISI. Ultrasonic testing is used for many critical components as the primary inspection method. Consequently, ultrasonic testing has had a pronounced role when characterising the performance of inspections. Ability to detect and size flaws by ultrasonic testing has been studied for several decades and clear progress has been achieved in the understanding of challenges of ultrasonic testing.

The first trials to quantify detection and sizing ability of UT were done under the Program for the Inspection of Steel Components, PISC, initiated in 1976, with the program called PISC I. The objective of PISC I was to investigate the ability of the 1974 PVRC (Pressure Vessel Research Council) procedure, based on the ASME XI Code, to detect, locate and size flaws in thick reactor pressure vessel steels by ultrasonic methods. Later program PISC II (1980-1986) for identification of the performance of the used inspection techniques was conducted and followed with program PISC III in 1988 for validation of results on real structures (Crutzen, 1985). PISC III was a major international program involving 15 countries and some 50 NDT teams from different institutions around the world (Crutzen et al., 1989).

The results of PISC I, II, and III studies revealed a need for a methodology to verify the capability of the used methods, inspectors and the whole inspection process. The developed qualification methodology ensures the reliability of different NDT methods and inspection processes. Depending on the national regulations, qualification may consist of practical tests and technical justification. Practical tests are conducted with mock-up samples similar to real components while technical justifications are written examinations covering different aspects of inspection in question. Different national qualification principles may have marked differences in qualification principles. For example, the recommendations for qualification principles of the European Network for Inspection and Qualification (ENIQ) in Europe and ASME Code (Section XI) in USA are different. The qualification in the USA is based on blind tests, while the technical justification has a more pronounced role in the European qualification (Waites et al., 1998). Development of qualification methodologies in Europe has favoured technical justification, partly because there has been lack of suitable flaw manufacturing techniques and partly because of the high costs of qualification mock-ups. If the qualification methodology followed

pronounces use of blind tests, it will increase the amount of qualification mock-ups needed. This results from the need of multiple samples and flaw sizes covering the whole fleet of inspected components and possible flaws. However, this way more data, i.e., better statistics is acquired and reliable results will be obtained, if the flaws used are representative.

Qualification mock-ups contain artificially introduced flaws aimed to resemble different types of flaws appearing in plant components related to manufacturing and service. There are a lot of different manufacturing flaws to be simulated in different components, as shown e.g. by Doctor et al. (1999). However, manufacturing flaws have different appearance from service-induced flaws and, hence, were excluded from this work.

Conventionally, flaws have been introduced by machining or by weld implanting separate, flawed coupons in the mock-ups. Flaw manufacturing methods have included processes such as manufacturing of starter notches and welding or other material treatments which have restricted the used component sizes and shapes. Quite often methods are practically applicable only to newly produced specimens. Furthermore, all the methods available, so far, introduce flaws with certain weaknesses and there is a clear need for new and better flaw manufacturing methods (Wüstenberg et al., 1994, ENIQ, 1999d). The weaknesses are, among others, extra material induced by any process applying welding, changed characteristics of flaws during flaw manufacturing (such as exaggerated openings, melted flaw tips, unrealistic residual stress conditions), uncontrolled flaw growth or uncertainty in nucleation of flaws, and destroyed material/sample integrity by notches required for flaw nucleation or braces required for transferring mechanical loads.

Artificially produced flaws in qualification mock-ups are intended to represent realistic, service-induced flaws. Hence, artificially produced flaws are often compared to real service-induced flaws found. Also, it is important to note that flaws detected during in-service inspections may represent only some fraction of the whole population of service-induced flaws. For example, differences in the flaw opening affect markedly the NDE response obtained from a flaw. Therefore, the flaws with a wider opening would be detected more probably than some tight flaws. Certain types of artificial flaws have been developed to emphasize only the simulation of NDE response at the expense of simulation of realistic properties of service-induced flaws. This has led to the development of different types of machined flaws such as PISC type A EDM-notches and, for certain cases, computerised simulation of the ultrasonic signal response. Often these simplified types of reflectors are representative in respect to certain properties but not in respect to other properties. For example, EDM-notches exhibit a good specular reflection but they do not show scattering or diffraction in a realistic way. Service-induced flaws are not ideal reflectors and their properties may have great variations depending on the effective loading conditions. Hence, the most realistic simulation is achieved with metallographically realistic flaws. The only way to have metallographically realistic flaws is to employ real, natural damage mechanisms as the manufacturing process of artificial flaws.

There are a number of natural damage mechanisms that can cause cracking in service conditions and each of them has specific characteristics. The ideal artificial flaw manufacturing method should have the possibility to alternate the characteristics of the produced flaws in order to simulate cases of different degrees of difficulties. Furthermore, it must induce only the intended flaw and no additional

deviations or discontinuities in the material. Thus, one must choose a method, which can be controlled accurately enough to produce different flaws in any desired location of freely chosen components.

The most challenging service-induced flaws are caused by mechanical and thermal fatigue and stress corrosion. Hence, the selection of a damage mechanism for flaw production is in practice done between mechanical fatigue, thermal fatigue and stress corrosion. In the case of mechanical fatigue, there is a need for mechanical loading. Mechanical loading always needs mechanical contact to the specimen and most often the contact is needed near the desired location of the produced flaw. The nature of mechanical loading restricts the applicability of the method and rules out large and many complex-shaped components.

Stress corrosion cracking causes the most challenging flaws for NDE in service conditions. However, utilization of it as the damaging mechanism for controlled flaw production meets considerable difficulties. Difficulties are related to control of environmental conditions, application of the loading and control of the flaw nucleation and growth. In service conditions the needed stresses are caused by manufacturing (both material and component) related residual stresses and operation related mechanical and thermal loads. These together with environment cause conditions where stress corrosion flaws are introduced to certain locations and growth directions. However, already in service conditions there may be a wide scatter in the flaw growth rates. It is very difficult to artificially achieve similar conditions, where growth of stress corrosion flaws would be well simulated with accurate control. Additionally, the loading of the specimen with mechanical loads meets similar difficulties as during mechanical fatigue loading and the loading by other means (by pressure, thermally etc.) is often restricted by the component size and shape.

Thermal fatigue damage induces often an area of shallow cracks creating so-called elephant skin cracking. However, in some cases individual thermal fatigue cracks grow bigger and become dominating cracks. Thermal fatigue in service conditions is caused by local, repeated temperature changes inducing cyclic strains. Consequently, both the flaw nucleation and growth are affected by local material and nature of temperature change (rate and amplitude). This is advantageous for artificial flaw production, as the sample size or shape does not restrict application of the loading. Practically, there is no need to mechanically touch the sample during thermal fatigue loading. Some limitations can be seen with thermal fatigue loading, as well. In thermal fatigue loading, characteristically, the strains induced by heating and cooling are constrained by the adjacent material. Thus, all the changes or irregularities in the microstructure and local shapes may rise or decrease the effective loads leading to uncontrolled flaw nucleation and growth. Furthermore, as seen in previous work with thermal fatigue, improper control of the loading will lead to uncontrolled nucleation and flaw growth probably resulting in multiple nucleation and growth of flaws.

The selection of the natural damage mechanism for artificial flaw manufacturing is not apparent, as all the three damage mechanisms have their advantages and restrictions. However, the limitations of application of mechanical fatigue and stress corrosion damage mechanisms and the benefits in application of thermal fatigue loading makes it the most interesting for artificial flaw manufacturing purposes. The benefits are, amongst others, that the component size or shape does not restrict the

application of the loading, the loading induces self-equilibrating stresses and very complex shaped load cycles can be induced by thermal fatigue.

With thermal fatigue one can accurately control the flaw nucleation and growth and produce desired flaws by understanding the combination of effects of different parts (heating period, cooling period, maximum and minimum temperatures etc.) of the loading cycle to the final characteristics of flaw growth. This work presents a new artificial flaw production method based on controlled, natural thermal fatigue damage mechanism. In order to produce representative artificial flaws it is crucial to identify the key characteristics of service and artificially induced flaws and to understand their effects on the ultrasonic response. The applicability of the flaw production method is demonstrated with simple specimens and real components. The characteristics of produced flaws are studied by non-destructive and destructive means. Realistic simulation is demonstrated by comparing artificially produced flaws with service-induced flaws, both non-destructively and destructively.

1.1 Damage and flaws

There are hundreds of field occurrences of different service-induced damage in different components and materials in nuclear power industry. Service-induced damage found has been caused by stress corrosion cracking (Kilian et al., 2005, Wesseling et al., 1999, Danko et al., 1981), corrosion fatigue (Enrietto et al., 1981), thermal fatigue (Lund et al., 1998), mechanical fatigue, corrosion, etc. Damage has occurred, e.g., in carbon steels (Enrietto et al., 1981), austenitic stainless steels (Danko et al., 1981) and Inconel alloys (Lagerström et al., 1994). Some of the damage incidences have ended in primary water leakage, which is always a safety issue and will lead to an emergency shutdown. Furthermore, many of incidents have happened in areas, which were not included in the original inspection program. Incidents have forced the operators to inspect and analyse all similar areas of the piping, where the leakages have been found. (Shah et al., 1994, Lund et al., 1998)

This study concentrates on thermal fatigue and understanding of characteristics of service-induced thermal fatigue cracks. Hence, damage related to the other mechanisms as mechanical fatigue and stress corrosion is only partly discussed. Service-induced thermal fatigue cracks and their characteristics are more comprehensively studied and respective properties of artificially produced flaws are compared to them. Results are used to judge the representativeness of artificially produced thermal fatigue cracks. Furthermore, the main focus is put on the austenitic stainless steels.

1.1.1 Thermal fatigue

Thermal fatigue has been known as a degradation mechanism of materials since the beginning of last century. It is a service lifetime limiting factor in many industrial applications including, e.g., gas turbine hot section components, recovery boilers, oil refining process components, and nuclear power plant components. In thermal fatigue degradation mechanism the material is exposed repeatedly to high and low temperatures. During exposure to alternating temperature the natural thermal expansion is restricted by adjacent components causing displacement controlled loads or by adjacent material causing strain controlled loads. Strain controlled thermal loads are self-induced by the temperature gradient when the uneven

temperature distribution prevents thermal expansion and gives rise to thermal strains and stresses. (Merola, 1995, Weronksi et al., 1991)

In thermal fatigue the successive temperature changes cause cumulative damage of the material. This accumulated damage is seen, e.g., in microstructural changes, residual stresses and cyclic hardening/softening of the material. Continued fatigue loading of the material will lead to thermal fatigue crack nucleation and growth whose final characteristics are determined by the active loads. Different aspects and characteristics of thermal fatigue damage mechanism for austenitic stainless steels are given in the open literature (Weronksi et al., 1991, Virkkunen et al., 1999, Virkkunen et al., 2000, Virkkunen, 2001).

Thermal fatigue is one of the life-limiting damage mechanisms in nuclear power plant conditions. A typical component where thermal fatigue cracking occurs is a T-joint where hot and cold fluids meet and mix (Chapuliot et al., 2005a and 2005b). The turbulent mixing of fluids of different temperatures induces rapid temperature changes to the pipe wall. The successive thermal transients cause varying, cyclic thermal stresses. These cyclic thermal stresses cause fatigue crack nucleation and growth similar to cyclic mechanical stresses (Virkkunen, 2001).

Thermal stresses are typically equi-biaxial and they are highest at the loaded surface. The loading is strain controlled and very high local stresses may arise. Already a 50°C temperature difference may be enough to initiate thermal fatigue cracking (Jansson, 1996). If the stresses locally exceed the yield strength of the material, thermal residual stresses arise (Virkkunen et al., 2000). Due to the high surface stresses, thermal fatigue cracks often form a mosaic-like crack pattern of shallow cracks, sometimes called elephant skin fracture. Some of the shallow cracks extend deeper into the material and can grow through the wall, as the example shows in Figure 1. Experience has shown that thermal fatigue cracks can occur in service conditions both in welded areas and in base metal sites (Lund et al., 1998).



Foto: Ringhals AB

Figure 1 Service-induced thermal fatigue crack causing leakage in a BWR reactor pipe elbow of the reactor water clean-up system (SKI, 2005).

Thermal loads present under service conditions induce residual stresses, as reported by, e.g., Gauthier (1998) and Jungclaus et al. (1998). Often these stresses are

connected to the manufacturing process of piping, such as mechanical grinding of the surface or welding of the pipes, as shown, e.g., by Faure et al. (1996).

Service-induced surface residual stresses are measured or analysed rarely. Long before crack growth there are irreversible changes in the material microstructure and the state of residual stresses. Virkkunen (2001) has studied thoroughly the relation between thermal fatigue cycling and residual stress accumulation with simple laboratory test samples. Corresponding information should be available also from service-induced damage to fully understand the thermal fatigue mechanism under service conditions. Results from laboratory tests can be used to simulate operationally induced residual stresses, but the difference between simple laboratory samples and real components is that in service conditions components have certain state of residual stresses from the material and component fabrication. Hence, the final state of residual stresses is determined by fabrication related initial residual stresses and loads present during operation. Furthermore, distribution and quantity of effective residual stresses near service-induced cracks through the wall thickness is even less known than the residual stresses in the surface layer.

During the operation of a power plant thermal fatigue cracks can initiate and grow in various components when larger than predicted thermal stress factors are present. The unpredicted large stress factors are caused by, e.g., mixing, striping and/or stratification of hot and cold water. Initiated cracks are tight, they grow transgranularly and may propagate through the pipe wall. During the last decades thermal fatigue has caused several primary water leakages resulting from through the wall crack propagation. The natural thermal fatigue damage appears locally and is affected by the local material condition. Local changes in the structure of the component, microstructure of the material, residual stresses, and operation related loads affect the damage nucleation and growth. Consequently, thermal fatigue damage in base material sites and welded areas has different appearance. (Hänninen et al., 1981, Stahlkopf, 1981, Hakala et al., 1990, Shah et al., 1994, Jansson, 1996, Hutin, 1998, Lund et al., 1998, SKI, 2005)

1.1.2 Thermal fatigue flaws in base material

There have been several failure cases where thermal fatigue cracking has occurred in base metal of pipes (Hänninen et al., 1981), nozzles, T-pieces (Jansson, 1996), elbows, vessel walls and valves (Hytönen, 1998). As an example of base metal damage Shah et al. (1994) have listed some incidents including a through-wall thermal fatigue crack in an elbow of high-pressure injection line, about 40 thermal fatigue cracks up to 6,4 mm deep at the inner surface of a cold leg, through-wall cracks in the counterbore region of a feedwater nozzle, about 400 thermal fatigue cracks in a feedwater nozzle, low- and high-cycle thermal fatigue cracks in the feedwater nozzle inside surface, and circumferential low-cycle thermal fatigue cracks in the vessel wall. Most of these flaws were discovered by leakage.

The most serious cracking incidences have led to through-wall leakage of radioactive primary water in components that cannot be isolated from the system. A through the wall leakage of a pipe elbow of the reactor water clean-up system was discovered in a BWR plant in Sweden (SKI, 2005). A through-wall crack in Finnish PWR plant was attributed to thermal fatigue caused by stratified flow (Hytönen, 1998). Crack appeared in a forged titanium stabilized austenitic stainless steel (X10CrNiTi189) valve body. Another through wall crack was detected in a Finnish BWR water clean-up system, after 4000 h of operation (Hänninen et al., 1981). In this case, the cracks

on the inner surface of the pipe were circumferential and longitudinal, forming a network of cracks, as shown in Figure 2. Additionally to the main crack, there were also two minor wall-penetrating cracks. Furthermore, cracking was transgranular, as shown in Figure 3.

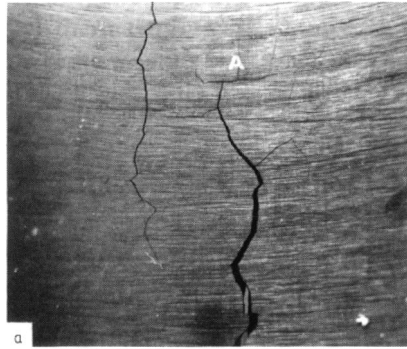


Figure 2 Service-induced thermal fatigue cracks on the inner surface of an austenitic stainless steel pipe of water clean-up system of a BWR (Hänninen et al., 1981).



Figure 3 A cross-sectional view of a service-induced thermal fatigue crack in austenitic stainless steel pipe of water clean-up system of a BWR (Hänninen et al., 1981).

1.1.3 Thermal fatigue flaws in welds

Thermal fatigue cracking of austenitic stainless steel welds has occurred in different components and plants as reported, e.g., by Shirahama (1998), Hytönen (1998) and Cipièrè et al. (2002a). The cause for cracking has been mixing and/or stratification of hot and cold water in the components. Common thermal fatigue damage has appeared as mosaic-like crack patterns in the ground areas and bigger, even through the wall penetrating cracks near the welds. Typically, through the wall penetrating cracks initiate at the fusion line assisted by the geometrical discontinuity between the weld and the base metal (Figure 4). Thermal fatigue crack growth rates can be seen on the fracture surface as variations of the fatigue striation spacing. Typical striation patterns at different depths of the cracks are shown in Figure 5. Thermal fatigue cracks initiated at the fusion line of the weld are propagating in the HAZ, but they may also penetrate into the weld material. An example is shown in Figure 6.

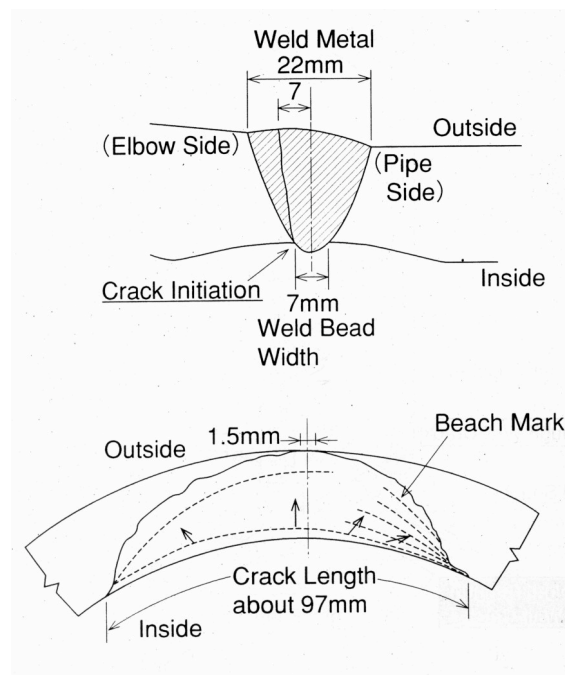


Figure 4 Illustration of a thermal fatigue crack in a weldment (Shirahama, 1998).

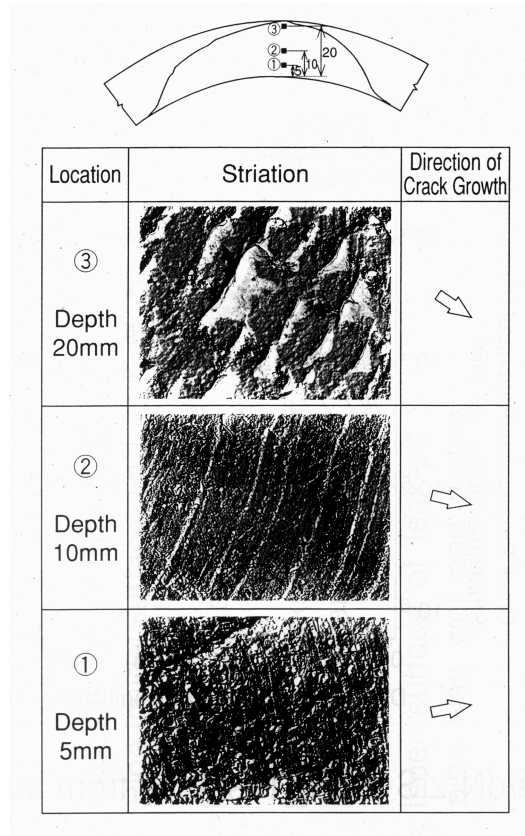


Figure 5 Typical striations on the thermal fatigue fracture surface (Shirahama, 1998).

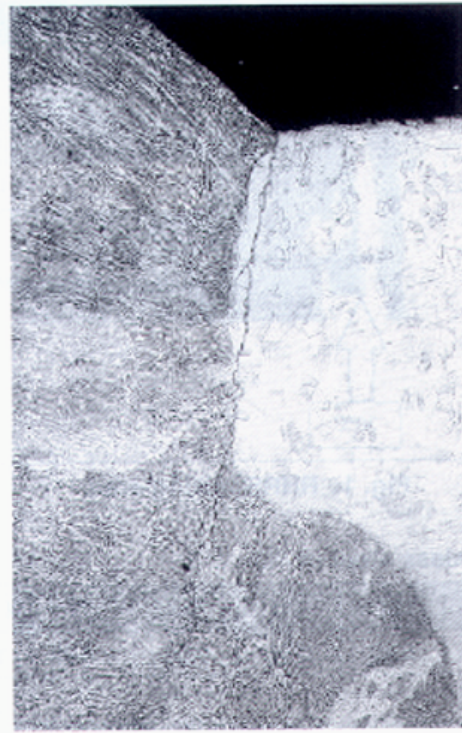


Figure 6 Thermal fatigue crack at the weld root of a French PWR plant piping component made of austenitic stainless steel (Cipière et al., 2002b).

Cipière et al. (2002a) reported the susceptibility to thermal fatigue cracking to be highest near the weld toe because of stress concentration at the geometrical discontinuity, a little bit lower at the weld counterbore where high mean stress, high surface roughness and tensile residual stresses enhance it, lower in the piping tee where high surface roughness and tensile stresses are present, and lowest in the straight pipe and elbow because of lower surface roughness and residual stresses. Faure et al. (1996) showed with cast austenitic-ferritic steel that machining might cause compressive residual stresses in the shallow surface layer of the pipe inner surface, although the subsurface residual stresses would be in tension. Faure et al. (1996) also showed that welding might cause tensile residual stresses in the inner surface layer of some millimetres thickness below which compressive residual stresses are present.

The final residual stress distribution of an operative component is a combination resulting from three different sources. These are material manufacturing, component manufacturing, and operation. The described conditions of residual stresses reported by Faure et al. (1996), are related to material and component manufacturing but, even though they are important to be aware of, they do not represent the whole distribution of residual stresses. The final distribution and level of residual stresses in an operational component is altered from the as-manufactured condition. The final distribution is determined by the effective operational loading as, e.g., operational temperature changes. As an example, Golembiewski et al. (1998) measured larger than 130°C temperature change of an operative power plant component. Such a temperature difference causes effective thermal loads easily inducing high enough strains causing plasticity of austenitic stainless steel. Furthermore, repeated cyclic thermal loads induce complex shapes of dynamic strain fields altering residual stresses differently in different depths of the wall.

1.1.4 Characteristics of service-induced thermal fatigue flaws

The macroscopic propagation path of a service-induced thermal fatigue crack is tortuous. As shown in Figure 3, the crack is narrow, propagates transgranularly in the microstructure and shows minor branching. The tortuous crack path has formed when the crack has changed direction crystallographically in grain boundaries of the microstructure. Fracture surface of a service-induced thermal fatigue crack is classified as acoustically rough surface (roughness typically between $\lambda/20$ and $\lambda/5$, where λ is the sonic wave length, Charlesworth et al., 2001). Typical surface roughness (R_z) values of service-induced thermal fatigue cracks in austenitic stainless steels vary between 6 and 140 μm (Wåle et al., 1995).

Service-induced thermal fatigue crack has largest opening (width) near the surface and it is tight in the vicinity of the crack tip. Typical width in austenitic stainless steels varies on the surface between 5 and 380 μm , in the middle of the crack between 2 and 190 μm and at the crack tip between 1 and 18 μm (Wåle et al., 1995). The opening of a crack is affected by the residual stresses along the crack depth. As the values show, service-induced thermal fatigue cracks exhibit narrow and tight crack tips. Figure 7 shows an example of the crack tip of a service-induced thermal fatigue crack. The crack tip has a small radius and the fracture surfaces near the tip are close to each other. However, all these pictures are taken from etched samples. It is known that etching makes the crack opening larger by rounding the flaw surface corners at the cross-sectional sample. Hence, if the flaw opening values through the

whole length of the crack are measured from etched samples, they tend to exaggerate the opening.

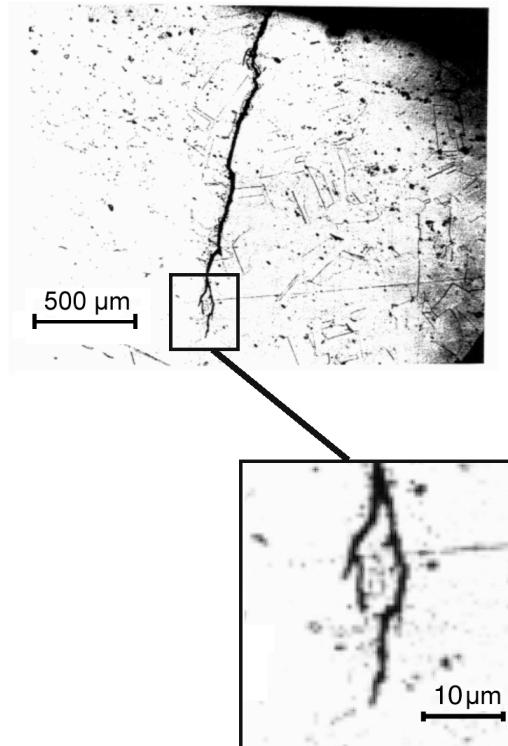


Figure 7 Crack tip of a service-induced thermal fatigue crack (Wåle et al., 1995).

Figure 8 shows an example of striations on the fracture surface of a service-induced thermal fatigue crack. Cipièrè et al. (2002a) reported the striation spacing of a service-induced thermal fatigue crack to be between 0,065 and 0,2 μm , nearly independently of the crack depth.

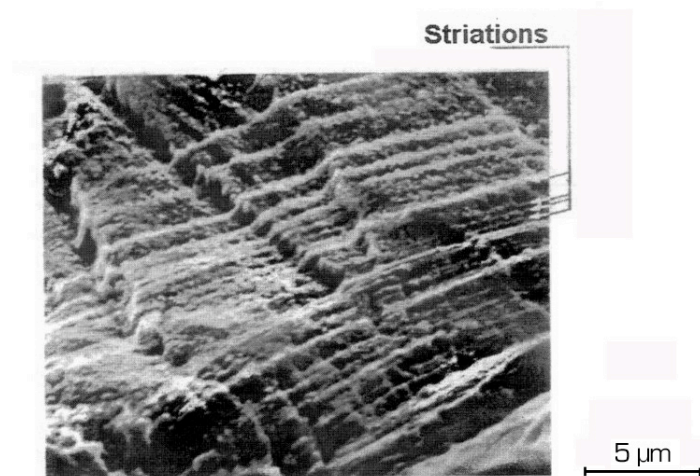


Figure 8 Fracture surface of a service-induced thermal fatigue crack in an austenitic stainless steel showing striation formation (Pirson et al., 1998).

Typically service-induced thermal fatigue cracks propagate transgranularly, are straight, show minor branching, have rough fracture surfaces and tight crack tip. Thermal fatigue creates clear striations on the fracture surface, which can be used to determine the crack growth rate. Characteristic values for service-induced thermal fatigue cracks are given in Table 1 (some values are given by the authors, some are measured from published micrographs).

Table 1 Characteristic value of different properties of service-induced thermal fatigue cracks in austenitic stainless steels. Some values are given by the authors (a.) and some are measured from provided micrographs (m.).

Reference	Surface opening (μm)	Tip radius (μm) ⁽⁰⁾	Striation spacing (μm)	Fracture surface roughness (R_z , μm)
Pirson et al., 1998	90 m.	< 35 m.	0,1-1,0 a.	-
Shirahama, 1998	200 a.	-	0,3-1,0 a.	-
Gauthier, 1998	< 30 m.	< 20 m.	-	-
Hänninen et al., 1981	115 m.	< 30 m.	-	-
Wåle et al., 1995	5-380/ 59,1 (* a.)	1-18/ 3,85 (** a.)	-	6-140/ 65,2 (** a.)
Cipièrè et al., 2002a	-	-	0,065-0,2 a.	-

(* = mean value for 18 cracks (minimum-maximum/mean value)

(** = mean value for 20 cracks (minimum-maximum/mean value)

(0) = values are given as widths by Wåle et al. (1995) and they were divided by the factor of two to get tip radius

Service-induced flaws are treated above as single and separate cracks in order to determine important flaw characteristics. This approach is practical as the characteristics treated determine the properties of an individual flaw as a reflector. In practice, however, service-induced flaws, especially thermal fatigue flaws, often appear as an area of multiple single cracks or combination of several cracks forming a mosaic-like crack field. Such a net of cracks consists of randomly orientated cracks increasing the challenge of NDE by causing scatter, diffraction and random reflection of ultrasonic energy.

1.1.5 Characteristics of service-induced mechanical fatigue and stress corrosion flaws

In addition to thermal fatigue, also the service-induced mechanical fatigue and stress corrosion cracks are among the main types of cracks to be detected and characterised during in-service inspections. The growth of these crack types is based on the crack tip propagation forced by effective loads. Table 2 gives typical characteristics of service-induced mechanical fatigue and stress corrosion cracks. Furthermore, Figure 9 gives two examples of service-induced stress corrosion cracks in austenitic stainless steel.

Table 2 Characteristic values of service-induced mechanical fatigue (MF) and stress corrosion cracks (both inter- and transgranular, IG and TG, respectively) in austenitic stainless steels. Values are given as the range between minimum and maximum values and calculated mean values of several cracks (e.g., 3-250/55,5, in micrometres (μm)).

Reference	Surface opening (μm)	Tip radius (μm) ⁽⁰⁾	Striation spacing (μm)	Fracture surface roughness (R_z , μm)
MF Wåle et al., 1995	3-250/ 55,5 ^(I)	0,5-30/ 4,7 ^(II)	-	10-212/ 49,3 ^(II)
IGSCC Wåle et al., 1995	5-200/ 43,2 ^(V)	1-25/ 2,7 ^(V)	-	8-169/ 71,9 ^(III)
TGSCC Wåle et al., 1995	3-500/ 49,1 ^(I)	1-100/ 4,3 ^(I)	-	10-90/ 37,4 ^(IV)

^(I) = mean value for 21/20 cracks

^(II) = mean value for 6 cracks

^(III) = mean value for 37 cracks

^(IV) = mean value for 24 cracks

^(V) = mean value for 33/32 cracks

⁽⁰⁾ = values are given as flaw tip widths by Wåle et al. (1995) and they were divided by the factor of two to get tip radius

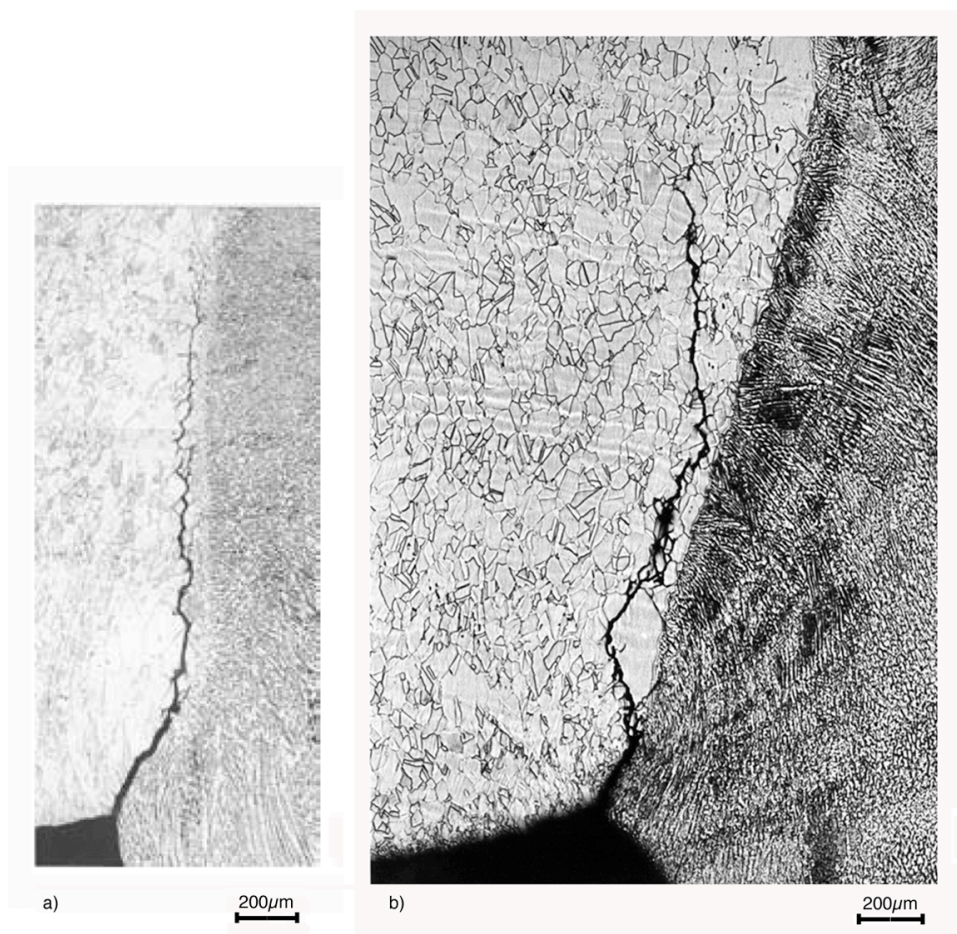


Figure 9 Two pictures showing typical IGSCC in austenitic stainless steel weld root notch and HAZ of a weld in BWR environment by a) Kilian et al. (2005) in Ti stabilized German 1.4541 material and b) Ehrnstén et al. (2001) in AISI 316 NG material.

The crack tips of mechanical fatigue cracks, thermal fatigue cracks and stress corrosion cracks are typically sharp. However, there are differences in appearances of these three types of cracks.

Mechanical fatigue cracks are initiated by mechanical loads and this mechanism typically results in growth of a single crack. This is a result of the growing crack concentrating the effective loads. A mechanical fatigue crack is transgranular and typically quite straight.

Thermal fatigue cracks are initiated and grown by loads induced when thermal expansion or contraction is constrained repeatedly. Consequently, they are fatigue cracks, but their nucleation and propagation are driven by applied temperature changes. Characteristically, thermal fatigue loads are not concentrated to the firstly initiated crack, but multiple cracking may occur. Furthermore, propagation and branching of thermal fatigue cracks are determined by the local condition of the material. Thermal fatigue cracks are most often transgranular with possible minor intergranular portions. Thermal fatigue cracks may exhibit branching and the propagation varies from straight to tortuous.

Stress corrosion cracks are initiated and grown by effective stresses caused by mechanical or thermal loads or residual stresses, and environment. Stress corrosion cracks exhibit both inter- and transgranular crack growth modes. Stress corrosion cracks may exhibit minor branching or be heavily branched and their propagation can be from quite straight to heavily tortuous.

1.2 NDE of flaws

In-service inspections are affected by numerous factors, the most important being type of material (e.g., base material, HAZ, weld etc.), type of material microstructure (e.g., ferritic, austenitic) and characteristics of flaws, when considered from the point of view of an artificial flaw used as a reflector. This work concentrates on austenitic stainless steels in nuclear applications and on challenges caused by service-induced cracks during inspections. Thus, e.g., environment, human and equipment related factors, as important as they are, are not treated in this work. Furthermore, the material-related problems are not thoroughly analysed. The focus is to understand and simulate the effects of the characteristics of natural, service-induced cracks on the NDT response. The main inspection technique treated in the study is ultrasonic inspection, while the other inspection methods are only shortly introduced.

All kinds of NDT methods are affected by the characteristics of inspected flaws. Thus, requirements set for the artificial flaw manufacturing method and produced flaws are similar and independent of the NDE method in question and need realistic simulation of the service-induced flaws. Non-destructive examination methods typically used include visual (VT), penetrant (PT), ultrasonic (UT), radiographic (RT) and eddy current (EC) testing. Three of these, visual, penetrant and eddy current testing, are most often performed on the damaged surface, while ultrasonic testing is performed mostly from the opposite surface. Time-consuming and expensive radiographic measurements are performed only in limited amount and rarely as the primary method. Visual, penetrant, eddy current, radiographic and ultrasonic testing are used for detection, while flaw sizing is mainly done by eddy current and ultrasonic testing and in some cases by radiography.

Ultrasonic testing is the most used method during in-service inspections and has a major effect on the performance of the whole in-service inspection. It is clear that ultrasonic testing has a pronounced position in the qualification of NDT personnel and processes. Therefore, inspection by ultrasonic means and the role of flaw characteristics in UT inspection are treated in more detail in the following.

1.2.1 Physical aspects of UT in relation to the flaw characteristics

Ultrasonic testing is based on an acoustic source applying periodically generated strains in the inspected material. Periodic strains are propagated as mechanical waves through the material. Both longitudinal and transverse waves can be used, called as compression and shear waves, respectively. Applied strain amplitudes remain in the elastic region of the material behaviour resulting in uniform propagation speed of acoustic energy with constant attenuation caused by the material. Physical characteristics affecting the propagation speed and attenuation coefficient are the nature and structure of the material, temperature, pressure and frequency of ultrasound. (Krautkrämer et al., 1990)

Induced mechanical waves transfer acoustic energy through the material by oscillating volume elements of the structure. Success of the energy transfer depends on the properties of different particles transferring the acoustic energy. This ability is connected to the differences in bonding, interfaces and acoustic properties of adjacent particles behaving as discontinuities in the route of the acoustic beam (Krautkrämer et al., 1990).

Propagation of acoustic waves may be disturbed by the discontinuities arising reflection, refraction, diffraction and scattering of the energy. Reflection and transmission of ultrasonic energy occur at the boundaries of different acoustic impedances (impedance is a product of material density and sound velocity). In a free boundary between solid material and empty space (vacuum) the incident wave will return in one form or other. With smooth boundaries specular reflection is seen while with rough boundaries both specular reflection and scattering (i.e., off-specular reflection) of the acoustic energy may occur. Furthermore, reflection with mode conversion, i.e., change from shear wave to compression wave or vice versa, may take place. Transmission of the acoustic energy may also occur over the boundaries between two materials capable of carrying acoustic waves (e.g., air, water, oxide, metal). However, transmission of shear waves happens only if there is a solid/solid boundary. In solid to fluid boundary (e.g., metal to air or water) either total reflection occurs or transmission by compression waves generated by mode conversion at the boundary takes place. (Krautkrämer et al., 1990)

Natural reflectors, such as cracks, may be tight and have fracture surfaces partly in contact, making them partially transparent to ultrasound. Furthermore, they may have wavy or rough surfaces decreasing the energy of specular reflection (Krautkrämer et al., 1990). Hence, a theoretical situation for pure reflection or scattering does not exist but they interfere always mutually at the uneven boundary conditions of the reflector surface. Furthermore, a flaw-like reflector may generate diffracted acoustic waves from its extremities such as tips, sharp corners or branches (Charlesworth et al., 2001). Figure 10 shows the principles of different phenomena occurring when an incident ultrasonic wave hits a crack-type natural reflector. Additionally, Figure 11 shows the principle of flaw tip diffraction from a flaw tip with a) wider opening and b) tighter and sharper flaw tip. With open flaw tip the strongest diffraction comes from the tip, but in cases where the deepest extremity of

the flaw is tight or possibly under compressive stresses, it may raise only a weak response. In such a case the strongest diffraction may arise from any source such as a corner or a root of a branch below the tight flaw tip, the principle shown in Figure 11 b). In order to find such a weak diffraction signal, high sensitivity and possibly special focused beam techniques may be needed.

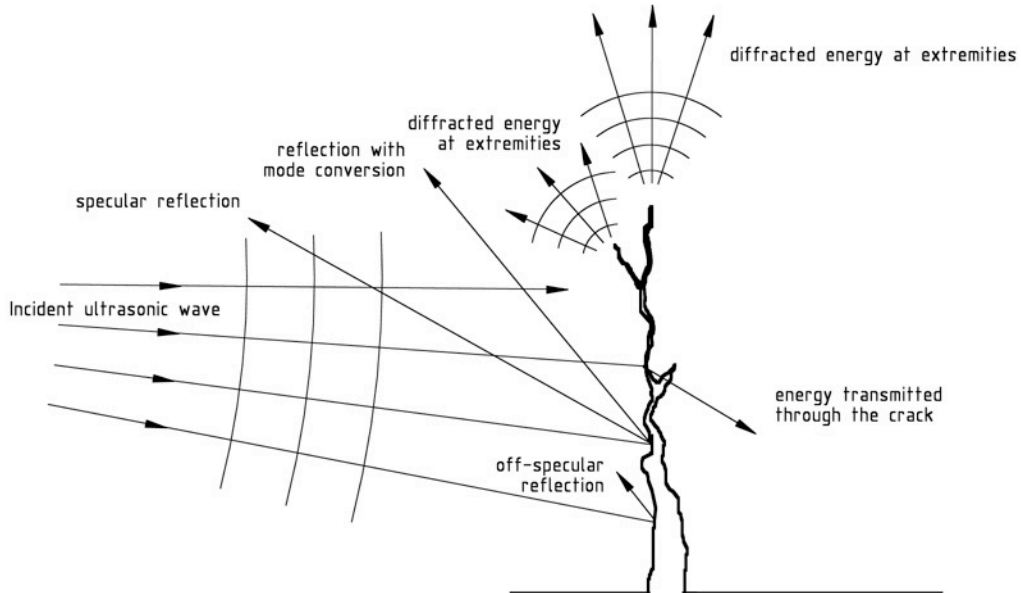


Figure 10 Schematic drawing of the interaction between a natural reflector and incident ultrasonic wave.

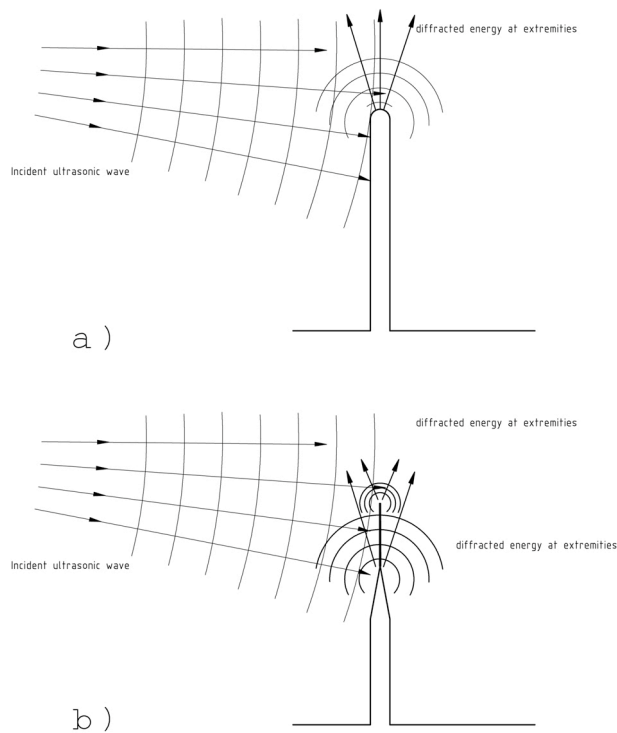


Figure 11 Schematic drawing of the diffraction from different flaw tips with a) open and b) tight tip.

In addition to phenomena occurring in the boundaries of a physical reflector, the state of residual stresses in the vicinity of it affects the propagation of the acoustic energy. In a situation where the direction of the residual stress is not known and the ultrasonic inspection technique chosen utilises a wave mode most seriously affected by the stress field present, a remarkable reduction in the inspection performance may occur. Hence, when the inspection procedures are chosen for different applications, it is justified, also from this point of view, to utilise several different techniques and not only rely on one specific technique.

Fundamentally, the effect of residual stresses on the ultrasonic wave arises from the displacement of atoms from their stress-free position as the wave propagation is based on the oscillation of atoms linked to each other with atomic bonds. Under compressive residual stress atoms are closer to each other and under tensile stress atoms are moved further away from each other. The atomic oscillation, i.e., the velocity of ultrasound of different wave modes is related to deformation if the atomic distance is shortened or enlarged from the stress-free position. For example, if compressive and shear waves arrive at the same angle and propagation direction to the same residual stress field where the atomic distance is shortened parallel to the propagation direction of applied waves, the bulk velocity of the compressive wave is increased, but the bulk velocity of the shear wave is decreased (Krautkrämer et al., 1990). Furthermore, if the utilised waves are polarized to certain direction, the effect is different. Although the direction of the bulk wave is the same, different wave modes move atoms to different directions and, as atomic distances are different to different directions, the effect to the velocity of the ultrasound is different. The principle is, that the velocity of the bulk wave is increased if the atomic distance is shortened on the direction to which atoms are moved by the wave mode. Correspondingly, if the atomic distance is enlarged the velocity is decreased. When the wave arrives to non-homogeneous stress field, the stress gradient may refract the propagation direction of the wave.

1.2.2 Ultrasonic inspection techniques

Ultrasonic techniques used for detection and sizing are based on the physical interaction of acoustic energy with the flaw. The most commonly used technique, pulse-echo technique, is based on the interpretation of reflected, scattered or diffracted ultrasonic energy from the flaw (Krautkrämer et al., 1990, Blitz et al., 1996). The principle is to measure the time difference between generated and returned pulse. Shape, size, orientation and surface condition of the reflector affect the measured amplitude of the returned pulse. The use and calibration of the pulse-echo method are widely standardized.

There are two principal sizing methods, the probe movement and amplitude method (Krautkrämer et al., 1990). Both methods can be used for small flaw sizing, but for large flaws exceeding the beam cross-sectional area, probe movement method is required (Blitz et al., 1996). Both methods rely on the reflected or diffracted ultrasonic energy received from the flaw which principle is shown in Figure 10.

Standardized probe movement techniques are the 6 dB drop (half-beam), the 20 dB drop technique and the time-of-flight diffraction method. When using dB drop method, the amplitude drop, either 6 or 20 dB, at flaw extremities is compared to the maximized value obtained from the flaw. Now half (6 dB) or minor (20 dB) part

of the ultrasonic beam reflects back from the flaw while the rest of the beam passes the flaw tip. In both methods, while moving the probe, the envelope curves showing the variations of flaw echo can be obtained. For a natural reflector dB drop methods do not work very accurately, as it is not known from which value the drop has to be calculated. As an example, Figure 12 shows schematic envelope curves obtained from different natural reflectors showing also the overall recording length, “s” of the envelopes. Different envelopes indicate different phenomena taking place at the boundaries of different reflectors, as indicated in Figure 10. As shown in the Figure 12, the actual length of the reflector differs from the length of the obtained envelope curve because of the directivity of the probe. (Krautkrämer et al., 1990, Blitz et al., 1996)

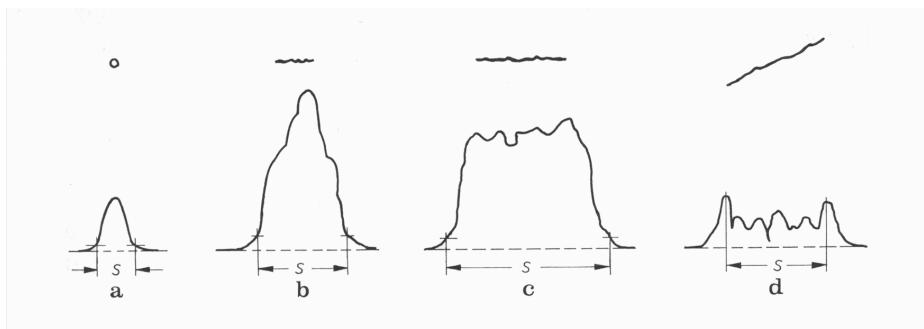


Figure 12 Schematic envelope curves obtained from different natural reflectors: a) round reflector as a pore smaller than the beam diameter, b) specular reflector equal to the beam diameter, c) specular reflector larger than the beam diameter and d) tilted, sharp-edged reflector with high amplification. (Krautkrämer et al., 1990)

The time-of-flight diffraction (TOFD) method is based on the phenomenon of diffraction at flaw edges. Wide beam spread longitudinal wave probes with angles from 40° to 60° are normally used. The method is most commonly employed with two probes located at a skip distance apart on opposite sides of the flaw, the other probe acting as transmitter and the other one as receiver. Longitudinal waves are used because of their uniform speed of travel. The earlier version of this method was called Delta method and an application of it to the flat plate specimens “pitch and catch technique” (Krautkrämer et al., 1990). While TOFD technique is a valuable sizing method, it meets some restrictions and hence in complicated geometries and flaws it should be used together with other techniques. For example, if a larger flaw obscures smaller one, the smaller one cannot be sized (Murgatroyd et al., 1988). This method may also indicate incorrectly the place of highest flaw tip as the extremities of branches or sharp corners (the principle shown in Figure 10) may diffract more ultrasonic energy than the probably tight and compressed highest flaw tip. (Blitz et al., 1996, Charlesworth et al., 2001)

Amplitude methods used for flaw sizing are the following: use of comparative blocks, distance amplitude correction (DAC) method and distance gain size (DGS) techniques. The use of comparative blocks is based on comparing echoes from artificial reference reflectors with the obtained echoes from flaws to be sized. Reference reflectors are located in a similar block than the inspected specimen and they must have similar size and location to those of the flaws to be sized. The distance amplitude correction (DAC) method is based on the fact that the ultrasonic

echo heights decrease in the far field. A curve indicating far-field attenuation, known as DAC curve, can be developed to indicate that a small echo signal at a remote distance from the probe may have a similar significance as a larger one closer to the probe. The distance gain size (DGS) method is a graphical representation of various echo amplitudes obtained from different sizes of reflectors located at different distances from the probe. In practice, DGS curves give an estimation of the minimum size of the inspected flaw. (Krautkrämer et al., 1990, Halmshaw, 1993, Blitz et al., 1996)

Even though different sizing methods listed above are widely used, there has been criticism on the applicability of echo amplitude based sizing techniques on real cracks. Several authors, as an example Becker et al. (1981), have indicated that the echo height is too sensitive to flaw tightness, roughness, orientation and selection of probing and instrumentation to be used reliably for crack sizing. The use of amplitude response for sizing has been deemed unreliable even for simple artificial flaws with both sides scanned. Posakony (1986) stated, that large flaws might be undetected if only a single transducer is used and/or if the flaw is viewed from only one direction.

1.2.3 Detection and sizing of flaws by UT

Detection of cracks is usually based on the corner effect, which is, to a certain amount, a combination of diffraction and reflection depending on the wave mode and incident angle. In detection different inspection probes have different sensitivity to flaw size, orientation and surface roughness.

The challenge in sizing of a realistic crack is caused by its tightness, surface roughness and small crack tip radius. Fracture surfaces of a tight crack are close to each other through the full length of the crack and closest at the crack tip. Fracture surface heights touching each other allow acoustic energy transmission through the crack, sometimes making the crack almost transparent in the ultrasonic testing.

Commonly used techniques for crack depth evaluation utilise crack tip diffraction of shear and longitudinal bulk waves, surface (Rayleigh) waves, back-scattering resonance and mode conversion. Characteristics of flaws affect remarkably the accuracy and reliability of flaw sizing based on all the different ultrasonic techniques.

In detection the echo amplitude height of an ultrasonic pulse is affected by the opening of the crack as different crack widths return different amplitude heights. When opening is increased, a saturation level can be reached after which the echo height does not change anymore. Saturation level seen is the result of maximum reflection met from the specific fracture surface. Consequently, as affecting the crack opening, the increased tensile stresses cause increase of the echo height and increased compressive stresses cause decrease of the echo height, respectively. In a static condition, the effective residual stresses determine the final opening of the crack and, hence, affect the obtained ultrasonic response in detection.

Studies with mechanical fatigue cracks have revealed that with high enough tensile loading the echo heights are almost identical to an EDM-notch. Comparative studies (e.g., Becker et al., 1981) of mechanical and thermal fatigue cracks have shown the difference in sensitivity to changes in fracture surface closing forces of these two types of cracks. Unlike mechanical fatigue cracks, the thermal fatigue cracks are difficult to detect already without loading and they are very sensitive to changes in closing forces.

In sizing the obtained echo height from the crack tip is affected by the crack opening and residual stresses in the vicinity of it. In time-of-flight measurements, there is a reduction in the strength of the diffracted signal from the crack tip caused by compressive residual stresses affecting the crack tip (Temple, 1985). Furthermore, residual stresses affect the rate of change of the amplitude height, if the crack is dynamically loaded. For example, when high compressive residual stresses are present at the crack tip and fracture surface closing is applied, the crack starts to close from the crack tip area. With continuing loading the rest of the crack follows and crack mouth closes last. This is seen as a gradual decrease of the ultrasonic amplitude height. In a stress-free condition, e.g., after annealing of the material, the amplitude change is much faster indicating that the whole crack closes almost at the same time. High enough fracture surface closing forces to partial (or even total) close the crack can be present under service conditions.

The fracture surface roughness has an effect on the ultrasonic response, since smooth surfaces (e.g., EDM-notch, mechanical fatigue crack) allow a strong reflection of coherent field while rougher surfaces (thermal fatigue cracks, stress corrosion cracks) destroy the coherency and cause increased scattering of the ultrasound. Increased fracture surface roughness reduces the detection sensitivity of the methods relying on specular signal. However, off-specular signals are increased because of increased diffuse field.

In sizing, similarly than in detection, the differences in the fracture surface roughness have an effect on the obtained ultrasonic amplitude height. Near the edges of a smooth flaw, the signal drop is sharp. When sizing rough flaws, no clear plateau region is seen, where the signal drop could be measured, but the signal fluctuates across the flaw. In the time-based sizing technique a smooth flaw gives two clearly separate pulses, but a continuous pulse may be obtained from rough flaws. If the fracture surfaces are covered by oxide film, it may affect the detectability of the crack tip and crack depth evaluation.

Small and closed cracks may be undetected because of their small size and high closing stress present. Enrietto et al. (1983) reported a limit value for crack depth to be 15% of the wall thickness, below which the reliability of detection is poor. Furthermore, if the crack is filled with water or oxide, the sensitivity of ultrasonic response to tightness of the crack is changed.

Different flaw characteristics are handled separately in the following, in order to get a closer idea of their effect on the obtained ultrasonic response.

1.3 Flaw properties affecting ultrasonic detection and sizing

There is a lot of experience confirming the difficulty to reliably detect and size service-induced thermal fatigue cracks as reported, e.g., by Edwards et al. (1993 and 1995), Pirson et al. (1998), and Gauthier (1998). The difficulty of the inspection is caused by typical characteristics of cracks, which affect, e.g., propagation, reflection, diffraction, transmission, attenuation and diffusion of ultrasonic energy (Becker et al., 1981, Ibrahim et al., 1981). Such flaw characteristics have been stated to be, amongst others, location, orientation and size of a crack (e.g., Waites et al., 1998), the opening of a crack and crack tip (e.g., Ahmed et al., 1998, Yoneyama et al., 2000, Wirdelius et al., 2000), the remaining residual stresses in the material (e.g., Gauthier, 1998, Iida et al., 1988), fracture surface roughness (e.g., Ogilvy, 1989, Wirdelius et

al., 2000), plastic zone (e.g., Saka et al., 1991), and filling of the crack with some substance (e.g., Becker et al., 1981).

1.3.1 Effect of fracture surface roughness on detection and sizing

The fracture surface of a realistic flaw is not ideally planar, but it has natural irregularities. The general effects of the fracture surface roughness of a reflector on the spatial distribution of scattered waves are well known and have been widely studied both practically and theoretically. The principle is that by increasing the reflection surface roughness, the forward scattered high amplitude is decreased and energy is redistributed into a more widely spread diffuse field (Ogilvy, 1989, Wirdelius et al., 2000). Figure 13 shows an example of the effect of surface roughness (from smooth to very rough) to the distribution of the scattered field. From a smooth surface a strong coherent field will arise because of the interference between all the scattered wavelets from all parts of the surface. Enhanced surface roughness destroys the summation as the phase of the wave varies with position along the flaw surface. Thus, the strength of the coherent field is reduced and a diffuse, widely scattered field of varying phase will be generated.

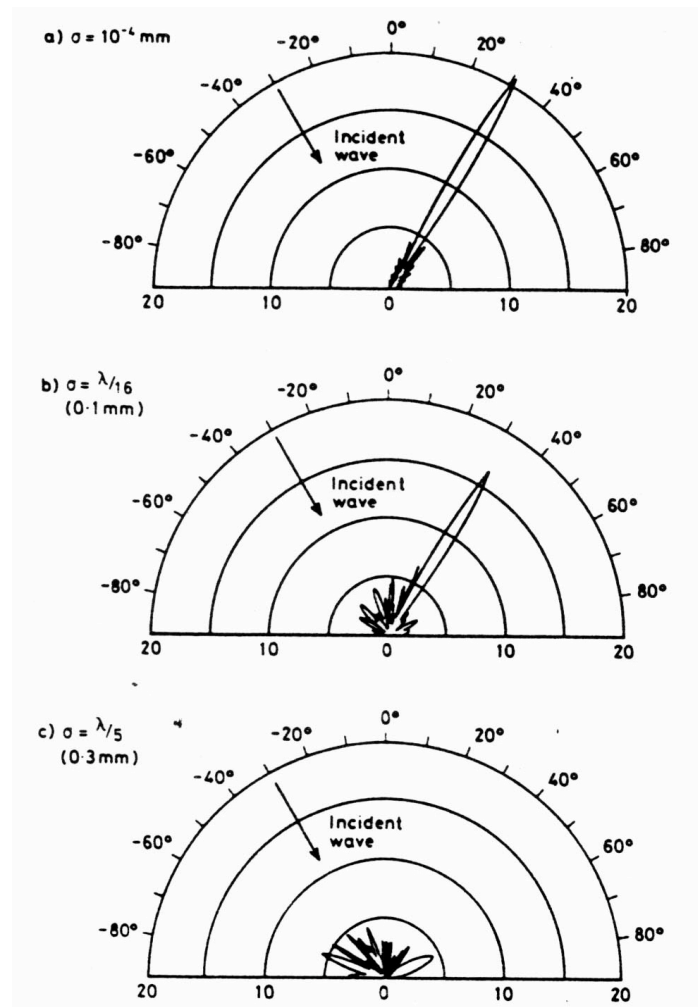


Figure 13 Polar plots of scattered amplitude distributions from surfaces of different roughness values (σ), when a 2 MHz monochromatic wave is incident at 30° . (Ogilvy, 1989)

Increased surface roughness reduces the detection sensitivity of the methods relying on specular signal. Off-specular signals may be increased because of the diffuse field. This effect was seen for certain inspection geometries in the PISC-II exercise, where small rough flaws were found to have higher detectability than the smooth flaws of the same size. Increased frequency of the used probe increases the scattering effect due to fracture surface roughness (Becker et al., 1981). Furthermore, if the surface has a regularly shaped fracture surface roughness profile, reflection of the incident sound wave may favour certain directions thereby decreasing the testing repeatability and reliability (Green, 1989). Effect of surface roughness on the scattered energy can be used qualitatively in flaw characterisation to separate smooth planar flaws, rough planar flaws and volumetric flaws. (Crutzen et al., 1989, Ogilvy, 1989)

Theoretical models and experimental work on the effect of surface roughness have shown quite good agreement with smaller surface roughness, but with increased values this is not the situation. For example, Ogilvy (1989) found an agreement between model predictions and experimental results to be typically within 3 dB, except for very rough surface where the theoretical prediction results did not agree with the experimental results.

The effect of fracture surface roughness on the detectability becomes advantageous, when the flaw is tilted. When the incident wave is normal to the reflection surface, the specular signal is detected and increased surface roughness decreases the amplitude hence decreasing the detectability. When the flaw is tilted, the increased surface roughness allows reflection of ultrasonic energy in different directions, as theoretically modelled by Ogilvy (1989). This means that by increased tilt the detection changes from specular to off-specular field. For example, Toft (1986) showed experimentally that increase of the fracture surface roughness of the flaw decreases the signal amplitude of well-oriented flaws (Figure 14). Furthermore, increase of the tilting angle decreases the signal amplitude, but with increasing surface roughness the rate of amplitude decrease is diminished. Through tilting the flaw, the signal amplitudes from rough flaws exceed those from smooth flaws as detection moves out from the main lobe of specular energy to the diffuse field.

The level of misorientation, after which the detection is enhanced, depends on the flaw size and shape. The larger is the flaw, the smaller is the degree of misorientation beyond which the surface roughness will enhance detection. It must be noted that, since the diffuse field amplitude will never exceed the amplitude of the coherent field, the detectability can be enhanced only with sufficiently large misorientation. The model predictions showed this to be more than 20° from normal angle (0°). (Ogilvy, 1989)

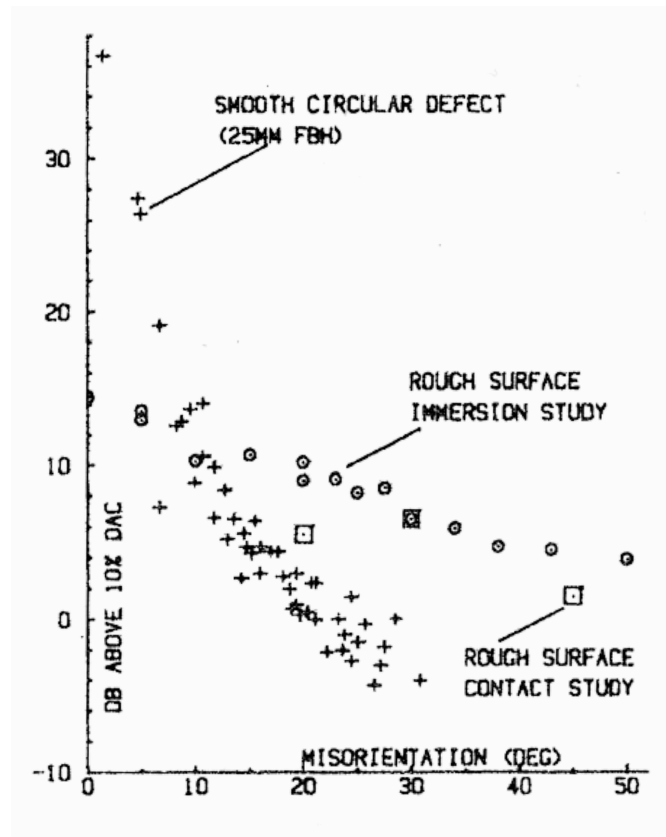


Figure 14 Signal levels of rough and smooth flaws as a function of flaw misorientation. (Toft, 1986)

However, there are studies that do not clearly indicate the effect. For example, Yoneyama et al. (2000) studied the effect with conventional 45° and focusing 45° and conventional 60° and 70° probes. In the experimental work they used mechanical fatigue cracks with maximum surface roughness values (R_a) varying from $40\ \mu\text{m}$ to $70\ \mu\text{m}$ and average values (R_z) from $34,6\ \mu\text{m}$ to $55,9\ \mu\text{m}$ (larger with deeper cracks). The difference in crack corner echo height was compared to the echo from a smooth corner. Authors found some differences between the echo heights from the smooth corner and corners of different fatigue cracks, but they considered them negligible and drew a conclusion that the difference of surface roughness between an EDM notch and a mechanical fatigue crack may be neglected when conducting flaw detection.

Amplitude differences at different locations of flaws are used to size flaws with techniques relying on amplitude changes at flaw extremities (Ogilvy, 1989). With smooth flaws, the signal amplitude drops clearly near the edges of the flaw. However, for rougher flaws there is not a clear plateau region from which the decibel drop could be measured, but the signal amplitude fluctuates across the flaw. The principle and difference between smooth and rough flaws is shown in Figure 15.

Surface roughness of the flaw affects also sizing techniques relying on the time-differences from flaw extremities (Ogilvy, 1989). Two clearly separate pulses are detected from a smooth flaw, from which the flaw size can be calculated. These distinct pulses arise from edge diffraction. From a rough flaw, a continuous pulse may be obtained which is a superposition of the edge-diffracted pulses and diffuse

scattering from all parts of the surface. Roughness may cause a loss of distinct diffracted pulses and hinder the timing measurements. The principle of the effect is shown in Figure 15.

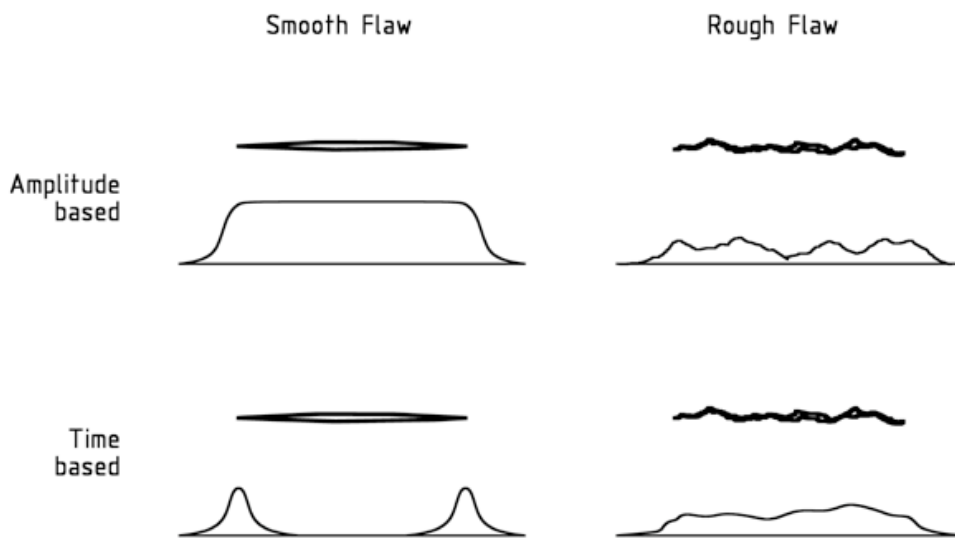


Figure 15 Principle of the effect of flaw surface roughness on the amplitude- and time-based sizing techniques.

1.3.2 Effect of opening and residual stresses on detection and sizing

Basically, with increasing crack opening the obtained ultrasonic echo amplitude increases and when the crack is closed, echo amplitude decreases. In the following the effect of flaw opening to the obtained ultrasonic response is introduced. Furthermore, the condition of residual stress is treated separately as an individual factor affecting the flaw opening and obtained ultrasonic response.

The recorded amplitude changes are related to the reflection surface movements. If the crack is open through its full length, the whole surface from the crack opening corner to the crack tip can vibrate freely as excited by the incident ultrasonic energy. If the crack is closed partly or through its whole length, the fracture surfaces pressed together hinder the free oscillation of the reflection surface. In this case, fracture surface heights touching each other allow transmission of the ultrasonic energy. Hence, the ultrasonic wave does not meet any boundary of different acoustic impedances. Vice versa, if the crack is open, there is a clear boundary of different acoustic impedances where reflection and scatter of the ultrasonic energy occur. By a continued increase of the flaw opening, a saturation level of the echo amplitude is reached where the reflection from the fracture surface is at maximum. For a mechanical fatigue crack, Iida et al. (1988) reported a saturation level to be at 10 μm width of the crack surface opening. When closing a crack, it is defined acoustically closed, when a large change in the ultrasonic signal is observed. However, according to Ibrahim et al. (1981), the signal does not necessarily disappear completely.

The effect of flaw opening to the detection sensitivity of different mechanical fatigue cracks has been studied, e.g., by Yoneyama et al. (2000). Yoneyama et al. (2000) loaded three different mechanical fatigue cracks by mechanical tensile and

compressive loads to study the effect of crack opening on the obtained crack corner echo height. In their results, the echo height from crack opening significantly changed with the changed surface opening width. Furthermore, echo height with the same opening width increased with increasing crack depth (Figure 16) finally being, with the largest opening widths ($>18 \mu\text{m}$), approximately the same as what was obtained from an EDM-notch. The authors attributed their results to the effect of crack opening width, but they did not discuss the reasons for this. The results may only reveal the effect of different cross-sectional areas taking part to the reflection of the acoustic energy.

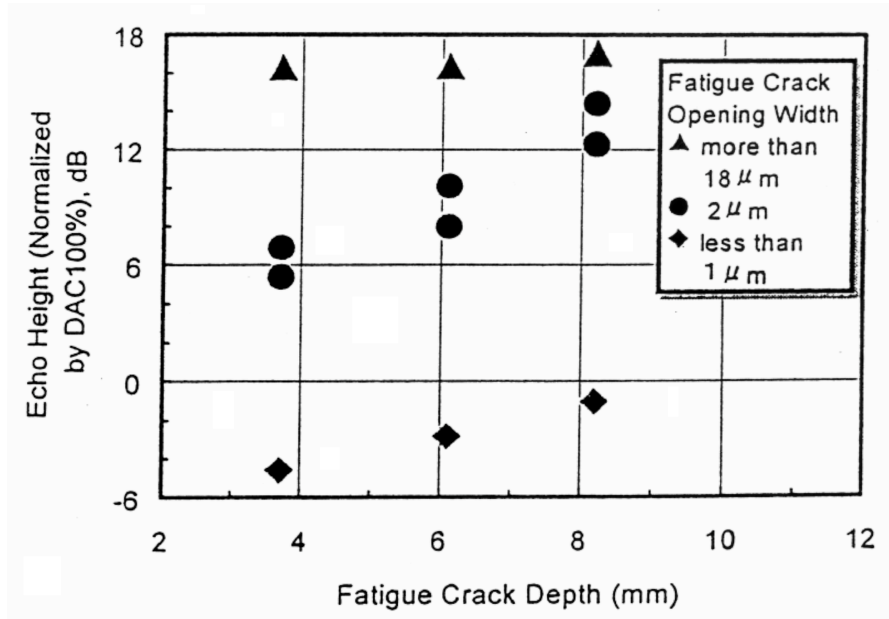


Figure 16 Relation between fatigue crack surface opening width and echo height of three different sizes of cracks (3,7 mm, 6,1 mm and 8,2 mm). (Yoneyama et al., 2000)

In the studies of detection sensitivity of mechanical fatigue cracks the effect of material condition to the interdependence of the opening of the crack and obtained ultrasonic echo amplitude height have been studied, e.g., by Becker et al. (1981). Ultrasonic amplitude height obtained from mechanically loaded fatigue cracks showed different behaviour with cold-worked and annealed materials. In the cold-worked condition, the amplitude height decreases gradually, when the crack is closed (compressive loading is increased). After annealing the sample, the change in amplitude height is much faster, i.e., the slope of amplitude change vs. applied load is steeper than that of the cold-worked sample. This was attributed to the material condition as in the cold-worked material the crack tip closes first and after that gradually the rest of the crack, and the last part to close is the crack mouth. This is seen in the change of the ultrasonic amplitude first as a slow decrease, when the less reflective crack tip closes, and then as faster decrease when the rest, more reflective parts of the crack close. In the annealed material, the whole crack closes practically at the same time. This difference was attributed to the compressive residual stresses present near the crack tip of the cold-worked specimen causing immediate increase of the compressive stress from the beginning of the compressive loading. In the annealed material sample there is no stress near the crack tip as unloaded.

Furthermore, the total signal drop was with the cold-worked material 32 dB and with the annealed material 22 dB, and both were reached at the yield stress of the material. Becker et al. (1981) attribute the difference in the total amplitude drop and the magnitude of the drop to the force the fracture surfaces bear. In the annealed material much less force is available, because the yield strength of the annealed material is lower, being half of that of the cold-worked material.

As a separated factor of the crack opening, the present stress state affects the echo amplitudes obtained from the crack opening corner, fracture surface and crack tip. Hence, the results from the open literature indicated here do not only show the crack opening differences, but also the effect of the present stress state. The effect of the stress state is handled as the effect of residual stresses in the following. This is the case also during the in-service inspection, where the present stresses are not dynamic but static.

The possible present residual stresses affect the detectability of a flaw, as tensile residual stress opens and compressive residual stress closes the flaw. Studies on the effect of residual stresses have been performed experimentally with external mechanical loading, e.g., by Iida et al. (1988), Yoneyama et al. (2000), Becker et al. (1981), Ibrahim et al. (1981) and Denby et al. (1984). Theoretical studies on this topic have been published, e.g., by Temple (1985) and Wirdelius (1992). Denby et al. (1984) mentioned that the reflection from fatigue flaws is most seriously affected by the compressive stresses, of all the flaws. Furthermore, flaw tips of the thermal fatigue flaws are considered to be the most challenging ones as the flaw tips are surrounded by a plastic zone already under compression.

The detectability is affected so, that the increasing tensile stresses (opening the crack) increase the echo amplitude and increasing compressive stresses (closing the crack) decrease the amplitude. With high enough loading, there will be a plateau in the amplitude value both in tension and compression. Similar phenomenon has been found for carbon steels (Iida et al., 1988) and austenitic stainless steels (Becker et al., 1981). With high enough tensile loading the echo amplitude obtained from a mechanical fatigue crack may be almost identical to the one obtained from an EDM-notch (Yoneyama et al., 2000).

The effect on the echo amplitude, and detection sensitivity, may be dependent on the direction of the load change, i.e., increasing or decreasing loading. As, in addition to plateau values obtained, a clear hysteresis may be recorded in the change of the ultrasonic amplitude during cyclic loading of a crack. This was shown by Becker et al. (1981) with a mechanical fatigue crack in an austenitic stainless steel. During cyclic loading between tension and compression, the first loading to tension did not change the height of the signal amplitude from the unloaded condition. However, by the followed high enough compressive stress, the amplitude height dropped markedly, finally stabilizing at a lower plateau at loads well over the yield stress of the material. During the second load cycle (unloading-tension-unloading-compression), while unloading from compression, the signal remained in the lower plateau, beginning to increase at a lower force than required to reach the plateau. In maximum tension, the same maximum value of the amplitude height was reached as in the first cycle. When the sample was loaded again in compression, lower force was needed to keep the lower plateau. Becker et al. (1981) attributed the seen hysteresis in the change of the amplitude height to the plastic deformation taking place during the first compressive loading cycle.

The detection sensitivity is differently affected by loading with mechanical fatigue and thermal fatigue cracks. Even though the basic phenomenon of ultrasonic echo amplitude change under cyclic loading is similar, there are some important differences. Typically, thermal fatigue cracks show low values of echo amplitude. Becker et al. (1981) reported that thermal fatigue cracks showed low values of echo amplitude already when no external load was applied. As Figure 17 shows, by application of an external load the thermal fatigue crack followed the theoretical behaviour of reflection amplitude as a function of crack opening (the theoretical amplitude curve is shown in Figure 18). That is, when the crack is under tension the plateau of high amplitude is obtained and under compression the low amplitude plateau of reflection is observed. When no external load is applied, the obtained echo heights lie in the lower part of the steep slope region between the plateaus. Consequently, unloaded thermal fatigue cracks are very sensitive to changes in the loading conditions. This is a result of the crack tightness and rough fracture surfaces allowing the surface heights to be, partly already as unloaded, in contact. Apart from this, mechanical fatigue cracks exhibit higher echo amplitudes as unloaded, hence being more detectable.

Although unloaded thermal fatigue cracks were undetectable (with 50% DAC criterion), the application of the tensile stress equal to the yield strength made most of them detectable. Detection of cracks with such tightness in service conditions substantially depends on stress condition. If cracks are filled with water, according to Becker et al. (1981), they can be undetectable under any realistic stress conditions as a result of the better acoustic energy transfer ability of water than air.

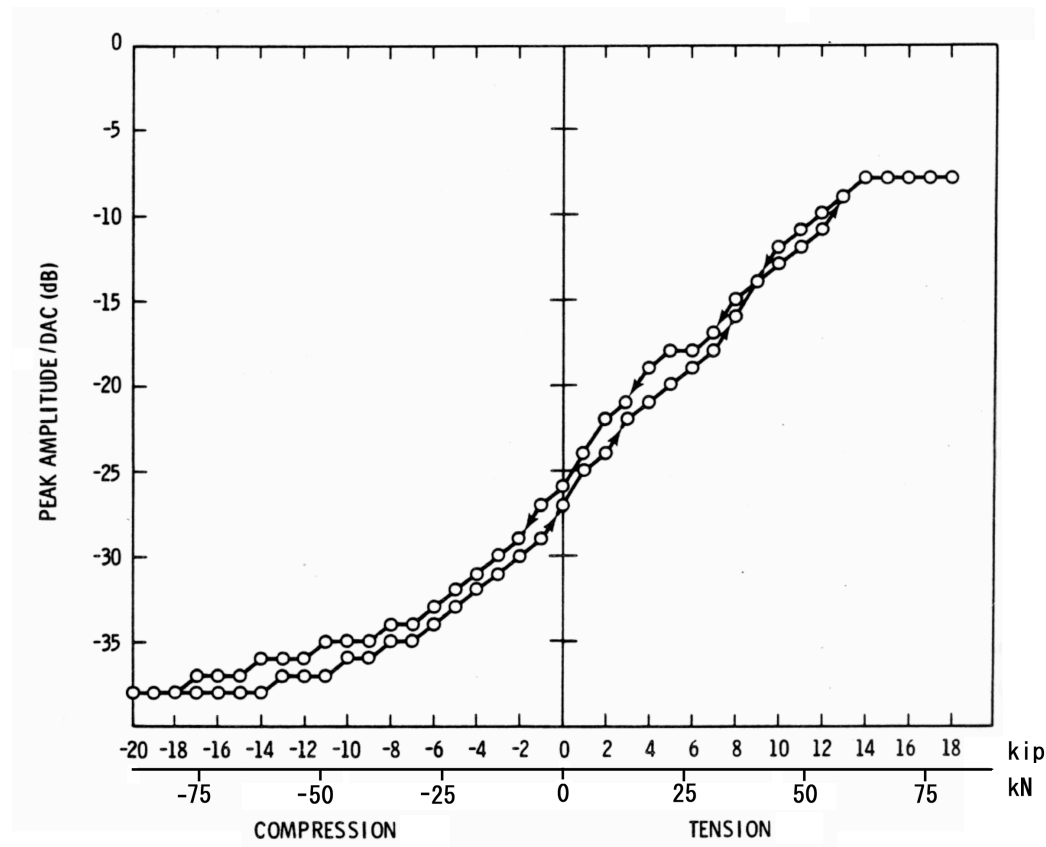


Figure 17 Different stress conditions affecting the obtained ultrasonic echo height from a thermal fatigue crack in AISI 304 type austenitic stainless steel. (Becker et al., 1981)

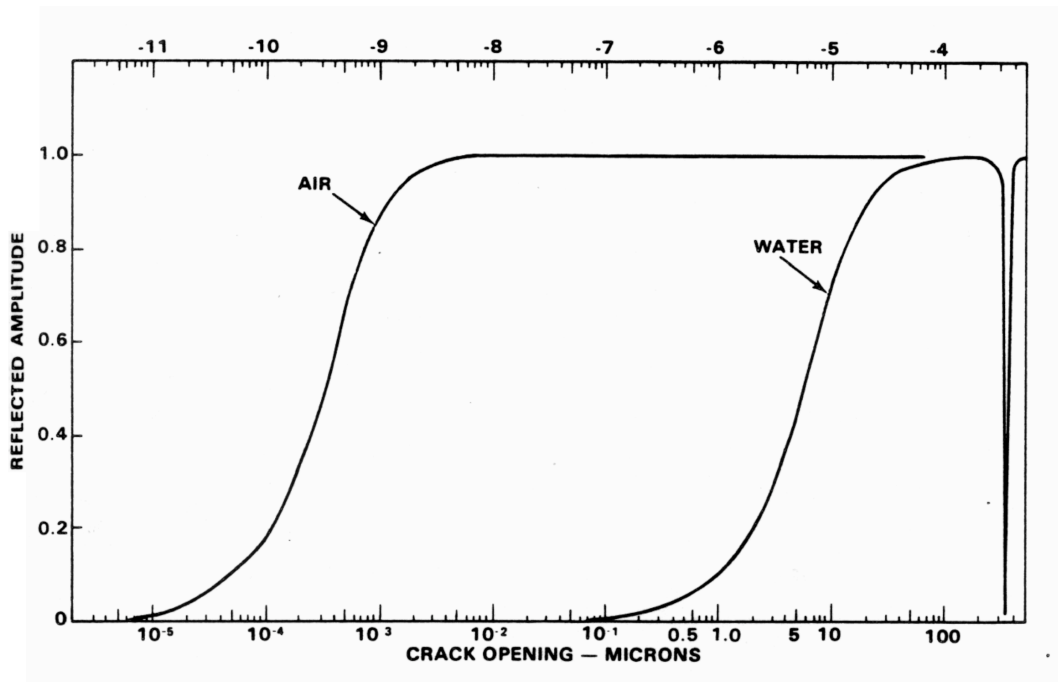


Figure 18 Theoretical ultrasonic reflection coefficient as a function of distance between parallel stainless steel plates separated by air and water (2,25 MHz, transverse wave at 45°). (Becker et al., 1981)

The obtained ultrasonic echo height, and detection sensitivity, under different stress conditions is also affected by the fracture surface roughness (i.e., planarity) of the flaw. The more planar the crack is, the bigger is the difference between the high and low plateau values (i.e., the smaller is the value of low plateau amplitude). This indicates that the non-planar geometry of the cracks may prevent their full closure. Under compressive loading, the smoother cracks can be acoustically more closed than the rougher ones having higher peaks on their fracture surface. This phenomenon has been reported for both carbon steel and austenitic stainless steel. (Becker et al., 1981, Ibrahim et al., 1981)

There are also theoretical studies on the impact of compressive loads to the crack detection including calculation of reflection coefficients for different fracture surface roughnesses (Temple, 1985) and evaluation of echo amplitudes as a function of tilt angle (Wirdelius, 1992) of flaws under different stress states. The smaller scale roughness shows higher effect on the reflection coefficient than the larger scale roughness with different tilting angles for the same probing frequency and applied load (Figure 19). With smaller roughness the higher amount of contact points allows a higher amount of energy transmission through the crack. The use of higher frequency reduces the influence of the compressive stress (Figure 20).

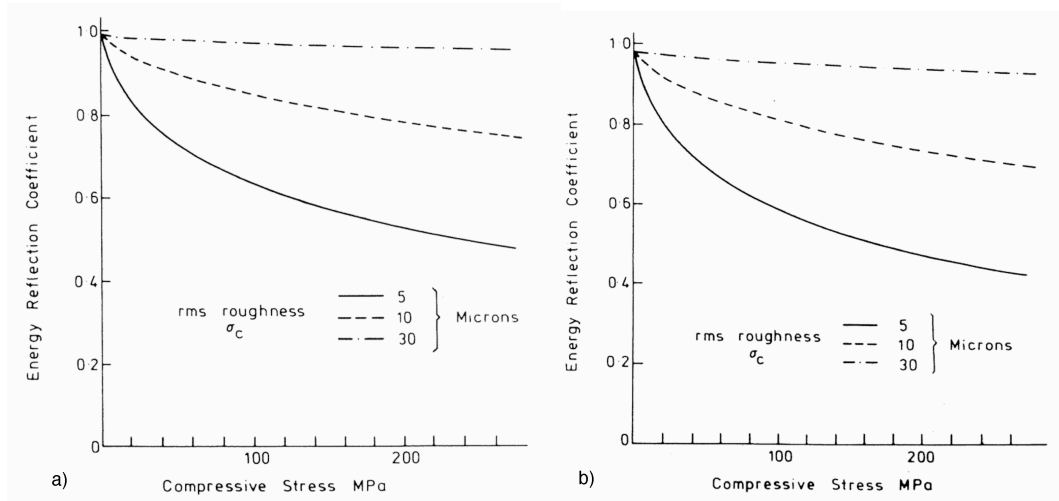


Figure 19 Energy reflection coefficient of 10 MHz longitudinal waves incident at a) 20° and b) 30° to the normal on the model crack under compressive stress. (Temple, 1985)

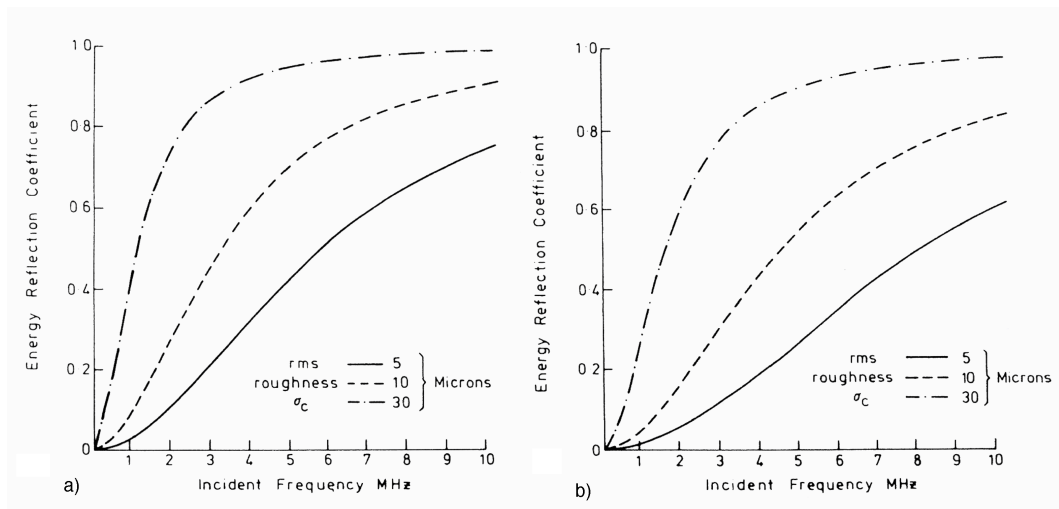


Figure 20 Energy reflection coefficient for longitudinal waves at normal incidence (0°) on rough cracks (three different rms values) under a) 60 MPa and b) 160 MPa compressive stress. (Temple, 1985)

Theoretical evaluations on detection sensitivity of Wirdelius (1992) show that the background pressure affects differently the obtained echo amplitude, when the flaw tilt angle is varied. In the specular reflection (Figure 21 a), the signal level is decreased until the background pressure reaches 200 MPa. In normal incidence (Figure 21 b), the tip-diffracted signal is dropped from the signal level of an open flaw markedly already with 50 MPa background pressure and increase to 200 MPa decreases the amplitude only a bit more.

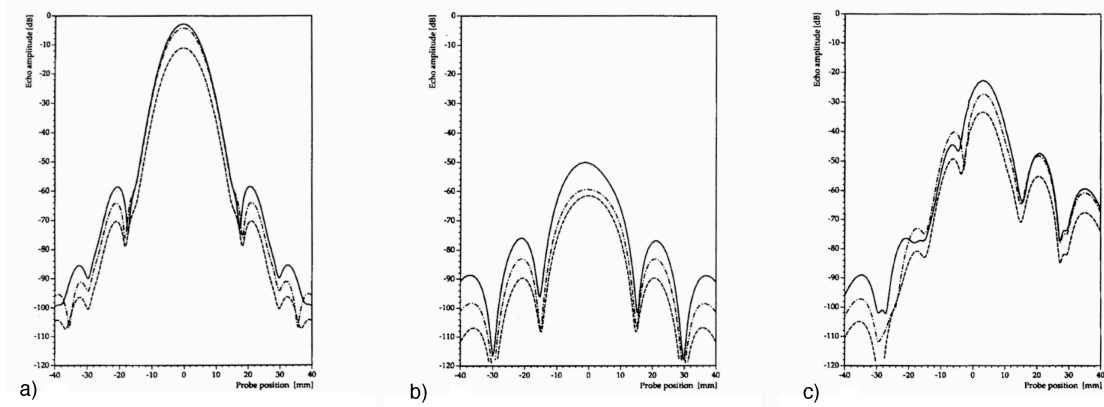


Figure 21 Theoretical evaluation of pulse-echo signal responses for a penny-shaped flaw (depth 60 mm, diameter 4 mm) at different tilts and under different background pressures, with a zero degree, 3 MHz longitudinal wave probe. Different line types indicate different stresses: 200 MPa (---), 50 MPa (-·-·-) and unloaded open crack (—). Tilts were a) 0° (parallel to scanning surface), b) 90° (perpendicular to the scanning surface) and c) 30° . (Wirdelius, 1992)

The effect of stress state and tilt angle to detection sensitivity was experimentally studied by Ibrahim et al. (1981) resulting in differences in the echo heights of different incident beam angles under different compressive stresses. Ibrahim et al. (1981) studied pulse-echo response from crack opening corners of three different mechanical fatigue cracks and, hence, their results are not directly comparable to the theoretical results given in Figure 21. However, the tendency shown in Figure 22, that the highest detectability is achieved with 45° probe, was also shown by Wirdelius et al. (1992). The good results of 45° probe were attributed to the favoured orientation of large portion of small facets on the flaw fracture surface.

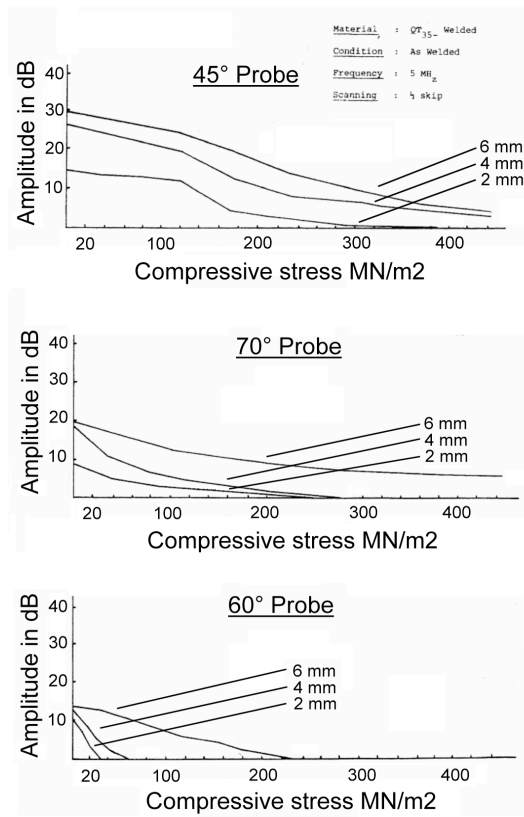


Figure 22 maximum signal responses from three different fatigue cracks as a function of compressive stress with three different 5 MHz angled transverse wave probes. (Ibrahim et al., 1981)

Sizing of the flaw, similarly than detection but probably with even stronger influence, is affected by the combined effect of the flaw opening width, residual stresses and material condition. However, there are no studies showing the effect of different flaw tip openings under different loading conditions, as was the case with detection sensitivity studies. Hence, all the sizing sensitivity studies are connected to different opening widths at the flaw mouth.

The effect of material condition to the obtained ultrasonic echo height from the flaw tip, i.e., sizing sensitivity, under different loading conditions has been studied, e.g., by Becker et al. (1981). The reported difference in the rate of change of the ultrasonic response from loaded crack tips of cold-worked and annealed materials was attributed to the different condition of residual stresses in the material. This was seen as slower change of obtained amplitude height with the cold-worked material and faster change with the annealed material. This difference was attributed to the first closing crack tip with the cold-worked material, while with the annealed material the faster amplitude drop indicates that the whole crack closes practically at the same time.

The growth of a fatigue crack always induces a plastic zone in the material around the crack tip, affecting the sizing sensitivity. With austenitic stainless steels the radius of the crack tip plastic zone can be from some hundred micrometres to some millimetres, depending on the loading used during the crack growth. The residual stresses inside the plastic zone are compressive, caused by the plastic tensile loads in

front of the crack tip during crack growth. Such compressive stresses around the crack tip promote closure of the crack tip.

In addition to the plastic zone around the crack tip, a plastic wake forms at the fracture surfaces of the crack in any material during fatigue crack growth. By annealing the material, the plastic areas are stress relieved resulting in stress-free material. Consequently, the echo amplitude from the crack and crack tip will behave differently during loading. However, although there are differences between cold-worked and annealed materials, the fatigue crack tips in both materials are very tight and sharp. They give, already as unloaded, a very weak ultrasonic response making the flaw sizing a difficult task. In case some loads are applied; the crack tip response is changed and if the loads are compressive they will result in marked difficulties in flaw sizing as the obtained amplitude is decreased.

The effect of residual stress on the flaw sizing sensitivity and accuracy has been studied, e.g., by Iida et al. (1988) and Temple (1985). In these studies, test specimens containing different types of flaws were mechanically loaded. Studies were performed with austenitic and ferritic steels under different stress conditions both with metallic fracture surfaces and surfaces covered with oxide layers. Ultrasonic measurement methods used were, amongst others, based on crack tip reflection and diffraction.

The sizing sensitivity is reduced as the obtained amplitude height from the crack tip is decreased with increasing compressive stress. However, the lateral scanning graphs of flaw tip reflection show similar shape under different stress states. On the contrary, the flaw tip echo height is increased by increased tensile stress. According to Iida et al. (1988) the sizing accuracy of DAC % method showed more sensitivity to stress changes than the amplitude drop method. The flaw tip reflection is measurable for deeper flaws, but that may not be the case with shallow flaws. Iida et al. (1988) mentioned the threshold depth to be 0,9 mm; with the smaller flaws they could not measure the tip reflection echo even under tensile loading.

The sizing sensitivity is reduced by increased compressive stresses also with flaw tip diffraction based sizing techniques. With these methods the strength of the crack tip diffracted signal show clear correlation to applied compressive stress. Temple (1985) has published results of correlation between theoretical calculations and experimental studies of stress vs. flaw tip diffraction (Figure 23), showing reduction in the strength of the diffracted signal with increasing compressive stress. However, in the studies of Temple (1985) the diffracted signal was not completely lost even with the maximum applied compressive stress. The maximum loss of signal strength was about 13 dB with maximum applied stress of 260 MPa.

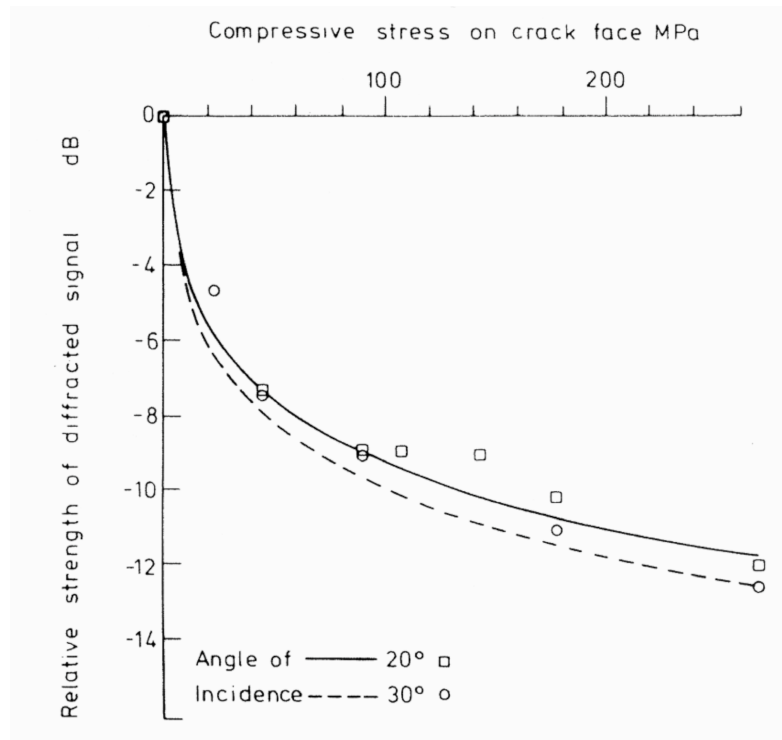


Figure 23 Interaction between compressive stress and relative strength of crack tip diffracted signal. (Temple, 1985)

1.3.3 Effect of crack orientation on detection and sizing

Detection is changed from specular to off-specular field as the tilt of the flaw increases (Ogilvy, 1989). Especially with flaws having rough fracture surfaces, the effect of tilt angle on the detectability is pronounced.

When detecting flaws, the inspection performed in normal (0°) position from the opposite surface, where the surface-opening vertical flaw is located, does not provide very good results. In this position the ultrasonic wave hits first the flaw tip. The tip of a natural flaw is tight and does not provide significant reflection surface. Instead the flaw may diffract quite a big portion of the ultrasonic energy, reflecting back only a small amount. Larger tilt angles provide higher echo amplitudes, when the fracture surface and the opening corner become more “visible” for the ultrasonic beam (Ahmed et al., 1998). This is due to the combination of the raising amplitude of the corner echo and the fracture surface reflection and scattering.

The different incident beams may cause a self-shadowing phenomenon, which may occur when a wave is incident onto a rough surface at a sufficiently tilted angle. Then part of the surface is not directly “illuminated” by the incoming wave, but it is shaded by other parts of the surface. Self-shadowing spoils the phase coherence of the adjacent surface scattered waves and, thus, the amplitude of the overall scattered field may be diminished (Ogilvy, 1989). Occurrence of self-shadowing depends on the surface profile and is therefore difficult to take into account precisely.

In some cases a small flaw may produce higher response than a similarly tilted large flaw (Becker et al. 1981). As a consequence, it is possible that when the flaw grows, repeated inspections would show decreasing signal amplitude. The degree of misorientation affects the strength of the diffracted ultrasonic signal from the flaw

tip (Toft, 1986). Figure 24 shows results obtained with three different 0° probes (different wave modes and frequencies). All the graphs show that by changing the angle of the incident of ultrasonic wave, the obtained amplitude height may be remarkably changed.

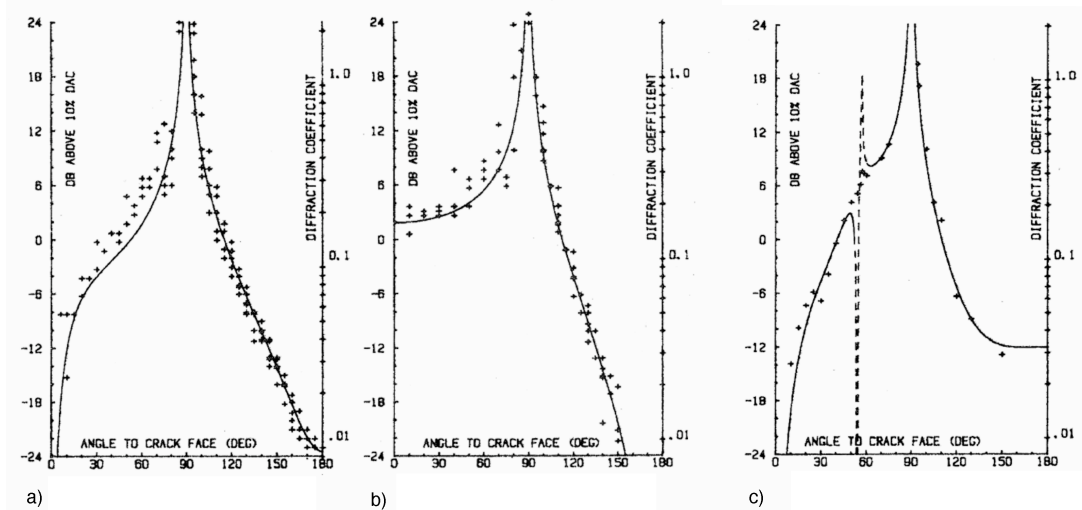


Figure 24 Pulse-echo response of a mechanical fatigue crack tip for a) 5 MHz longitudinal waves, b) horizontally polarised 2,25 MHz transverse waves and c) vertically polarised 2,25 MHz transverse waves. Solid lines show results of theoretical modelling and crosses are measured data. (Toft, 1986)

1.3.4 Effect of oxide film on detection and sizing

During in-service inspection the tested flaw may be filled with air, water and/or have an oxide layer on its fracture surfaces entailing different acoustic impedances and, hence, affecting the reflection and transmission of ultrasound. According to Crutzen et al. (1996), the presence of corrosion products in the flaw enhances its transparency during ultrasonic inspection decreasing detectability. Filling the crack with oxide or water results in higher sensitivity to amplitude drop, when the crack is closed as with an air-filled crack (Becker et al., 1981). That is, the transmission of ultrasound through the crack occurs earlier if the crack is filled with oxide or water. The sensitivity to tightness is ranked to be highest with water-filled cracks, second highest with oxide-filled cracks, while metallic, air-filled cracks are the least sensitive. The theoretical calculations (pulse-echo, 45° , 4 MHz) of Temple (1984) show similarly that a narrow (opening $2\ \mu\text{m}$) water-filled flaw gives 9,6 dB lower signal than air-filled one. Similar drop is obtained with a $4\ \mu\text{m}$ wide flaw in 2 MHz inspection.

Some authors report opposite results from their studies. For example, Iida et al. (1988) reported that if an oxide layer is present on the fracture surfaces, the changes in the ultrasonic echo heights, when closing the crack, are remarkably reduced. This was explained as a cause of air present in the crack hindering changes of the reflection coefficient of the sound pressure. Iida et al. (1988) made a conclusion from their results that, even if compressive stresses are present in a component during the shutdown of a plant, the oxide films present on the fracture surfaces do not reduce the detectability of cracks.

During flaw sizing the oxide film grown on the fracture surfaces affects the sizing capability. This is due to the oxide layer on the fracture surfaces holding the metallic surfaces separate. The difference in the impedances of the metal and the oxide affects the obtained ultrasonic amplitude from the oxide filled flaws, as shown, e.g., by Iida et al. (1988).

1.3.5 Comparison of ultrasonic responses of an EDM notch and a fatigue crack

Traditionally machined notches and drilled holes have been used as artificial reflectors in samples employed, e.g., in ultrasonic training and calibration. However, machined notches and drilled holes are not similar reflectors to service-induced flaws. There are some published comparative results between machined notches and more realistic flaws reported, e.g., by Yoneyama et al. (2000) and Becker et al. (1981).

A clear difference between ultrasonic echo height from the flaw-opening corner of an EDM-notch and a mechanical fatigue crack is observed. However, the magnitude of the difference varies between different authors. For example, the results of Yoneyama et al. (2000) showed 6 to 17 dB difference (Figure 25), while the results of Becker et al. (1981) showed only a minor difference (Figure 26) between EDM-notches and unloaded mechanical fatigue cracks. The difference is based on different reflection properties of the EDM-notches and fatigue cracks. In the case of similar ultrasonic response, the mechanical fatigue crack is acoustically fully open, while in the case of lower amplitude there is also energy transmission through the fatigue crack.

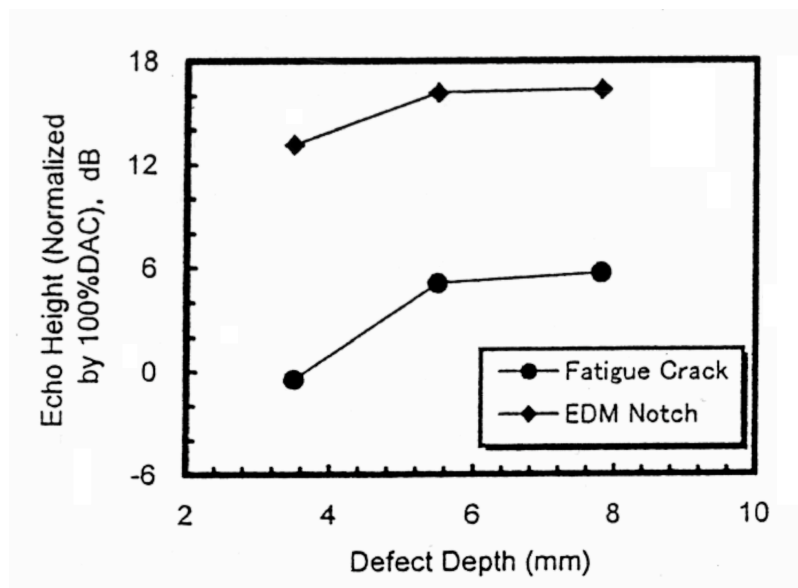


Figure 25 Comparison of corner echo height between EDM-notch and mechanical fatigue crack (45° , 5 MHz). (Yoneyama et al., 2000)

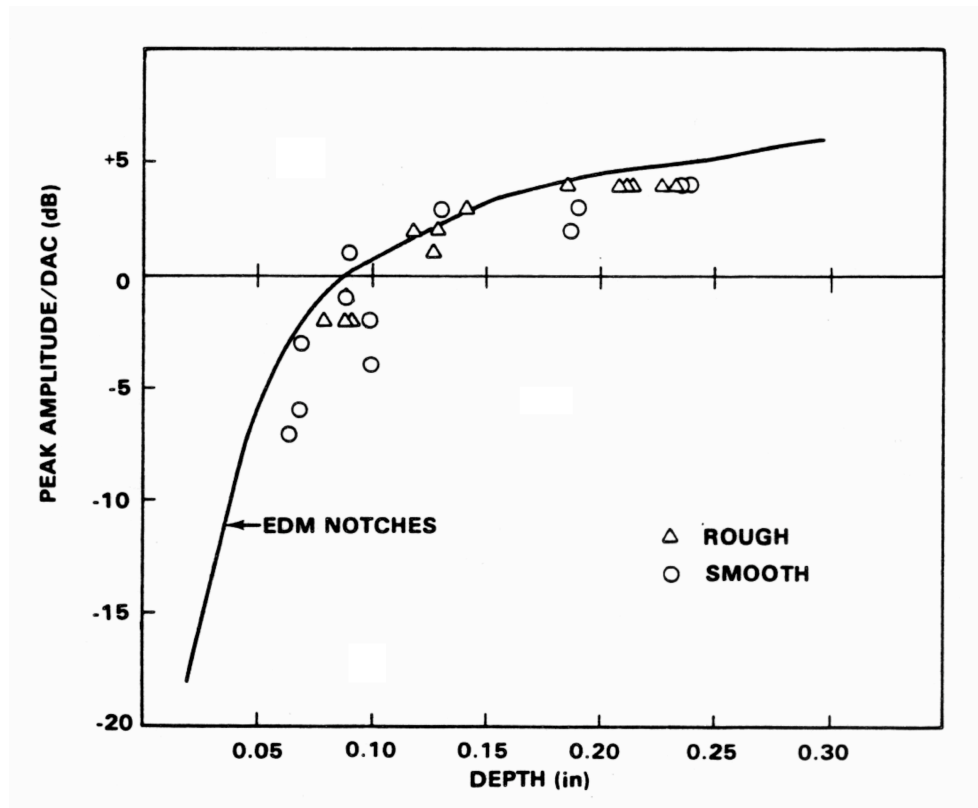


Figure 26 Ultrasonic responses of vertical EDM-notches and several bending fatigue cracks (half skip, 45°). (Becker et al., 1981)

Results obtained with unloaded thermal fatigue cracks were quite different, since all the cracks showed low values of echo amplitude. All the thermal fatigue cracks studied by Becker et al. (1981) were undetectable with 50% DAC criterion, although they were all of rejectable size according to the criteria of ASME Boiler and Pressure Vessel Code.

Sizing of a flaw with ultrasonic methods relies on the flaw tip condition and its characteristics as a reflector. Comparison between realistic flaws (cracks) and machined flaws indicates the difference between these two types of reflectors. The difference has been shown, e.g., by Yoneyama et al. (2000). Yoneyama et al. (2000) obtained a difference of 22 dB between tip echo amplitudes of an EDM-notch and a mechanical fatigue crack. This was unchanged regardless of the depth of the flaws.

The mechanical fatigue crack tip showed almost constant tip echo heights, when different crack sizes were studied. However, echo heights from both the unloaded and loaded (maximum tensile loading) cracks differed remarkably from the echo heights of different EDM-notches (Figure 27). Also by TOFD method the diffraction wave amplitude from realistic flaw tip was smaller than what was obtained from the tip of an EDM-notch. Yoneyama et al. (2000) noticed that the amplitude of the diffracted wave from the crack tip with TOFD had larger values than the amplitude measured with the tip echo method.

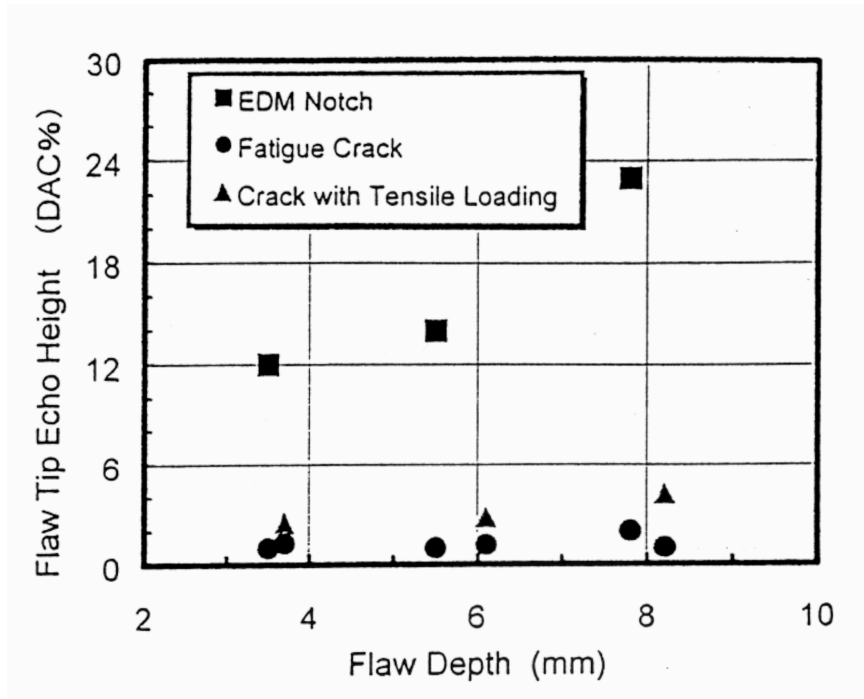


Figure 27 Comparison of flaw tip echo heights between EDM-notch and mechanical fatigue crack. (Yoneyama et al., 2000)

The effect of plastic zone at the fatigue crack tip has been studied by comparing fatigue cracks and EDM-notches in an austenitic stainless steel. The introduced fatigue cracks were machined away with EDM and the resulting notch was compared to similar size of EDM-notch machined in the virgin material (without a plastic zone). In the studies of Saka et al. (1991), the time-of-flight measurements showed difference between these two notches and they attributed this to an effect of the plastic zone left to the crack tip attenuating the time-of-flight signal. When calculating the size of the plastic zone (equations given, e.g., by Anderson, 1991) with parametric values given by Saka et al. (1991) resulting values in the range of about 200 μm to 700 μm are obtained. Furthermore, not only the plastic zone at the crack tip but also the plastic wake on the fracture surface left by the propagating crack tip is present. Hence, by introducing a 300 μm wide notch in the middle of the crack it is possible to have an area of plastic wake in both sides of the flaw and an area of plastic zone in front of the notch tip extending from about 50 μm to 500 μm .

Electrical discharge machining affects the material condition in the vicinity of the tool and marked changes maybe left around the notch. In ferritic TMPC steel Gripenberg et al. (2000) showed that different intensities (fine, medium and rough) used in EDM processing affect markedly the material structure near the machined surface. Machining of stress-relieved material induced tensile residual stresses between 400 and 600 MPa in the surface layer of 50 μm to 150 μm related to the machining intensities, respectively. In addition to this, EDM with oil as the rinsing fluid induces a carbon rich layer (named as white layer) on the surface of the machined material. Thickness of this layer depends on the machining intensity being thinnest with fine and thickest with rough machining. Gripenberg et al. (2000) reported the layer thicknesses from about 10 μm to about 30 μm , respectively. This brittle layer contains micro cracks extending through the whole thickness of the layer.

Saka et al. (1991) did not mention the used machining intensities, but let us consider that they used medium level machining intensity, hence causing a tensile residual stress field with a depth of about 100 μm in front of the notch tip. Furthermore, if they removed totally the fatigue crack tip, with a size of plastic zone of 200 μm (plane strain condition), EDM changed the state of the whole plastic zone. Thus, the results do not necessarily show effect of plastic zone on the diffracted signal, but the effect of EDM on the material condition. If the crack tip was not totally removed, the results show only the effect of the existing crack tip ahead of the EDM-notch.

Despite of the uncertainty in the results of Saka et al. (1991), the effect of plastic zone around the crack tip to diffracted ultrasonic energy maybe significant. However, it is not clear how this effect could be distinguished from the effect of residual stress affecting the crack tip.

1.4 Essential properties of artificially produced flaws

Representativeness of artificially produced flaws is attributed to certain properties that can be quantitatively or at least qualitatively specified. The most important ones are the flaw size, location, propagation path, opening, branching, fracture surface roughness, residual stresses in the vicinity of the flaw and possible oxide products in the flaw. These have marked effect on the NDE response obtained from the flaw and determine its representativeness. Hence, characteristics shown schematically in the Figure 28 should be controlled when artificial flaws are chosen for NDE purposes.

Representative flaw sizes (Figure 28 a) are based on the calculations performed on different components taking into account the local loading conditions, component structure and material. Furthermore, experience from in-service inspections is used to determine the appropriate flaw sizes needed for aimed training and qualification purposes. Hence, the applied artificial flaw manufacturing method has to be able to produce different flaw sizes with adequate tolerances and reproducibility.

Representativeness of flaw location (Figure 28 b) is based and determined by the natural nucleation site of service-induced flaws. It can be in the base material, weld, fusion line or HAZ, as the examples show in Figures 3, 1, 6, and 9, respectively. The appearance of service-induced flaw is such, that it is surrounded by certain microstructural elements resulting from the manufacturing of the component in question. In order to be representative, the artificially produced flaw should have similar microstructure in its surroundings. Hence, the artificial flaw production should not induce any other deviation or microstructural change to the component than those being representative to actual components. If flaws are made to ready-made components only the intended flaw should be induced.

Propagation (Figure 28 c) of the flaw should follow the naturally weakest path through the microstructure, as does the service-induced flaw. Most often this is seen as tortuous propagation caused by the local microstructure. Hence, representative propagation exhibits tortuousness arousing the uneven NDE response similar to those obtained from service-induced flaws.

Quantitative values for representative flaw opening (Figure 28 d, e and f) for different types of service-induced flaws are given in Table 1 and Table 2. A representative flaw is narrowest at the flaw tip and has its maximum opening in the part nearest the surface area. The principle of the effect of the flaw opening to the NDE response is that, the bigger the opening, the higher is the obtained ultrasonic

amplitude from it. However, a saturation level can be reached after which increase of the opening does not increase the amplitude any more. Saturation values of 10 μm and 18 μm of the surface opening for mechanical fatigue flaws have been given by Iida et al. (1988) and Yoneyama et al. (2000), respectively. The given saturation values corresponded to the values obtained from smooth EDM-notches. Narrow and tight flaws allow transmission of energy through them resulting in a weak or uneven NDE response. Consequently, the opening of artificially produced flaws should be controlled and adjustable for simulation of different flaw openings.

Service-induced flaws sometimes exhibit branching (Figure 28 g) disturbing the NDE-response obtained. Hence, artificially produced flaws should optionally be branched, as well. However, there are no guidelines for quantitative determination of the amount of the branching. Neither is there quantitative information available about the amount of branching determined from service-induced flaws.

Service-induced flaws do not have ideally planar fracture surfaces, but they have natural irregularities resulting in different values of fracture surface roughness (Figure 28 h) typically from relatively smooth to medium roughness, as seen in Table 1 and Table 2. Enhanced surface roughness destroys the uniform reflection of incident ultrasonic waves reducing the detection sensitivity of ultrasonic testing. With increased surface roughness, through scattering, the off-specular signals are increased and the amount of specularly reflected energy is decreased. Artificially produced flaws should exhibit representative values of fracture surface roughness to obtain realistic interaction behaviour of ultrasonic energy (e.g., reflection, scattering and diffraction) at the flaw boundaries and extremities.

The state of residual stresses (Figure 28 i) in the vicinity of the flaw is significant, but not very well understood as a property of an artificially produced flaw. Compressive or tensile residual stresses close or open the existing flaw, respectively. With representatively tortuous, narrow and tight flaw the change of residual stresses changes the obtained NDE response markedly. Natural flaws with tight tips exhibit low values of ultrasonic amplitudes already as unloaded, thus, being sensitive even to small changes in the loading conditions. The artificial flaw production technique should allow production of flaws with representative residual stresses and at least qualitative (compression/tension) control of them.

Oxide products (Figure 28 j) in the flaw clearly have an effect on the detection and sizing sensitivity of the flaw. However, there are results in the literature indicating both that the oxide layer increases and decreases the sensitivity (Becker et al., 1981 and Iida et al., 1988, respectively). Despite of that, it should be optional for the artificially produced flaws to have a representative oxide layer on their fracture surfaces.

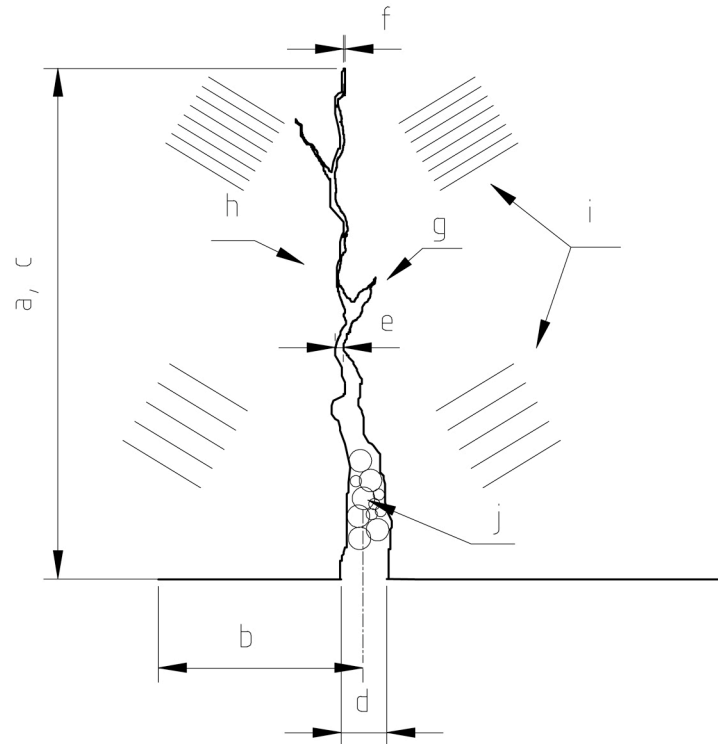


Figure 28 Essential properties of artificially produced flaws: a) size, b) location, c) tortuous propagation, d) opening at flaw mouth, e) opening through the length of the flaw, f) flaw tip opening/radius, g) amount of branching, h) fracture surface roughness, i) residual stresses in the vicinity of the flaw and j) oxide products in the flaw.

1.5 Artificial flaw manufacturing in relation to qualification procedures

There are certain factors that have to be considered when a non-destructive testing personnel qualification is planned and artificial flaws are used as reflectors. Flaw specifications should define factors influencing the inspection method in question in the same way as service-induced flaws do. These factors include correspondence of reflector dimensions and dynamic range of echo amplitude, representativeness of position, orientation, fracture surface roughness and reproducibility of the artificial reflector both metallographically and echo-dynamically (Wüstenberg et al., 1994). Evidently these criteria include requirements of nonexistent artefacts as extra welds, machined notches or microstructural changes. Furthermore, there should be enough information from service-induced flaws from point of view of all the criteria to judge the representativeness of an artificial reflector. (Waites et al., 1998)

The ASME Section XI Code and its Appendices VII and VIII are followed in the USA for NDE qualification. The method described in Appendix VIII requires only test-piece trials and it is mainly used in the USA. As a comparison, there is a clear difference in NDE qualification procedures in the USA and Europe. In Europe each country has their own regulations for qualification and, therefore, it has been impossible to set detailed requirements for qualification that would be commonly valid. The approach of the established European Network for Inspection Qualification (ENIQ) has been to create a methodology to set a framework for qualification. This framework includes the principles and the responsibilities of different involved parties. Furthermore, ENIQ gives series of recommended

practises (ENIQ 1998a, 1998b, 1998c, 1999a, 1999b and 1999c) to assist the developing of detailed qualification systems based on the methodology. The principles of the methodology include the following:

- Qualification is a combination of practical trials and technical justification.
- Procedures and equipment can be qualified by using open trials, in which the operators have knowledge about the flaws in the test pieces.
- Personnel test piece trials should be conducted as blind, i.e., personnel should not have information about the flaws in the test pieces.

The trend in qualification procedures in different countries is towards more widespread adoption of performance demonstration. The form of adoption can be national system based on ASME Code Section XI or ENIQ or consultancy of an organisation already having the expertise. The expense of ASME Code based on the large numbers of specimens is a clear disadvantage. On the other hand, the ENIQ approach requires countries to develop detailed qualification systems of their own, which requires expertise many countries do not have (Waites et al. 1998, Waites et al., 2002). Procedures relying only on practical trials have more confidence based on the statistical aspects, as there are more flaws to be inspected during qualification. However, development of technical justification is seen as one of the key issues, since it offers use of fewer number of test pieces with high effectiveness as test pieces have been designed to focus on the important issues. Furthermore, technical justification brings additional confidence not achieved through practical trials.

The ENIQ steering committee conducted a pilot study to investigate the feasibility of the recommended practises and to explore the details of its implementation (ENIQ, 1999d). This pilot study was carried out with austenitic stainless steel components. The study included several aspects of qualification procedures, but here the interest is on the flaw manufacturing issues. There were different artificially produced flaws used, e.g., EDM-notches, realistic fatigue cracks and implanted IGSCC simulating flaws (ENIQ, 1999e). However, the flaws used were not satisfactory as there were a lot of artefacts produced resulting to false interpretation of the NDE results. Conclusions made from the results of the pilot study were that the used flaws, although produced by several leading manufacturers, were not satisfactory to be used for the qualification purposes. Hence, a statement was given that further work is needed to resolve the problems encountered with the used flaws.

1.6 Flaw manufacturing techniques

Different techniques are used to manufacture flaws for the NDE training, practising and qualification purposes. The aim of each manufactured flaw is to reach such an NDT response that it either is a simplified simulation or could be regarded as a realistic simulation of a service-induced flaw. This is reached with varying success depending on the manufacturing technique. The limitations of the different types of manufactured flaws restrict their use as realistic simulation of service-induced flaws.

The reflection behaviour of a test reflector is commonly compared to real indications. For this comparison Wüstenberg et al. (1994) state that the minimum demand for similarity in morphological sense is as follows: for slag inclusion

simulation at least a side drilled hole should be used, for circular shaped hydrogen-induced crack in a forging simulation at least a flat bottom hole should be used, for near surface crack detected by the corner effect simulation at least a notch should be used. The reflector dimensions should correspond to actual simulated flaw size and its dynamic range of echo amplitude should be comparable. Location of the reflector should represent the same geometrical conditions (e.g., sound path, focal distance, relation to surface) as the actual flaw. Production of the reflector should ensure high reproducibility both in dimensions and in the ultrasonic response.

The necessity is emphasised to make definition of the artefact as being a reflector or an object for crack tip simulation. The most frequently used artificial reflectors and their typical physical interaction to produce an indication are listed in Figure 29. There are two main categories of interactions: mirror-like reflection and diffraction from tips and corners. (Wüstenberg et al., 1994)

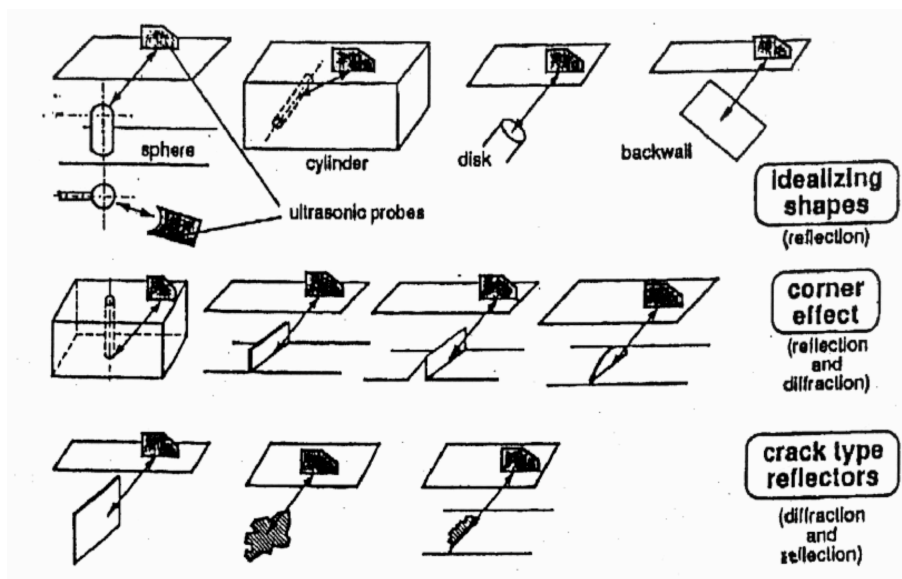


Figure 29 Different types of test reflectors. (Wüstenberg et al., 1994)

Conventional approach has been to base the ultrasonic signal analysis on an absolute amplitude threshold, which implies an assumption of proportionality between echo amplitude and flaw size. For small flaws, in the range of wave lengths, the echo amplitude increases monotonically with the flaw size, but this is not the case for larger (2 to 5 times the wave length and more) and tilted flaws. The relation between echo amplitude and flaw dimensions for different artificial flaws is visualised in Figure 30.

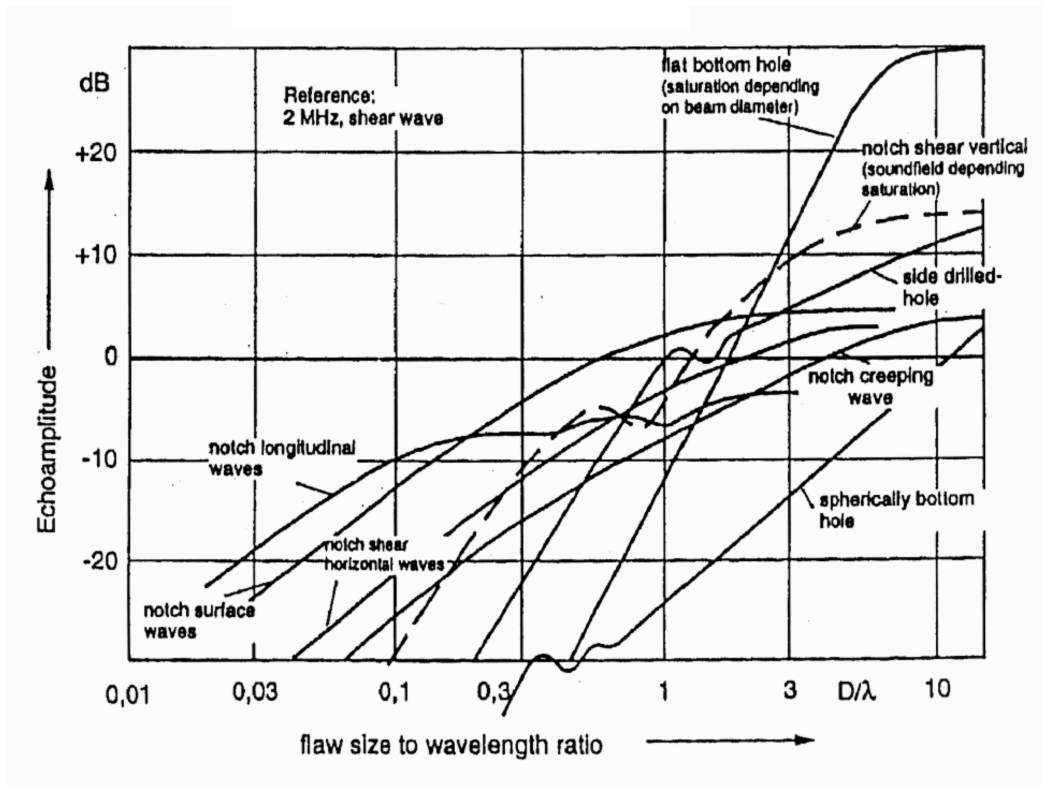


Figure 30 Dynamic range of echo amplitudes for different artificial reflectors. (Wüstenberg et al., 1994)

The traditional way to produce an NDE calibration flaw is machining (drilling, milling, grinding, EDM). Although machined grooves can be narrow and there are improved shapes as PISC type A notch (ENIQ, 1999d, ENIQ, 1999e), they are not similar to fatigue or stress corrosion cracks from their NDE response point of view. Reason is that the walls of grooves are smooth and planar and the tip radius is large, while a real crack has rough surfaces and the tip radius can be very small. Furthermore, fracture surfaces of a real crack are sometimes pressed together, especially near the crack tip. Hence, the physical phenomena of machined flaws and real flaws are of different nature and there is no practical correlation between them (Crutzen, 1986).

Comparative studies on the difference of ultrasound diffraction of real and artificial realistic flaws have shown that the flaw tip condition should be under strict consideration when choosing artificial reflectors. Lemaitre et al. (1993) mentioned that already small changes in the flaw tip condition changed dramatically the ability to detect the tip diffraction. Hence, they concluded that the flaw tip of an artificial realistic flaw should be as tight as possible to have the most demanding simulation of the real flaws. Crutzen et al. (1996) clearly distinguished the NDE response of any artificial flaw (flat bottom holes, side drilled holes, saw cuts, electro-discharge machined notches) from NDE response of real flaws. Wüstenberg et al. (1994) state that if the main interaction is based on the crack tip diffraction, then there is no other possibility than to use real cracks as cut outs from components. The reason for the statement is that any available production method for realistic cracks has not been able to produce sufficiently representative weak tip diffraction.

1.6.1 Implanted flaws

Implantation techniques mainly include implanting of different kinds of flaws by welding. Flaws implanted are intended to accurately replicate the real ones occurring in the plant components. In addition to flaws manufactured with different techniques, flaws can be cut out from real components and implanted into mock-ups. There are requirements for the accuracy of certain factors (location and size) of the implanted flaws that are equal to or exceed the sizing capability of UT measurements. Generally accepted tolerances are ± 1 mm for flaw depth and ± 2 mm for flaw length. Some authors, e.g., Pherigo et al. (1993), state that if the implanted flaws cannot be accurately characterized by mechanical measurements, final destructive tests are needed to confirm the flaw size.

The flaw implantation method is considered cost effective, because several flaw types can be implanted in one specimen during the same manufacturing process. The method provides good means for controlling flaw accuracy (size, shape, orientation, etc.). There are two common types of implantation processes used for manufacturing of flawed specimens: 1) welded implant process, and 2) in-situ implant process. The first one is typically used to introduce flaws in carbon steel pressure vessel, nozzle and plate materials. Figure 31 describes the process where a flaw is implanted underneath the cladding in a pressure vessel specimen.

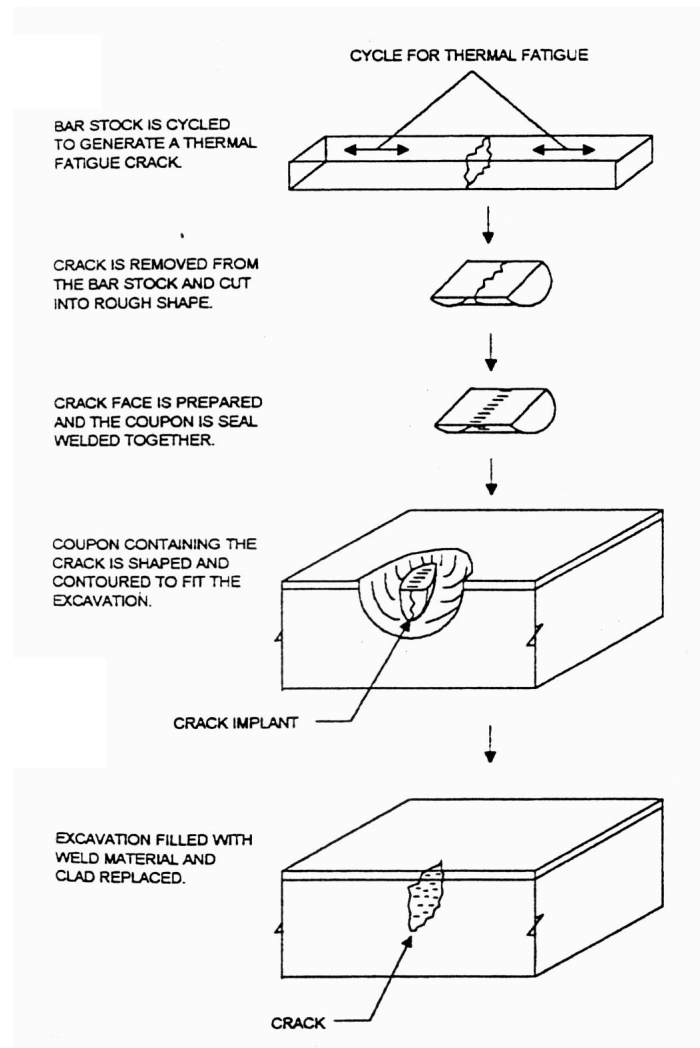


Figure 31 Principle of the welded implant process. (Pherigo et al., 1993)

Flaws to be implanted by welded flaw implant process are manufactured separately and implanted in a machined cavity of the specimen. With this process almost any type of flaw can be implanted. Flaw location can be accurately measured during the process, which provides confidence of location tolerances. The disadvantages are the new material and extra weld seam introduced and the effect of the welding residual stresses on the final flaw opening and flaw tip condition. The extra weld around the implanted flawed coupon is “visible” for ultrasonic testing and the depth of the implantation may give an idea of the flaw depth although the flaw tip would not be detected (ENIQ, 1999d). During implant welding of the cracked coupon in the prepared excavation, the flaw tips are melted down. Hence, the final flaw has melted tips without natural sharpness and tightness. Furthermore, the weld solidification induces marked tensile residual stresses on the weld that open the flaw through the full length from the initial, as-introduced state.

In the in-situ flaw implant process the flaw is created directly in the original material. This method is typically used for pipes. The advantage is that the UT beam will reach crack face from one direction without having to propagate through the weld material. This is particularly important for stainless steels, where the extra weld material causes deleterious effects on the UT beam. The in-situ flaw implant process is described in Figure 32.

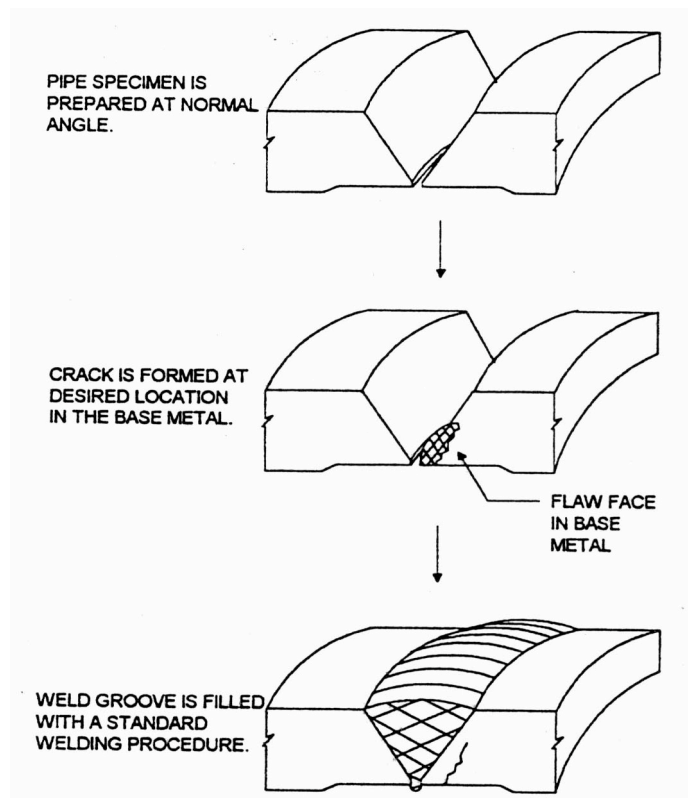


Figure 32 Principle of the in-situ flaw implant process. (Pherigo et al., 1993)

Thermal and mechanical fatigue cracks can be produced in the pipes of different diameters by the in-situ flaw implantation process. Flaws can be grown in the weld preparation area of other part before the weld groove is filled with the weld metal. When thermal fatigue cracks are grown, they are produced under tensile loads by

subjecting the area to a number of heating and cooling cycles. After the flaw has been formed, its location is determined with physical measurements to a given reference surface. Finally, the groove is seal welded with a GTAW welding process. The welding phase is critical, because the final penetration of weld cannot be measured by mechanical means. Disadvantage of this process is the solidification of the seal welding of the groove inducing residual stresses that affect the final opening of the flaw. This process induces extra weld on one side of the flaw and, hence, cannot be used to simulate a base metal flaw. (Pherigo et al., 1993, Paussu et al., 2003)

Typical tolerances for the in-situ flaw implantation, as given by Pherigo et al. (1993), are shown in Figure 33. Although accurate mechanical measurements are made during the manufacturing process for flaw size and location, the seal welding process affects the final measures. Furthermore, even when the described manufacturing process allows ultrasonic beam to reach the flaw without passing through the weld metal from one direction, the other direction does have this weakness. Practically the flaws can be produced only during manufacturing of the whole test sample.

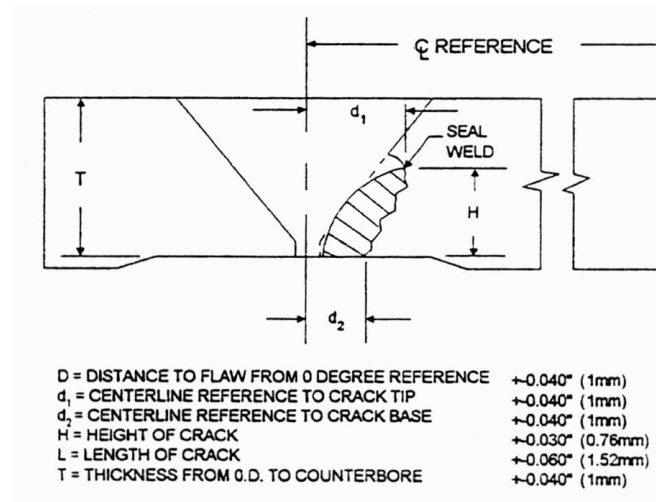


Figure 33 Typical implant tolerances for an in-situ implantation process. (Pherigo et al., 1993)

1.6.2 Natural flaws

Flaw manufacturing techniques inducing natural flaws produce weld-induced cracks (solidification cracks), thermal fatigue cracks, mechanical fatigue cracks and stress corrosion cracks (SCC). These cracks can be produced into final, full-scale qualification mock-ups simulating actual plant components. The advantage of the natural flaws is that they are aimed to induce only natural changes in the microstructure. (Araki et al., 1998)

1.6.2.1 Weld-induced cracks

Surface breaking cracks can be introduced by welding, as described by Edwards et al. (1993 and 1995), Watson et al. (1996) and Paussu et al. (2003). These methods are based on control of the welding procedure so that a solidification crack will arise. Before welding a narrow cavity is machined to the wanted location. This cavity is then filled with a special weld metal susceptible to solidification cracking, hence

producing a centreline crack during solidification. Produced crack can show branching and secondary cracking. An example of this type of crack is shown in Figure 34.

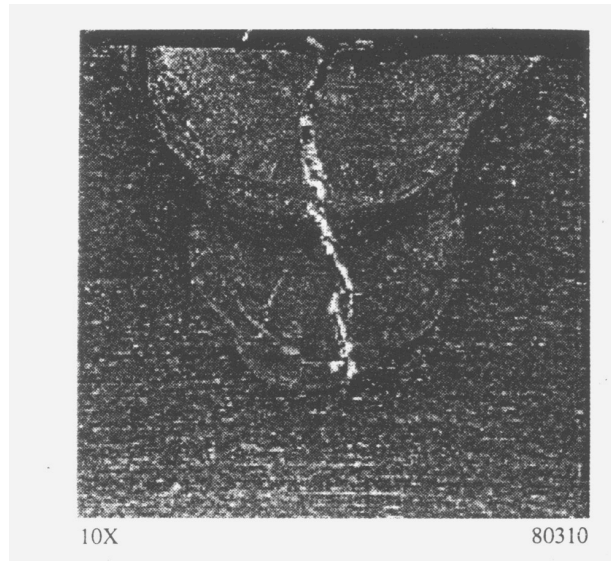


Figure 34 Weld solidification (WS) crack in AISI 304 type stainless steel. (Watson et al., 1996)

Weld solidification technique reduces the amount of weld metal as compared to the traditional implanting of a crack-containing coupon into a cavity (Edwards et al., 1995). Weld solidification technique is suitable for both ferritic and austenitic steel components. This type of crack can be generated to any component, mock-up or geometry without any restrictions for location or orientation. The flaw size (length and depth) can be controlled to some extent, but as the true penetration of the solidification crack varies it results in large tolerance of reproducibility of the flaw size. The limitation of the production is the needed access with a gas-tungsten-arc (GTA) welding torch. Disadvantage of this method is the introduced weld seam affecting the detection of the site where the flaw is located. Hence, as the weld seam causes, e.g., scatter of the acoustic energy it may be detected although the flaw inside it would not be detected. Furthermore, opening of the flaw cannot be controlled but it has random variations affected by the welding procedure and its solidification causing tensile residual stresses in the last weld bead. Particularly important property is the induced large crack tip radius. As a result, flaws produced by weld solidification technique are representative to natural weld flaws, but cannot be used to simulate base metal flaws or flaws with tight crack tip.

1.6.2.2 Thermal fatigue

Some researchers, as Araki et al. (1998) and Becker et al. (1981), have used artificial flaw production methods based on thermal fatigue. In these works, EDM-notches were used as starters for thermal fatigue cracks in order to accurately locate and orientate the produced cracks. In the work of Araki et al. (1998) the starter notch was machined in an additional layer built-up only for this purpose, while Becker et al. (1981) machined the starter notch into the material surface. In both cases the starter notch and certain layer of the material surface were machined away

afterwards. Thermal stress cycling was locally applied by infrared heater (Becker et al., 1981) and high frequency induction heating (Araki et al., 1998) and water-cooling. In the method used by Araki et al. (1998), heating and cooling was performed from the same surface where the starter notch was located. In the method developed by General Electric Ltd. used by Becker et al. (1981), the constant heating was performed from the opposite surface and cycled cooling from the same surface as where the starter notch was located. Both methods mentioned were capable of producing single thermal fatigue cracks in the bottom of the starter notches. Clear disadvantage of these methods is the needed starter notches and extra initiation layer. This restricts the use to samples where machining of the specimen is allowed after flaw manufacturing. The control of flaw characteristics is affected by the final machining procedure and it may close the crack on the machined surface.

1.6.2.3 Mechanical fatigue

Artificial flaw production method based on mechanical fatigue has been used, for example, by Araki et al. (1998), Becker et al. (1981) and in the first ENIQ pilot study (ENIQ, 1999d). Methods of Araki et al. (1998) and Becker et al. (1981) were mentioned to be capable to be used for thick specimens and complicated structures. Araki et al. (1998) and Becker et al. (1981) used EDM-notches as starters for growth of mechanical fatigue flaws similarly than with their thermal fatigue techniques. Mechanical loads were locally applied by specially produced braces welded in the specimen and a hydraulic cylinder (Araki et al., 1998) or by four-point bending (Becker et al., 1981). Both methods were capable of producing single mechanical fatigue cracks at the bottom of the starter notches. Disadvantages of these methods are the needed load bearing braces, starter notches and extra initiation layer. Application of mechanical loading is either restricted to simple components (loading by bending) or braces welded to the component are needed to transmit mechanical loads into the notch tip. The starter notch is needed to accurately locate and orientate the intended flaw. These facts restrict the use of the method to the samples with simple geometry allowing mechanical loading and machining of the specimen after the flaw manufacturing. Equally to thermal fatigue technique, the control of flaw characteristics is affected by the final machining procedure.

1.6.2.4 Stress corrosion

In the work of Araki et al. (1998) stress corrosion cracking was introduced by subjecting the specimen to tensile loading at elevated temperature and high-pressure pure water environment in a static autoclave. Cracks were produced in the heat affected zone (HAZ) of stainless steel pipe welds by covering the area in question first by graphite fibre wool. The methods used were called CPT (Crevised Pipe Testing) and modified CPT methods (modifications were made to the artificial gap geometry and water quality control). Although the methods used were reported to be applicable to introducing stress corrosion cracks in a short time also in large-scale specimens, the difficulty to control quantitatively the depth and length of the cracks was mentioned. Furthermore, flaw manufacturing methods based on stress corrosion require application of the corrosive environment and appropriate loading. These facts restrict the sample size and geometry for which any such method is applicable.

2 AIMS OF THE WORK

The aim of this work is to develop and verify a novel artificial flaw manufacturing method showing the capability of producing representative and realistic flaws. These single and separated flaws are suitable for NDE qualification and training, when true simulation of different service-induced flaws including the most challenging service-induced mechanical fatigue, thermal fatigue and stress corrosion cracks is required.

Present artificial flaw manufacturing methods and manufactured flaws show deviations from the real flaws making them unrepresentative and unsuitable from the NDE point of view. Deviations from real flaws are caused by unrepresentative characteristics of the flaws or additional changes induced during the flaw production processes. Weaknesses are inherent in the nature of applied manufacturing methods and cannot be avoided. Thus, there is a need for development of a manufacturing method introducing more representative flaws.

Natural thermal fatigue damage mechanism is applied and its controllability studied during this study. Thermal fatigue was selected based on its applicability to any component. The developed method is evaluated by studying the characteristics of produced flaws both non-destructively and destructively. Features to be evaluated are control of locating, orienting and sizing of single and separate cracks so that they can be freely located, oriented and sized in a component of any size and shape. Furthermore, when the crack growth is under accurate control, the ability to use the developed method for controlling the final characteristics of produced cracks is verified. Finally, the aim is to prove by NDE measurements the achieved level of realistic simulation of service-induced cracks. The realistic appearance both metallographically and in non-destructive testing is verified through comparing the results to properties of service-induced thermal fatigue, mechanical fatigue and stress corrosion cracks.

3 MATERIALS AND METHODS

Thermal fatigue damage mechanism was utilised for all the crack nucleation and growth tests by using a thermal fatigue testing equipment. Test materials were mainly austenitic stainless steels used widely in nuclear power plants. In order to evaluate the NDE response of the produced flaws, different NDE methods were used. Finally, some of the produced flaws were destructively analysed by metallographic means using optical and scanning electron microscopy.

3.1 Test materials

Test materials were austenitic stainless steels and a Ni-based alloy. Types of austenitic stainless steels were 08X18H10T, SA 376 TP 304, X 5 CrNi 18 10 and AISI 321, the two first of which are typically used in the Finnish nuclear power plants. Ni-based alloy was Inconel 600 (AST M B 166), which is typically used in the safe-ends of the pressure vessel nozzles. Chemical compositions of the alloys are given in Table 3 and Table 4.

Table 3 Chemical compositions of austenitic stainless steels.

Material	C	Mn	Si	Cr	Ni	S	P	Ti	N/ Mo/ Cu
08X18H10T	0,07	1,40	0,55	17,95	10,45	0,008	0,025	0,55	0,015/ 0/ 0
SA 376 TP 304	0,047	1,47	0,34	18,37	10,20	0,009	0,028	-	0/ 0/ 0
X 5 CrNi 18 10	0,02	1,20	0,30	18,20	9,10	0,00	0,028	-	0,06/ 0/ 0
AISI 321	0,08	2,00	1,00	17,00 – 19,00	9,00-12,00	0,03	0,45	Min 0,4	0/ 0,5/ 0,5
ASTM A-351, Grade CF-8A	0,08	1,5	2	18,00-21,00	8,00-11,00	0,04	0,04	-	0/ 0,5/ 0
AISI 316	0,03	-	-	16,50-18,50	10,00-13,00	0,015	-	-	0,11/2,0/ 0

Table 4 Chemical composition of Inconel 600.

Material	C	Mn	Si	Cr	Ni	Fe	Cu
Inconel 600 / AST M B 166	0,15	1,00	0,50	14,0-17,0	min 72,0	6,0-10,0	0,50

3.2 Thermal fatigue

Thermal fatigue damage nucleation and growth is based on repeated strain cycling inducing microscopic plastic deformation. Accumulated damage leads to crack nucleation and growth being strongly dependent on the properties of the loaded material. Characteristics of the final thermal fatigue damage depend on the applied temperatures and loading rates, i.e., heating and cooling rates. Consequently, by controlling the heating and cooling, accumulated damage can be controlled. To do

this, suitable equipment allowing accurate control of heating and cooling in loading cycle is required.

3.3 Test methods

Test samples were subjected to thermal fatigue cycling by applying successive heating and cooling periods. High frequency induction was used as the heating method, because of its high efficiency and good controllability. Water and gas sprays were used for cooling. With the selected methods high and fast enough temperature amplitudes were obtained to induce accelerated thermal fatigue crack growth. Cycles were selected so that no unwanted changes of the microstructure (e.g., grain growth, phase transformation etc.) occurred.

3.3.1 Sample geometry

Experiments were carried out with different sample geometries and sample sizes including plate samples (Publications V and VI), pipes without welds (Publications II and IV), butt-welded pipes, a thick-walled primary pipe section (Publication VII), a piece of real collector head of a VVER PWR steam generator with three threaded holes (Publications II and IV), and a feed water nozzle safe-end specimen (Publications VI, VII and VIII).

3.3.2 Thermal fatigue loading facility

Thermal fatigue loading unit consisted of a high frequency induction heater (300 kHz, 20 kW), water and/or gas cooling system and a control unit (Figure 35). Kemppainen (1997) has described the unique testing installation in more detail. Originally the installation was designed for small sample thermal fatigue laboratory testing. Modifications of the basic set-up were done, e.g., in tooling, fixtures, positioning systems and data acquisition to perform the experiments of this work. Inductors play the main role as the heating power is transferred to the specimen through them.

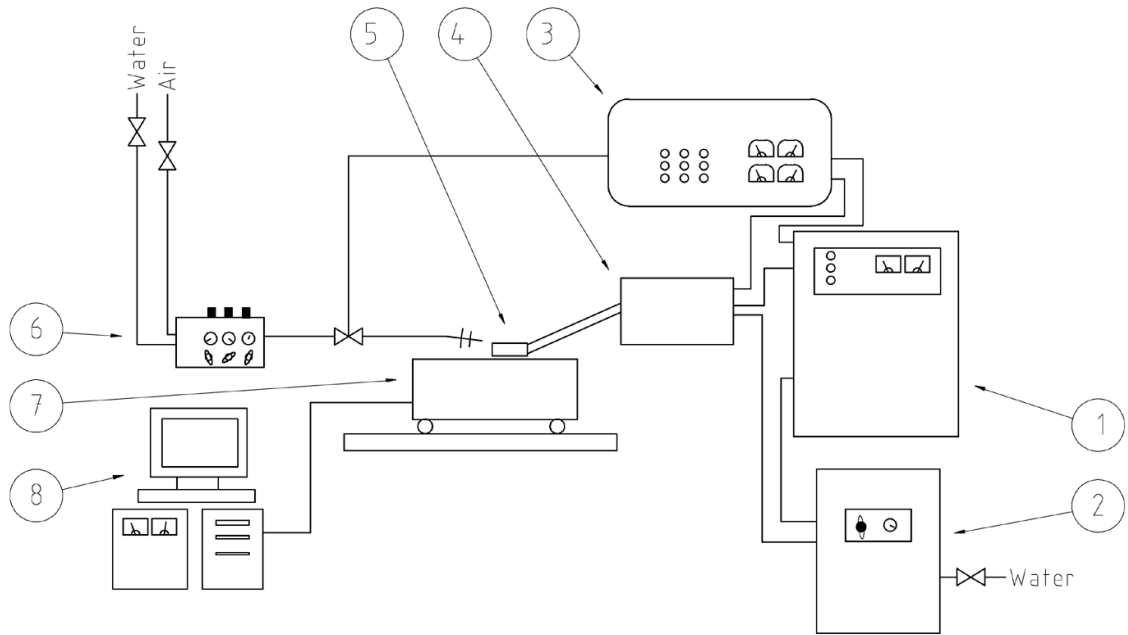


Figure 35 Schematic drawing of the experimental thermal fatigue installation. 1. generator, 2. water cooler, 3. control unit, 4. high frequency unit (HF), 5. inductor, 6. water and air spray cooling system, 7. sample and 8. data acquisition.

Induction heating is a known physical phenomenon and its principles, as well as design of inductors have been described, e.g., by Zinn et al. (1988) and Rudnev et al. (2003). The material is heated up by losses of eddy currents and by losses from hysteresis of changing the polarisation of magnetic domains. The previous occurs with all electrically conductive materials and the latter only with ferromagnetic materials. The basic principle of inductor design is to use Cu-tube wound to shape of a coil and to use alternating current to produce magnetic fields around the coil. Magnetic field induces eddy currents to the test material brought in the close vicinity of the inductor. The principle of the induction is shown in Figure 36.

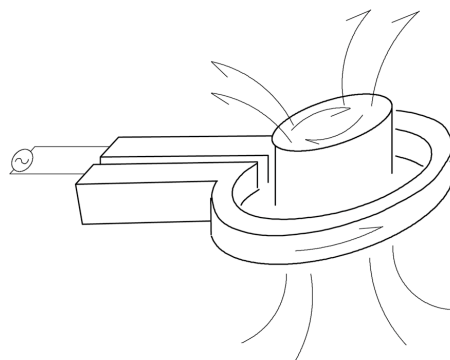


Figure 36 Working principle of an induction heating coil.

3.3.3 Temperature measurement

Temperature cycles were measured and calibrated prior to the actual flaw manufacturing with calibration samples prepared for the purpose. Calibration samples were instrumented with thermocouples and painted with thermal chinks. Temperature cycles to be used were calibrated for different inductors, samples and materials. Some inductors were used for one specific thermal cycle, but most of them were used for several different cycles. By the calibration the needed output power and heating and cooling rates were adjusted to reach the aimed thermal cycle.

Thermocouples and thermal chinks were used for the temperature calibration. Due to limited space between the induction heating coil and the work piece, the thermal chinks turned out to be the most practical method of measurement. On the other hand, thermocouples are suitable for the continuous temperature measurement. Due to limited space, thermocouples cannot be attached close enough to measure the maximum temperatures, which led to a combined use of thermal chinks and thermocouples in the cycle calibration. Thermal chinks with melting temperatures of 302°C, 316°C, 399°C, 427°C, 510°C, 593°C, 621°C and 788°C were used. In practice, the maximum temperatures were measured with thermal chinks and the temperature change during the heating and cooling cycles with thermocouples. The maximum temperature at different times during the cycle was estimated by combining the results from both measurements.

A wide variety of thermal cycles were applied during the work. Different thermal cycles were used for different materials and different stages of the crack growth process. As examples, next figures show the temperature change during chosen heating and cooling cycles in air-cooled (Figure 37) and water-cooled (Figure 38) cycles.

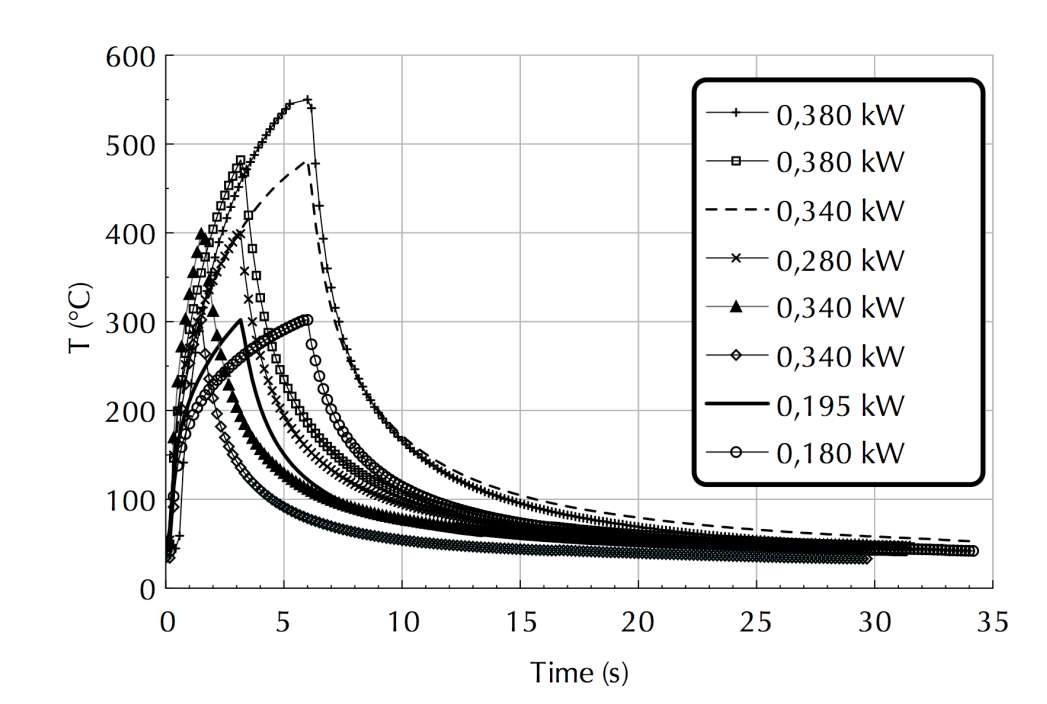


Figure 37 Different air-cooled thermal fatigue cycles with different heating output. Temperatures are shown as a function of time.

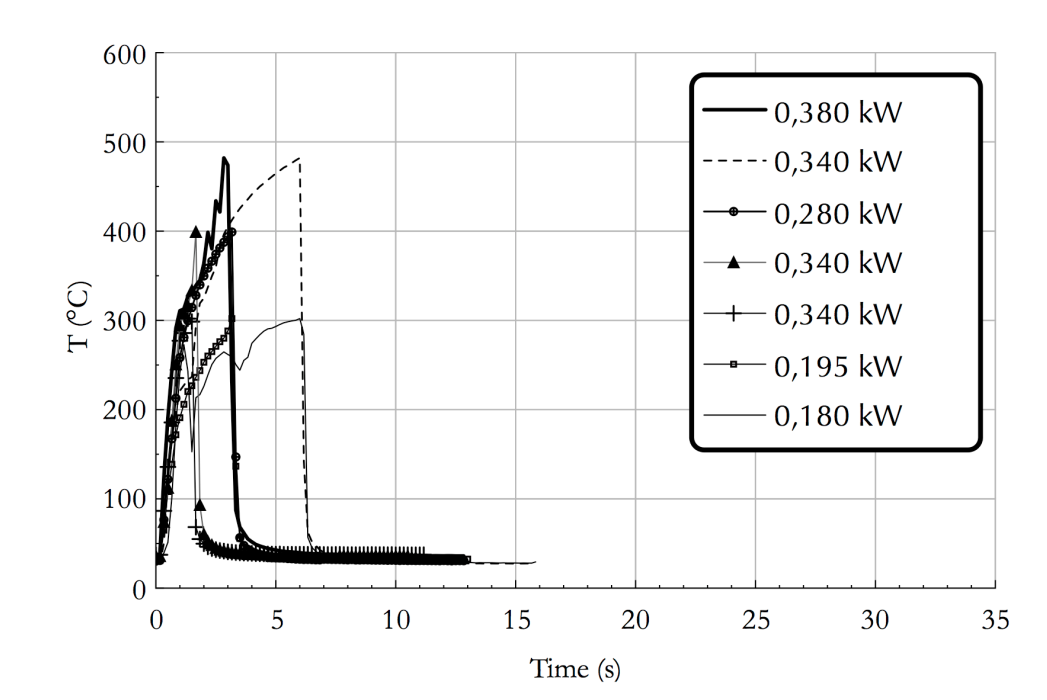


Figure 38 Different water-cooled thermal fatigue cycles with different heating output. Temperatures are shown as a function of time.

3.3.4 Finite Element Modelling

In Publications VII and VIII finite element modelling (FEM) was applied in order to analyse the cyclic strain behaviour at different depths induced by different temperature cycles. Applied thermal loads were analyzed by one-dimensional linear-elastic model giving two-dimensionally the dynamic strain distribution in the surface direction of the sample through the wall thickness. The model was loaded with temperature cycles measured on the sample surface. The numerical cycle was allowed to stabilize for nine cycles and the strains were solved for the tenth thermal cycle. Calculation was performed with commercially available ANSYS 5.5 FE-code (ANSYS Release 5.5.1, 1998). This model is made for solid material and it shows the temperature and strain distributions during loading through the sample wall thickness. The model does not take into account possible flaw in the material and hence the tensile loads that are not carried by the flaw are erroneously shown in the area where the flaw is located. However, as the loading caused by thermal cycling is induced by thermal expansion and contraction of the material, solid material near the flaw still experiences strain cycling.

3.3.5 Residual stress measurements

Surface residual stresses were measured (Publication II and IV) by X-ray diffraction utilizing the $\sin^2\psi$ -method (Noyan et al., 1987). Residual stress measurement device was XSTRESS 3000 (Stresstech Finland Ltd.) (Figure 39). The $\text{MnK}\alpha$ -radiation ($\lambda = 2,10314 \text{ \AA}$) was directed to the sample through a 3 mm in diameter collimator with or without a lead plate mask (with a rectangular slit $0,6 \times 3 \text{ mm}$) attached in front of the collimator mouth (Figure 40). The mask was used to distinguish measured residual stresses in different directions. Total applied exposure times were from 450 s to 650 s.

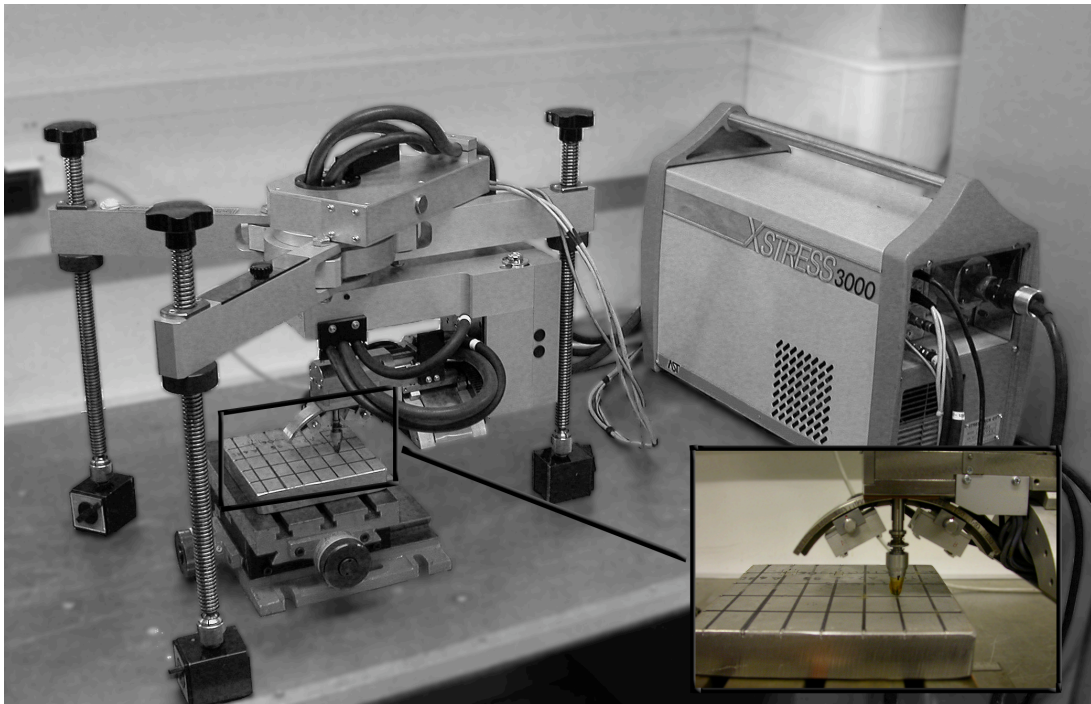


Figure 39 General view of the residual stress measurement device.

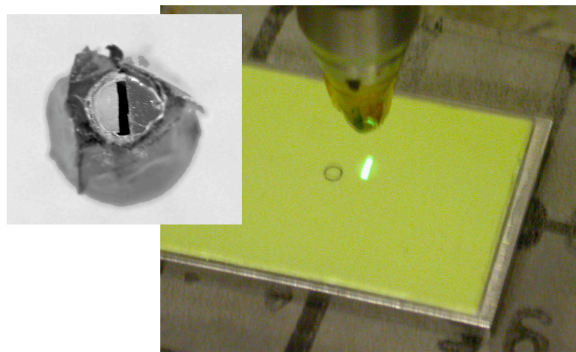


Figure 40 Mouth of the X-ray collimator covered by a Pb-mask with 0,6 x 3 mm slit and irradiated area visualized by an indication plate.

3.3.6 Microscopy and replication method

Replicas, surface cracks and microstructures were studied by light optical microscope Nikon Epiphot. Microstructures, surface cracks and fracture surfaces were studied by a scanning electron microscope Zeiss DSM 962 equipped with an EDS analyser.

Crack nucleation and growth were followed on the surface and documented by cellulose acetate and silicone-based replicas. Replicas were taken before tests and after predetermined fatigue cycles. Crack nucleation and growth were determined afterwards from replicas by light optical microscopy.

3.3.7 Ultrasonic examination

Ultrasonic measurements were carried out with pulse-echo method and time-of-flight diffraction (TOFD) techniques. Phased array equipment, delta-technique and RF- or logarithmic data acquisition were also used. VIT Industrial Systems and Inspecta Testing performed the ultrasonic examinations. There were totally several tens of different probes used during the study, but only some of the results were taken in this work. Probes included in this work are presented in the publications and listed in Table 5.

Table 5 Probes used during ultrasonic examinations.

Probe	Used in Publication	Frequency	Angle	Phase mode (T = transverse, L = longitudinal)
WSY 70-2	II, III, IV, V	2 MHz	70°	mode conversion
MWK 70-2E	II, III, IV	2 MHz	70°	T
MWK 45-2	II, III, IV, V	2 MHz	45°	T
ADEPT60	II, III, IV	5 MHz	60°	L
V110-0°L	II, III, IV	5 MHz	0°	L
41°T	II, IV	1 MHz	41°	T
70°TRL	II, IV	2 MHz	70°	L
45° T	VI	4 MHz	45°	T
55° T	VI	1.5 MHz	55°	T
45° TRL	VII	1 MHz	45°	L
41° T	VII, VIII	1.5 MHz	41°	T

3.3.8 Eddy current testing

Eddy current testing was performed (Publications II and IV) for artificially produced thermal fatigue cracks in austenitic stainless steel base material and cladding. Eddy current testing was performed with 100 kHz probe (Zetec 195-801P02 Fe).

3.3.9 Calculation of fracture surface roughness

Fracture surface roughness value was calculated as a mean roughness value of ten measurements (R_z). Measurements were performed digitally from cross-sectional pictures taken of polished and etched metallographic samples. The following equation was used:

$$R_z = \frac{\left(\sum_1^{10} a - \sum_1^{10} b \right)}{10},$$

where a is distance from surface peak to reference line and
 b is distance from surface valley to reference line.

3.3.10 Thermal fatigue loading vs. UT measurements

Ultrasonic in-situ measurements were performed to artificially produced flaws under dynamic thermal loading. Flaws were first produced with the method developed in this work and then loaded with the same method. Measurements were performed with the probes attached to the samples close to the loaded flaw to obtain a clear enough ultrasonic response. Measurements were performed with simple, plate-like samples (Publications V and VI) and realistic mock-ups (Publications VI, VII and VIII).

Reference measurements were performed in order to separate the effect of temperature to the ultrasonic amplitude change. The local change of the temperature influences measurements due to the change of velocity of the ultrasound. Measurements were done with the same probes using a virgin reference sample with thermocouples attached. Measurements were performed on the edge of the sample to simulate the flaw opening corner and fracture surface of the flaw and their effect on the ultrasonic wave. As a result from the measurements, the effect of temperature changes on the monitored ultrasonic amplitude was separated from the effect caused by the loading. Hence, the final calculation results show only the effect of different loading conditions.

Test specimens having artificially produced, surface opening thermal fatigue cracks were an austenitic stainless steel plate (150 x 150 x 25 mm) with a 20 x 7,5 mm (length x depth) crack in the middle of the plate (Publications V and VI), a section (400 x 190 x 60 mm, length x width x thickness) of a centrifugally cast large grain size austenitic stainless steel primary circuit pipe with a 34 x 17 mm (length x depth) crack in it (Publication VII) and a core spray nozzle mock-up (constructed from A508 carbon steel, Inconel 600 and AISI 316 austenitic stainless steel) with a 15 x 5 mm (length x depth) crack in the heat affected zone of the weld in AISI 316 (Publication VI) and with a 14,2 x 5 mm (length x depth) crack in the heat affected zone of the weld in Inconel 600 (Publications VII and VIII). Loading was applied to the crack opening surface and cycling was recorded by a digital video camera. Simultaneously with thermal cycling, ultrasonic signals were gathered from all used probes. An average of 15 different thermal cycles were applied for each specimen and each type of cycle was run for 5-20 times.

4 RESULTS

During the study thermal fatigue flaws were artificially produced in different austenitic stainless steel base materials (Publications II, III, IV, V and VI), welds (Publications VI, VII and VIII) and claddings (Publications II and IV) and Ni-based alloy Inconel 600 (Publications VII and VIII). Thermal fatigue was used as the damage mechanism for flaw nucleation and growth. The crack growth was accurately controlled and the resulting representative thermal fatigue cracks are among the most challenging flaw types for different NDE techniques.

The produced flaws were studied with different non-destructive and destructive methods in order to evaluate their representativeness. The final evaluation of flaw properties and their representativeness was based on combined results of all studies performed.

4.1 Metallographic representativeness

Requirements set for representative NDE response of artificially produced flaws are fundamentally based on the physical phenomena occurring when the ultrasonic energy confronts the flaw. The response is primarily based on the metallographic characteristics of the flaw. Thus, the flaw characteristics were studied carefully and compared to service-induced flaws. Studied characteristics included crack opening, fracture surface roughness, crack tip tightness and crack propagation in the material. Furthermore, surface residual stresses in the vicinity of the produced flaw were shortly studied.

Produced flaws show transgranular, tortuous growth and very tight tip and small tip radius. Opening of the flaw in different locations (at flaw mouth, fracture surface and tip) is similar to service-induced flaws as shown in Publications III and IV. Flaw propagation follows the weakest path through the microstructure. The growth is based on local high strains and stress intensity at the flaw tip. The flaw grows on a cyclic basis, when the flaw is cyclically loaded causing flaw tip opening and closing. Microscopically, the flaw tip is alternately blunted and resharpened and the plastic zone in front of the flaw tip is experiencing cyclic tensile and compressive straining.

The size of the produced flaw is controlled during the flaw growth process. The understanding and control of the applied thermal fatigue cycles, examples shown in Figure 37 and Figure 38, are used to control the flaw size. Figure 41 shows, as an example, four flaws produced to have different sizes. The exhibited non-correspondence between flaw sizes and applied total cycles is a result of used different thermal loads. Furthermore, flaws shown exhibit the effects of different loading conditions on flaw characteristics such as straightness and amount of branching in propagation and opening conditions. Flaws in Figures 40 a) and b) are about the same size, but a) is much more tortuous and has branches as a result of smaller load amplitude and higher loading frequency while bigger load amplitude in production of b) has forced the crack to grow straighter. Furthermore, Figures 40 b) and c) show flaws with size difference at only about 35%, but with clear difference in the flaw opening. In production of the flaw in c) different loading parameters were used resulting in bigger opening than in b). Similarly, the flaw in d) has the biggest opening extending down to the flaw tip. These pictures show the controllability of the flaw size and effect of different load conditions on the final characteristics of the produced flaw.



Figure 41 Four different flaws in AISI 304 austenitic stainless steel samples produced by the developed method. Flaws after approximately a) 30 000, b) 2770, c) 6500 and d) 167 000 thermal fatigue cycles.

The residual opening of the produced flaws is a result of the used thermal fatigue loading cycles and can be controlled during the production. Flaw opening can also

be changed afterwards by employing proper additional loading cycles. An example of this is shown in Figure 42, where a ready-made flaw with the final size (length 20 mm, depth 7,5 mm) is shown prior to and after a flaw opening post-treatment. Furthermore, a cross-section of the flaw after post-treatment is shown in Figure 43 exhibiting that the severe treatment has changed the flaw opening along the whole length of the flaw.

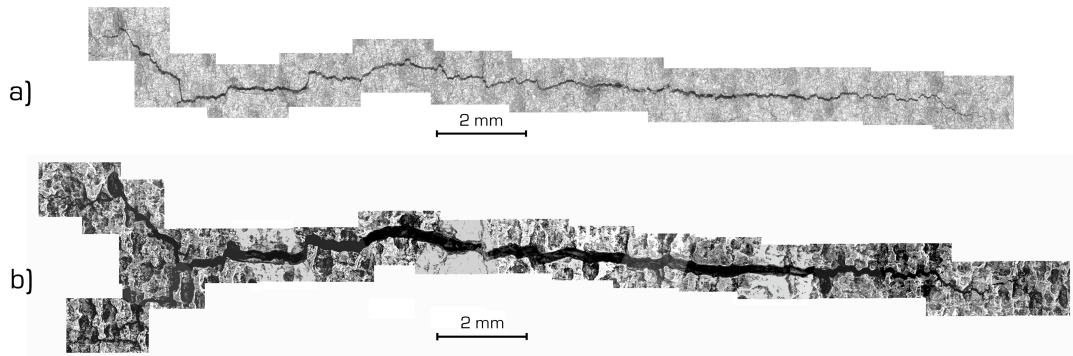


Figure 42 Two pictures showing different opening conditions of the same flaw: a) after 167 000 cycles as ready-made flaw with an intended size – maximum opening 55 μm and b) after severe post-treatment of the flaw with 250 cycles – maximum opening 250 μm .

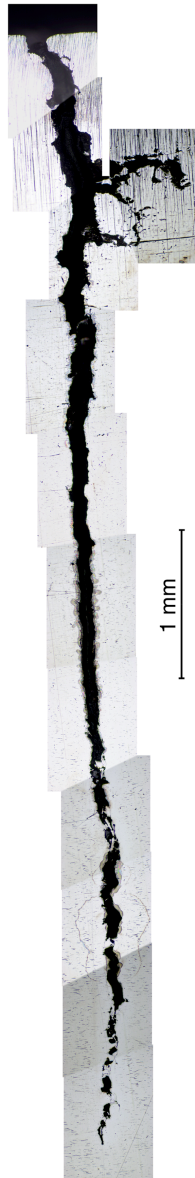


Figure 43 Cross-section of the flaw after severe post-treatment for opening of the flaw.

The micrographs in Figure 41 show that method does not cause any additional disturbance, as weld metal or microstructural changes in the material. This is different from flaws produced by other qualification flaw manufacturing techniques as the comparison shows in Publication IV.

4.2 Metallographic comparison to service-induced MF, TF and SC cracks

The produced flaws were compared to service-induced thermal fatigue cracks published in the open literature to assess the reality of the simulation. Compared characteristics included crack propagation, tortuosity, crack opening, crack tip tightness and radius, and fracture surface roughness. The macroscopic propagation of service-induced and artificially produced thermal fatigue cracks is similarly

tortuous and both flaws are narrow, propagate transgranularly and show minor branching. Both flaws have the larger width near the surface and are tight in the vicinity of the flaw tip. The results of the comparison are shown in Publications III and IV.

In addition to comparison to service-induced thermal fatigue cracks, the characteristics of the produced flaws were compared to corresponding ones of the service-induced mechanical fatigue and stress corrosion cracks. The values given in Table 2 show that the values measured from the produced flaws (see Publications III and IV) are representative for the service-induced mechanical fatigue and two types of SC cracks shown. Furthermore, comparison of Figure 41 and Figure 9 clearly indicates a good simulation of service-induced SC cracks achieved by the produced thermal fatigue flaws.

4.3 NDE representativeness

Verification of the representativeness of the NDE response was done as a comparison of responses of the artificially produced flaws and service-induced thermal fatigue cracks. The produced flaws were representative and, thus, challenging for all used NDE methods. The challenge is based on the characteristics of the flaws, as they are narrow and rough with tight crack tips. From NDE point of view, the produced flaws give a realistic crack-like indication. Flaws are representative to service-induced thermal fatigue cracks and give a good simulation of service-induced stress corrosion cracks.

4.3.1 Ultrasonic inspection

Characteristically ultrasonic comparison of flaws produced artificially and service-induced thermal fatigue flaws shows similar responses from flaw opening corner, fracture surface and flaw tip. The dynamic ultrasonic response of the produced flaws is realistic showing uneven amplitude levels as scanned over the flaw (Publications II and IV). Furthermore, the rough fracture surfaces and tortuous propagation disturb the coherent forward reflected acoustic field by scattering the energy randomly. The tight flaw tip gives only a weak tip response during inspections (Publications III and IV). In some cases the flaw tip has been too tight for both pulse-echo and time-of-flight based ultrasonic inspection methods and has led to marked underestimation in sizing when qualified procedures were applied. Furthermore, sometimes the tip-like response has appeared in a location of some curvature or root of a branch of the flaw misleading the inspector.

The weak tip response is a realistic simulation of the real service-induced cracks and, as shown in Publications III and IV, tip S/N-ratios of both the artificially produced and service-induced thermal fatigue flaws lie very close to the 6 dB detection limit.

4.3.2 Eddy current inspection

In the eddy current inspections performed during this work the response of the flaw tip is seen quite weakly and the tortuous propagation requires concentration when analysing the results (Publications II and IV). Most often the detection and sizing was possible with good results. However, during inspections there appeared also clear deviations between obtained eddy current testing results and actual flaw sizes.

The results show that the eddy current inspection is also markedly affected by the characteristics of the inspected flaw.

4.4 Residual stresses

The applied flaw production method characteristically induces residual stresses in the material during the flaw growth process. Induced residual stresses affect the ultrasonic response obtained from the flaw. Hence, studies on development of residual stresses during thermal fatigue loading were shortly included in this work (Publications II and IV).

The significance of the effect of residual stresses on the obtained ultrasonic response became apparent during the work. Tens of flaws produced and inspected revealed marked differences in the detection and sizing performances, when different ultrasonic techniques were applied. Furthermore, in some cases different parts of flaws were under different residual stress conditions making part of the flaw visible, but allowing transmission of ultrasonic energy in an other part making it invisible (Publications II, III and IV). The effect is dependent on the type and propagation direction of the induced ultrasonic wave (Krautkrämer et al., 1990).

4.5 Ultrasonic response during dynamic thermal fatigue loading

In an operating power plant the alternating loads open and close the growing crack. Furthermore, when the plant is shut down, the cracks possibly present are affected by the residual stresses, as discussed above. The technique developed in this work gave an opportunity to study in a flexible way the effects of different loading conditions on the obtained NDE response (Publications V, VI, VII and VIII).

There are several publications in the open literature describing studies of ultrasonic response from different dynamically loaded flaws. However, in all published studies mechanical loading has been applied, most often as a bending load. All applied mechanical loads have the same characteristics; the whole flaw is loaded with the same load, in tension or compression. However, this is not the common situation in service conditions, where the mechanical loading conditions are more complex and when service-induced thermal loads are present, there is a thermal strain gradient in the component causing also stress gradient. The developed method enables application of such complex load cycles. Furthermore, if the sample has representative residual stresses from manufacturing as compared to the simulated operational one, the induced strain cycles are representative to those induced during operation.

During the study ready-made flaws were loaded with different thermal cycles and the ultrasonic response was monitored. Analyses of the results show clear time differences between ultrasonic maximum amplitudes obtained from different parts of the flaw. This indicates that different parts of the flaw are experiencing different loads at the same moment, as shown in Publications VI, VII and VIII. Furthermore, from the ultrasonic response it is seen that with the applied loads the flaw tip is experiencing opening and closing behaviour causing increase and decrease of the obtained amplitude. Some of the loads applied were of such magnitude that they could appear during normal operation of a power plant.

4.6 Real components

The last part of this study was to apply the technique to the real components and verify the result by non-destructive means. The technique was used in production of flaws in several realistic samples and mock-ups, as shown in Publications II, IV, VI, VII and VIII and in the separate work of Kemppainen et al., 2004. The results also show that the flaws are produced with a reproducible manner without causing any additional disturbances in the material and specimen. The technique was proven to be very well applicable to different real components without limitations if the location is reachable with the loading tools.

5 DISCUSSION

Artificial flaw manufacturing technique based on controlled thermal fatigue damage mechanism was developed. The method is used to produce realistic thermal fatigue cracks. It was shown that the developed technique allows reproducible production of thermal fatigue cracks to components of any shape, size and weight without any unwanted alterations of the material or specimen. Developed technique has been patented (Publication I).

5.1 Metallographic representativeness

The developed technique produces flaws exhibiting different characteristics when different loading parameters are applied, as shown in Publications II, III and IV. The effect is seen metallographically as different crack growth rates, branching, tortuosity of the propagation paths, crack opening and crack tip conditions of different flaws. This is seen in Figure 41, where all the four flaws have been produced with different loading parameters. Such differences in flaw characteristics have an effect on the obtained NDE response and result in markedly different NDE fingerprints from differently produced flaws. Controllability of one of such characteristics, the residual opening of the produced flaw was only shortly studied during this work, but the results (examples shown in Figure 42 and Figure 43) clearly indicate the possibility to control the flaw opening. This is advantageous as the real, service-induced flaws show quite a large range of openings to be simulated, as shown in Table 1 and Table 2. There are no limitations for application of the artificial flaw production method and the flaws can be produced to have a wide variation of different characteristics.

The developed method produces controlled realistic and natural thermal fatigue cracks exhibiting realistic characteristics. Furthermore, the method does not cause any additional disturbances in the material and specimen as shown in Publication IV.

5.2 Metallographic comparison to service-induced MF, TF and SC cracks

Produced flaws were found to give excellent simulation of service-induced thermal fatigue cracks with similar characteristics (crack propagation, tortuosity, crack mouth opening, crack tip tightness and radius, fracture surface roughness). The macroscopic propagation of service-induced and artificially produced thermal fatigue cracks is similarly tortuous and both cracks are narrow, propagate transgranularly and show minor branching. In addition to service-induced thermal fatigue cracks, produced cracks give very good simulation of service-induced mechanical fatigue and stress corrosion cracks. All the cracks have the largest width near the surface and are tight in the vicinity of the crack tip. The results show that the produced cracks are metallographically representative. However, certain extreme flaw types as, e.g., corroded wide open corrosion fatigue flaws and heavily branched transgranular stress corrosion flaws are not perfectly simulated by the developed artificial flaw production technique.

The flaw tip tightness of service-induced thermal fatigue, mechanical fatigue and stress corrosion cracks and artificially produced thermal fatigue cracks is similar. This is a result of the flaw tip growth process where stress concentration at the tip is the driving force for the growth with all the flaws. Hence, NDE response based on the flaw tip interaction should be similar from all these flaws.

In service conditions often a mosaic-like thermal fatigue crack pattern appears. This is also one type of service-induced damage to be simulated for NDE qualification and training purposes. Simulation of a random crack pattern allowing random appearance of cracks is not too challenging a task but controlling the size of each crack inside the area is it. The developed method is suitable for this kind of flaw production as well, but it requires modification of the load cycles used in the production of single flaws. This study was focused on production of single flaws and further application is to use the technique for simulation of mosaic-like crack pattern without uncontrolled and random cracking but with controlled size and location of all cracks. However, this application was excluded from the study and is suggested as part of the future work.

The aim of the study was to develop a method for producing single and separate flaws, i.e., without random, multiple cracking. The results show that this aim was successfully reached, and only very shallow and minor secondary cracks appear in the surface of the samples. However, if the sample has microstructural or structural discontinuities as, e.g., weld microstructure or changes in the shape of the surface contour, there may appear secondary cracking caused by these weak discontinuities or stress raisers near the loaded area.

5.3 NDE representativeness

Obtained results show that the flaws produced with the developed method are representative for different NDE methods, as shown in section 4.3 of this work. The metallographic representativeness is based on the characteristics of flaws, as they are narrow and rough with tight crack tips. From NDE point of view, and based on the metallographic similarity, the produced flaws give a crack-like indication representing both service-induced thermal fatigue cracks and service-induced stress corrosion cracks. Metallographic differences to service-induced SC cracks are that SCC may have unbroken ligaments and in some cases more branches than these artificially produced thermal fatigue cracks. However, artificially produced thermal fatigue flaws can be produced to have representative branching and/or unbroken ligaments in the surface.

The ultrasonic response of produced artificial flaws is realistic and similar to the responses from the service-induced flaws. This includes the dynamic response obtained during scanning over the flaw showing varying and low level echo amplitude. Furthermore, tips of the artificially produced flaws show very low echo and diffraction amplitudes. The cases where the inspector cannot detect or size the flaw because of a missing signal from the flaw fracture surface and/or flaw tip, are considered in simulation to belong among the worst-case flaws met under in-service inspections. These kinds of tight, tortuous and branched flaws cause scattering, transmission and do not allow flaw tip diffraction of the incident ultrasonic energy. The developed method allows production of such flaws simulating the worst-case flaws in service.

Eddy current inspections performed during the study showed that the produced flaws give realistic weak response because of tight flaw tip and tortuous propagation. In most cases the results of eddy current inspections were, however, reliable. The performance of the eddy current inspection, similarly to the ultrasonic inspection, is markedly affected by the characteristics of the inspected flaws. Results emphasize the challenges set by the realistic flaws to different NDE techniques. Eddy current inspections were not widely done in this study and the performance of EC

techniques should be further studied. Further studies should be focused on the differences between EDM-notches used widely in calibration of eddy current equipment and realistic flaws. Such studies would reveal the possible differences between responses from notches and realistic flaws giving motivation for further development of eddy current inspection techniques and procedures to enhance the reliability of the testing.

The obtained NDE results show, that the produced flaws give a good simulation of different service-induced flaws. The obtained NDE response with different inspection techniques proved to be realistic. Response depends on the flaw characteristics.

5.4 Residual stresses

The effect of residual stresses on ultrasonic inspection performance has substantial importance and it is studied widely around the world. Residual stresses may be present during in-service inspections, as caused by the fabrication of the component, operation of the plant and possible repair works made. During in-service inspections, residual stresses affect the flaw by opening or closing it, which in turn affects the NDE response obtained from the flaw. When an artificially produced thermal fatigue crack is used as a reflector, the opportunity to control the induced residual stresses is an important option. As a result of this work, a better understanding on the development of the residual stresses during the flaw growth process was achieved. Publications II and IV show that by controlling the loading the surface residual stresses in the vicinity of the crack can be left either in tension or compression.

The key feature of the developed method is to initiate and grow natural thermal fatigue cracks under accelerated conditions as compared to service conditions. The nucleation and growth lifetime of service-induced flaws may be calculated in years, but the growth of the artificial thermal fatigue cracks is calculated in hours or days. This is achieved by using higher load amplitudes than occur or can occur in service conditions. The applied load amplitudes and maximum temperatures are selected so that they are not too high to cause any microstructural changes. From the point of view of residual stress conditions this leads to interesting phenomena caused by the plastic deformation of the material. Characteristic to thermal fatigue load, the material around the flaw is plastically deformed by compressive stresses during heating. This deformation results in tensile residual stresses in the material surrounding the flaw after the flaw manufacturing. The higher the maximum temperature of the thermal cycle is, the bigger is the amount of plastic deformation and the higher are the resulting tensile residual stresses. As a result of this, if there are any differences, the artificially produced thermal fatigue flaws, as they are produced under enhanced conditions, should be under higher level of tensile residual stresses than the service-induced cracks. Hence, artificially produced flaws tend to exhibit similar or bigger openings than the service-induced flaws caused by similar loads.

5.5 Response during dynamic thermal fatigue loading

The dynamic loading of the flaws with online ultrasonic measurement revealed the nature of thermal fatigue crack growth. During loading the fracture surfaces of the flaw in different areas (near the surface, along the fracture surface and at the flaw

tip) are moved in different directions simultaneously (Publications VI, VII and VIII). This is caused by the thermal waves penetrating the thickness of the sample.

The principal behaviour of the ultrasonic response is similar under thermal loading and mechanical loading; during dynamic loading the ultrasonic amplitude either increases or decreases when the flaw is opened or closed, respectively. However, mechanical loads open or close the flaw linearly from surface to the crack tip, while cyclic thermal loads open and close different parts of the crack differently. In the study, when the near surface part of the flaw was closed and the corner echo amplitude reached its minimum, the crack tip amplitude was at its maximum, and vice versa, when the surface part was fully open showing the maximum ultrasonic amplitude, the crack tip amplitude almost disappeared. For some other types of loads the relationship was not the opposite, but there was a time-dependent delay between the maximum amplitudes of corner and tip echoes.

The applied loads affect the stress/strain behaviour at different parts of the flaw. The effect is seen both in the time response as well as in the magnitude of the maximum/minimum amplitudes of corner and tip echoes. Thus, depending on the applied loads and the time when the flaw manipulation is interrupted, the flaw is left in different conditions. Obtained results indicate, that as the different loads result in different strain amplitudes at the flaw tip, they also grow the flaws differently during the process. This was also shown by the results of the destructive metallographic testing exhibiting different appearances of differently produced flaws.

Obtained results revealed that different loads left the flaw to different opening condition leading to different ultrasonic response, as shown in Figure 41. This encourages to the idea that the method could be used to manipulate indications (i.e., supposed flaws) found during in-service inspections to make them more detectable and easier to characterise. This option should be considered in further studies.

5.6 Real components

The applicability of the technique to realistic components was shown during the work. It is a marked advantage of the developed technique, that the artificial flaw manufacturing process is separated from the sample manufacturing process. It was shown that the method is applicable to practically any size, weight and shape of components (Publications II, IV, VI, VII and VIII, Kemppainen et al., 2004) with a reproducible manner. There are no practical limitations in application of the method. Both the heating and cooling are applied locally without any mechanical contact to the sample. Hence, the only limitation is that the intended location of the flaw has to be reachable by the loading tools, i.e., induction coil and cooling nozzles.

5.7 Representativeness of the produced flaws

Although the metallographic representativeness of the produced flaws has been proven, the flaw characteristics and the non-destructive representativeness of the flaws have raised discussion among inspectors. Some of the ultrasonic testing results obtained during the study revealed that the flaws were not correctly characterised by experienced inspectors having experience from real, service-induced flaws. However, by giving more information about the flaw location and size, the results were markedly better although sometimes a clear deviation from the actual size appeared in the sizing results.

Service-induced flaws have been detected and sized during ISIs, but there have also been flaws passing ISIs without being detected. Some of the non-detected flaws have been found by leakage as they have grown through the pipe wall. It may be asked, what is the difference between the flaws that were detected during in-service inspections and those that were not detected. Fundamentally the flaw growth process is similar in all similar damage mechanism cases, but the final characteristics and, hence, the obtained NDE responses of the flaws are determined by the effective damage mechanism and the loads. The affecting loads determine the flaw nucleation and growth controlling the whole process; incubation time, nucleation site, propagation path through the material, branching, growth rate, induced residual stresses, etc.

One issue is the flaw opening condition as very tight flaws may not be detected during in-service inspections. The literature shows that service-induced flaws found exhibit a wide range of different flaw openings. The tighter flaws are more challenging to detect and size than the ones with bigger opening. Flaws produced with the developed method can be manufactured with different opening conditions. Similar to the service-induced flaws, the tighter flaws force all the inspection techniques to their physical limits. Hence, the tightness of produced flaws should be considered as one characteristic affecting the inspection performance and it should be used as an adjustable parameter in NDE qualification.

Another issue is the possible oxide layer on the fracture surfaces of a flaw. In the literature, the metallic fracture surfaces have been mentioned to be both less and more sensitive to amplitude drop caused by the residual stresses, when compared to water- or oxide-filled flaws. Depending on the study, the conclusion can be either that the oxide layer increases (Iida et al., 1988) or decreases (Crutzen et al., 1996 and Becker et al., 1981) the detectability and sizing capability of the flaws.

There is, however, always some kind of oxide layer on the fracture surfaces of the flaw. Thickness of the oxide layer induced during service may be different. Thickness of the oxide may be affected by the flaw growth rate as generally longer time results in thicker oxide layer. However, water inside the crack in many cases is supposed to contain no oxygen and should not enhance large oxide growth at least in stainless steels and Ni-based alloys, although cracks filled with oxide are found in service. This subject was excluded from this study, but correlation studies between the thickness of the oxide layer and the NDE response from the service-induced flaws should be performed.

The developed technique is based on a natural damage mechanism and hence the produced flaws are similar to the service-induced flaws. There are also differences in the thickness of the oxide layers of the service-induced flaws. Similar oxide growth on the fracture surfaces of artificially produced flaws is possible by exposure to a corroding environment. If the thickness of the oxide layer on the flaw surface plays a critical role on the obtained ultrasonic amplitude, i.e., the thicker oxide layer enhances detection and sizing, artificially produced flaws with thin oxide layer can be considered as the worst case simulation of the service-induced flaws.

Aspects described above have been realized, e.g. by Crutzen (1986), and this has led to an understanding that practically each service-induced flaw may be considered, more or less, unique. Based on this, the artificial flaw production technique has to be capable to simulate a wide variety of different flaw characteristics. However, there is no extensive information available about the variations of the flaw characteristics of service-induced flaws. Actually, the lack of information may lead to an assumption

that, when an inspector is once capable of detecting and sizing a service-induced flaw, that inspector is capable of detecting and sizing all real flaws. When the information on flaw characteristics and NDE response in service will be available, the developed method can be used to simulate accurately different real characteristics and to give an opportunity to learn more about their effects on the NDE response.

5.8 Further studies

Two areas of interest can be seen to be studied further: 1) control of residual stress fields and 2) use of the method to change characteristics of the different flaws including flaws produced also by some other artificial flaw manufacturing technique or cut-outs from actual plants. These will lead to enhanced use of existing qualification mock-ups and test samples. The developed method is used for commercial purposes and the primary research and development work consists of applying the method to different practical applications concentrating on new materials and challenging component geometries. Successful development with ferritic steels and Ni-based alloys has already been made and application to aerospace materials is seen in the future.

Comparative studies related to the NDE responses from the artificially produced flaws and service-induced flaws have to be continued. These include analyses of the residual crack opening and residual stress conditions of the service-induced flaws and simulation of them by the artificially produced flaws. In this way better understanding on different conditions met during in-service inspections can be obtained, and their effect on the NDE response and potential changes between successive periodic inspections of the same indication is explained.

The developed flaw manufacturing technology gives a marked opportunity to broaden the knowledge on challenges set by the realistic flaws. The utilities, the NDE vendors and the authorities can enhance their understanding on plant degradation, inspection and maintenance requirements.

This can also include development of the existing and new NDE techniques and procedures to better meet the challenges of the realistic flaws. The first few experiences obtained with different qualified UT and EC inspection procedures, have revealed surprisingly bad performance indicating that a realistic flaw pushes the inspection techniques to their limits. However, by using the equipment and procedures beyond the qualified specifications (i.e., increasing sensitivity), inspectors have been able to characterise the flaws. Further studies will open possibility for a further development of the inspection equipments, techniques and procedures.

One new area of interest arising in the nuclear field is the study of the amount of leakage as connected to properties of through-wall-penetrating crack. For such studies the developed flaw production method suits very well as the component dimensions or other specifications do not limit the flaw growth. Furthermore, the flaw opening and residual stress fields in the vicinity of the produced flaws can be modified by the technique and the conditions can be changed during the leakage rate studies.

6 CONCLUSIONS

The developed artificial flaw manufacturing technique was shown to perform well. The applicability of the method was verified by means of non-destructive and destructive testing. Similarity of the produced flaws to the service-induced flaws was evaluated by metallography, penetrant, ultrasonic and eddy current testing. Furthermore, the potential of the method to control the characteristics of the produced flaws was shown. The following conclusions can be drawn based on the research conducted.

1. An artificial flaw production method was developed based on the controlled thermal fatigue damage mechanism and its ability to production of the controlled realistic flaws was shown.
2. The developed method does not cause any additional disturbances in the material and specimen.
3. The reproducibility of the flaw production (accuracy in location, control of size and characteristics) was demonstrated by several experiments.
4. Representativeness of metallographic and NDE response was good in comparative studies carried out with the flaws produced by the developed method and the service-induced flaws.
5. Produced flaws are realistic and natural thermal fatigue flaws exhibiting realistic propagation path, opening (at flaw mouth, along the fracture surface and at flaw tip region), residual stress conditions and NDE response.
6. Produced flaws are an excellent simulation of the service-induced thermal fatigue cracks and a very good simulation of the service-induced mechanical fatigue and stress corrosion cracks.
7. NDE response of the produced flaws was evaluated and shown to be realistic by different inspection procedures and techniques. Response depends on the flaw characteristics generated during the flaw growth process and/or afterwards by a post-treatment of the flaw.
8. It was shown that the flaws can be produced to realistic mock-ups without size, weight or shape restrictions.
9. It is suggested that the flaws produced by the developed method should be used in NDE personnel qualification, practising and training in order to achieve highest level of NDE knowledge and skills among inspectors. The more experience the inspectors have on the realistic flaws, the higher the level of their skills will be to detect and size the service-induced flaws.
10. Further studies were proposed for control of the residual stresses and changes of the flaw characteristics as compared to the service-induced flaws. These studies include both non-destructive and destructive analyses of both types of flaws to obtain a true connection between them.

REFERENCES

Anderson, T.L., 1991. *Fracture Mechanics, Fundamentals and Applications*. CRC Press, Inc., Boca Raton, Florida, USA, 793 p. ISBN 0849342775

ANSYS Release 5.5.1.1998.UP19981001.SAP IP Inc.

Araki, K., Sakamoto, H., Nakagawa, A. and Higuchi, M., 1998. Fabrication of Mock-Up Specimens with Natural Flaws. *Proceedings of First International Conference on NDE in Relation to Structural Integrity for Nuclear and Pressurised Components*, 20-22 October 1998, Amsterdam, The Netherlands, pp. 112-123.

Ahmed, S.R. and Saka, M., 1998. A Sensitive Ultrasonic Approach to NDE of Tightly Closed Small Cracks. *Journal of Pressure Vessel Technology, Transactions of the ASME*, November, Vol 120, pp. 384-392 .

Becker, F.L., Doctor, S.R., Heasler, P.G., Morris, C.J., Pitman, S.G., Selby, G.P. and Simonen, F.A., 1981. *Integration of NDE Reliability and Fracture Mechanics - Phase I Report*. NUREG/CR-1696 PNL-3469, Vol 1, 170 p.

Blitz, J. and Simpson, G., 1996. *Ultrasonic Methods of Non-destructive Testing*. First Edition, Chapman & Hall, London, UK, 264 p. ISBN 0412604701

Chapuliot, S., Gourdin, C., Magnaud, J.P., Mermaz, F., Monavon, A., 2005a. Hydro-Thermal-Mechanical Analysis of Thermal Fatigue in a Mixing Tee. *Collection of Papers of the International NuPEER Symposium*, June 2005, Autorite de Surete Nucleaire, Dijon, France. 14 p.

Chapuliot, S., Gourdin, C., Payen, T., Magnaud, J.P., Monavon, A., 2005b. Hydro-Thermal-Mechanical Analysis of Thermal Fatigue in a Mixing Tee. *Nuclear Engineering and Design*, Vol 235, pp. 575-596

Charlesworth, J.P. and Temple, J.A.G., 2001. *Engineering Applications of Ultrasonic Time-of-Flight Diffraction*. Second Edition, Research Studies Press Ltd., Philadelphia, USA, 254 p. ISBN 0863802397

Cipière, M.F. and Le Duff, J.A., 2002a. Thermal Fatigue Experience in French Piping: Influence of Surface Condition and Weld Local Geometry. *Welding in the World*, Vol 46, No 1/2, pp. 23-27.

Cipière, M.F. and Le Duff, J.A., 2002b. Thermal Fatigue Experience in French Piping: Influence of Surface Condition and Weld Local Geometry. *IIW Document No. XIII-1891-01*, International Institute of Welding, 11 p.

Crutzen, S.J., 1985. PISC Exercises: Looking for Effective and Reliable Inspection Procedures. *Nuclear Engineering and Design*, Vol 86, pp. 197-218.

Crutzen, S., 1986. Influence of Defect Characteristics on Inspection Performance, PISC II. *Proceedings of 8th International Conference on NDE in the Nuclear Industry*, ASM, Orlando, USA, pp. 23-34.

Crutzen, S.J., Jehenson, P., Nichols, R.W. and McDonald, N., 1989. The Major Results of the PISC II RRT. *Nuclear Engineering and Design*, Vol 115, pp. 7-21.

Crutzen, S., Lemaitre, P. and Iacono, I., 1996. Realistic Defects Suitable for ISI Capability Evaluation and Qualification. Proceedings of the 14th International Conference on NDE in the Nuclear and Pressure Vessel Industries, 24-26 September 1996, Stockholm, Sweden, pp. 153-163.

Danko, J.C., Stahlkopf, K.E. and Rossin, A.D., 1981. An Overview of Boiling Water Reactor Pipe Cracking. International Journal of Pressure Vessels and Piping, Vol 9, pp. 401-419.

Denby, D. and Duncumb, A.C., 1984. the Effects of Stress on the Ultrasonic Detectability of Defects. Proceedings of the Conference of Nondestructive Testing in the Fitness-for-Purpose Assessment of Welded Constructions. The Welding Institute, Cambridge, UK., pp. 73-81.

Doctor, S., Schuster, G. and Simonen, F., 1999. Fabrication Flaws in Reactor Pressure Vessels, U.S. Nuclear Regulatory Commission Workshop on Flaw Distribution in PVRUF & Structural Integrity Assessment, AL, February 25-26, 1999.

Edwards, R., Gruber G. and Watson, P., 1995. Fabrication of Performance Demonstration Initiative Specimens with Controlled Flaws. Proceedings on 13th International Conference on NDE in the Nuclear and Pressure Vessel Industries, 22-25 May 1995, Kyoto, Japan, pp. 167-176.

Edwards, R.L., Watson, P.D. and Gruber G.J., 1993. Fabrication of Specimens with Controlled Flaws for Procedure Development and Personnel Training and Qualification. Proceedings on 12th International Conference on NDE in the Nuclear and Pressure Vessel Industries, 11-13 October 1993, Philadelphia, Pennsylvania, USA, pp. 93-100.

Ehrnstén, U., Aaltonen, P., Nenonen, P., Hänninen, H., Jansson, C. and Angelu, T., 2001. Intergranular Cracking of AISI 316NG Stainless Steel in BWR Environment. 10th International Conference on Environmental Degradation of Materials in Nuclear Power Systems - Water Reactors. Nevada, USA, 5 - 9 August. ANS; NACE; TMS (2001), 10 p.

ENIQ, 1998a. ENIQ Recommended Practice 1: Influential/Essential Parameters, Issue 1. ENIQ Report nr 6, EUR 18101 EN, European Commission, JRC Petten, 16 p.

ENIQ, 1998b. ENIQ Recommended Practice 2: Recommended Contents for a Technical Justification, Issue 1. ENIQ Report nr 4, EUR 18099 EN, European Commission, JRC Petten, 30 p.

ENIQ, 1998c. ENIQ Recommended Practice 3: Strategy Document for Technical Justification, Issue 1. ENIQ Report nr 5, EUR 18100 EN, European Commission, JRC Petten, 25 p.

ENIQ, 1999a. ENIQ Recommended Practice 4: Recommended Contents for the Technical Qualification Dossier, Issue 1. ENIQ Report nr 13, EUR 18685 EN, European Commission, JRC Petten, 16 p.

ENIQ, 1999b. ENIQ Recommended Practice 5: Guidelines for the Design of Test Pieces and Conduct of Test Piece Trials, Issue 1. ENIQ Report nr 14, EUR 18686 EN, European Commission, JRC Petten, 16 p.

ENIQ, 1999c. ENIQ Recommended Practice 6: The Use of Modelling in Inspection Qualification, Issue 1. ENIQ Report nr 15, EUR 19017 EN, European Commission, JRC Petten, 11 p.

ENIQ, 1999d. Final Report of the First ENIQ Pilot Study, ENIQ Report nr 20, EUR 19026 EN, European Commission, JRC Petten, 38 p.

ENIQ, 1999e. Results of the Destructive Examination of the ENIQ Pilot Study: Defect Catalogue, ENIQ Report nr 19, EUR 19024 EN, European Commission, JRC Petten, 90 p.

Enrietto, J.F., Bamford, W.H. and White, D.F., 1981. Preliminary Investigation of PWR Feedwater Line Cracking. International Journal of Pressure Vessels and Piping, Vol 9, pp. 421-443.

Enrietto, J.F. and Pade, E.R., 1983. An Assessment of the Reliability of Detecting Fatigue Cracks in Cast Stainless Steel Pipe Weldments. American Welding Society (AWS) Annual Meeting, Abstracts of Papers presented at AWS Convention, Philadelphia, Pennsylvania: 64th American Society Annual Meeting, April 25-29, 14th AWS-WRC Brazing and Soldering Conference, April 26-28, USA, pp. 76-77.

Faure, F. and Leggat, R.H., 1996. Residual Stresses in Austenitic Stainless Steel Primary Coolant Pipes and Welds of Pressurized Water Reactors. International Journal of Pressure Vessels & Piping, Vol 65, pp. 265-275.

Gauthier, V., 1998. Thermal Fatigue Cracking of Safety Injection System Pipes Non Destructive Testing Inspections Feedback. Proceedings of NEA/CSNI Specialists' Meeting on: Experiences with Thermal Fatigue in LWR Piping Caused by Mixing and Stratification, 8-10 June, Paris, France, pp. 436-453.

Golembiewski, H-J., Kleinöder, W. and Hoch, G., 1998. Experiences Made in Continuous Long-Term Monitoring of Thermal Stratification Processes and their Implications on Material Fatigue. Proceedings of NEA/CSNI Specialists' Meeting on: Experiences with Thermal Fatigue in LWR Piping Caused by Mixing and Stratification, 8-10 June, Paris, France, pp. 415-434.

Green, E.R., 1989. Worst-Case Defects Affecting Ultrasonic Inspection Reliability. Materials Evaluation, Vol 47, pp. 1401-1407.

Gripenberg, H., Siiriäinen, J., Saukkonen, T. and Hänninen, H., 2000. Effects of EDM on Surface Residual Stresses in a TMCP Steel. The Sixth International Conference on Residual Stresses ICRS-6, Oxford, UK, July 10-12, pp. 1004-1011.

Hakala, J., Hänninen, H. and Aaltonen, P., 1990. Stress Corrosion and Thermal Fatigue - Experiences and Countermeasures in Austenitic SS Pipings of Finnish BWR-Plants. Nuclear Engineering and Design, Vol 119, pp. 389-398.

Halmshaw, R., 1993. Non-Destructive Testing. Second Edition, Edward Arnold A Division of Hodder & Stoughton, London, UK, 323 p. ISBN 0-340-54521-6

Hutin, J-P., 1998. Thermal Fatigue Experiences and Strategies in EDF Nuclear Power Plants. Proceedings of NEA/CSNI Specialists' Meeting on: Experiences with Thermal Fatigue in LWR Piping Caused by Mixing and Stratification, 8-10 June, Paris, France, pp. 19-35.

Hytönen, Y., 1998. Two Leakages Induced by Thermal Stratification at the Loviisa Power Plant. Proceedings of NEA/CSNI Specialists' Meeting on: Experiences with Thermal Fatigue in LWR Piping Caused by Mixing and Stratification, 8-10 June, Paris, France, pp. 115-160.

Hänninen, H. and Hakala, J., 1981. Pipe Failure Caused by Thermal Loading in BWR Water Conditions. International Journal of Pressure Vessels and Piping, Vol 9, pp. 445-455.

Ibrahim, S.I. and Whittaker, V.N., 1981. The Influence of Crack Topography and Compressive Stresses on the Ultrasonic Detection of Fatigue Cracks in Submerged Arc Welds. British Journal of NDT, September 1981, pp. 233-240.

Iida, K., Takumi, K. and Naruse, A., 1988. Influence of Stress Condition on Flaw Detectability and Sizing Accuracy by Ultrasonic Inspection. The Ninth International Conference on Nondestructive Evaluation in the Nuclear Industry, 25-28 April, Tokyo, Japan, pp. 563-567.

Jansson, C., 1996. Pipe Cracking Experience in Swedish BWRs. International Journal of Pressure Vessels and Piping, Vol 65, pp. 277-282.

Jungclaus, D., Voswinkel, A. and Négri, P., 1998. Common IPSN/GRS Safety Assessment of Primary Coolant Unisolable Leak Incidents Caused by Stress Cycling. Proceedings of NEA/CSNI Specialists' Meeting on: Experiences with Thermal Fatigue in LWR Piping Caused by Mixing and Stratification, 8-10 June, Paris, France, pp. 465-534.

Kemppainen, M., 1997. Design and Implementation of Thermal Fatigue Testing Facility. Master's Thesis (in Finnish), Helsinki University of Technology, Laboratory of Engineering Materials, Espoo, Finland, 110+11 p.

Kemppainen, M. and Virkkunen, I., 2004. Qualification of the Future. Technical Report No. 162AER001, Trueflaw Ltd, March 23, 14 p. + 90 p.

Kilian, R., Hoffmann, H., Ilg, U., Küster, K., Nowak, E., Wesseling, U. and Widera, M., 2005. German Experience with Intergranular Cracking in Austenitic Piping in BWRs and Assessment of Parameters Affecting the In-Service IGSCC Behavior Using an Artificial Neural Network. Proceedings of 12th International Conference on Environmental Degradation of Materials in Nuclear Systems-Water Reactors. The Minerals, Metals & Materials Society. 8 p.

Krautkrämer, J. and Krautkrämer, H., 1990. Ultrasonic Testing of Materials. 4th Fully Revised Edition, Springer-Verlag, Berlin, Germany, 677 p. ISBN 3-540-51231-4

Lagerström, J., Wilson, B., Persson, B., Bamford, W.H. and Bevilacqua, B., 1994. Experiences with Detection and Disposition of Indications in Heat Penetrations of Swedish Plants. Service Experience and Reliability Improvement: Nuclear, Fossil, and Petrochemical Plants, PVP-Vol. 288, ASME, USA, pp. 29-40.

Lemaitre, P., Lakestani, F., Crutzen, S., Dombret, Ph. and Maes, G., 1993. Diffraction of Ultrasound by Cracks: Comparison of Real with Artificial Realistic Flaws. Proceedings of 12th International Conference on NDE in the Nuclear and Pressure Vessel Industries, 11-13 October 1993, Philadelphia, Pennsylvania, USA, pp. 303-308.

- Lund, A.L. and Hartzman, M., 1998. USNRC Regulatory Perspective on Unanticipated Thermal Fatigue in LWR Piping. Proceedings of NEA/CSNI Specialists' Meeting on: Experiences with Thermal Fatigue in LWR Piping Caused by Mixing and Stratification, 8-10 June, Paris, France, pp. 41-72.
- Merola, M., 1995. Normative Issues in Thermal Fatigue Design of Nuclear Components. Nuclear Engineering and Design, Vol 158, pp. 351-361.
- Murgatroyd, R.A., Highmore, P.J., Burch, S.F., Bann, T. and Ramsey, A.T., 1988. PISC II Parametric Study on Flaw Characterisation Using the Tandem and TOFD Techniques. International Journal of Pressure Vessels and Piping, Vol 35, pp. 137-169.
- Noyan, I.C. and Cohen, J.B., 1987. Residual Stress Measurement by Diffraction and Interpretation. MRE Materials Research and Engineering, Springer-Verlag, Berlin, Germany. 276 p. ISBN 0-387-96378-2
- Ogilvy, J.A., 1989. Model for the Ultrasonic Inspection of Rough Defects. Ultrasonics, Vol 27, pp. 69-79.
- Paussu, R., Kemppainen, M., Pitkänen, J., and Sarkimo, M., 2003. Practical Examples of Application of Different Qualification Defects. Journal of Nondestructive Testing, Vol 8, pp. 1-6.
- Pherigo, G.L. and Pherigo, A.L., 1993. Using Flaw Implants to Qualify Nuclear NDE Personnel. Proceedings of 12th International Conference on NDE in the Nuclear and Pressure Vessel Industries, 11-13 October 1993, Philadelphia, Pennsylvania, USA, pp. 81-84.
- Pirson, J. and Roussel, G., 1998. Emergency Core Cooling System Pipe Crack Incident at the Tihange Unit 1 Plant. Proceedings of NEA/CSNI Specialists' Meeting on: Experiences with Thermal Fatigue in LWR Piping Caused by Mixing and Stratification, 8-10 June, Paris, France, pp. 103-114.
- Posakony, G.J., 1986. Experimental Analysis of Ultrasonic Responses from Artificial Defects. Materials Evaluation, Vol 44, pp. 1567-1572.
- Rudnev, V., Loveless, D., Cook, R. and Black, M., 2003. Handbook of Induction Heating. Marcel Dekker Inc., New York, USA, 777 p. ISBN 0-8247-0848-2
- Saka, M., Fukuda, Y., 1991. NDT of Closed Cracks by Ultrasonic Propagation along the Crack Surface. NDT&E International, Vol 24, No 4, pp. 191-194.
- Shah, V.N. and Ware, A.G., 1994. Inservice Inspection of Base-metal Sites Susceptible to Thermal Fatigue Damage. PVP-Vol 286, Changing Priorities of Codes and Standards, ASME, pp. 9-18.
- Shirahama, S., 1998. Failure to the Residual Heat Removal System Suction Line Pipe in Genkai Unit 1 Caused by Thermal Stratification Cycling. Proceedings of NEA/CSNI Specialists' Meeting on: Experiences with Thermal Fatigue in LWR Piping Caused by Mixing and Stratification, 8-10 June, Paris, France, pp. 73-101.
- SKI, 2005. Kärnsäkert 1/2005. Newsletter from the Swedish Government's Regulatory Body. (available online at: <http://www.ski.se/> 23.10.2005)

- Stahlkopf, K.E., 1981. IAEA Specialists' Meeting on Environmental Factors Causing Cracks and Degradation in Primary System Components: Conclusions and Recommendations. *International Journal of Pressure Vessels and Piping*, Vol 9, pp. 467-470.
- Temple, J.A.G., 1985. The Effects of Stress and Crack Morphology on Time-of-Flight Diffraction Signals. *International Journal of Pressure Vessels and Piping*, Vol 19, pp. 185-211.
- Toft, M.W., 1986. Experimental Studies of Ultrasonic Reflection from Various Types of Misoriented Defect. *Proceedings of 21st Annual British Conference on Non-Destructive Testing – NDT 86*, pp. 193-206.
- Uddcomb, 1999. *Testblock med Implanterade Defekter*, Brochure from Uddcomb Engineering AB.
- Virkkunen, I., 2001. Thermal Fatigue of Austenitic and Duplex Stainless Steels. *Acta Polytechnica Scandinavica, Mechanical Engineering Series No. 154*, Espoo, 2001, 115 p. (available online at: <http://lib.hut.fi/Diss/2001/isbn9512256878/>)
- Virkkunen, I., Kemppainen, M. and Hänninen, H., 1999. Thermal Fatigue Crack Growth in Austenitic Stainless Steels. *The Seventh International Fatigue Congress, Fatigue '99*, June 8-12, Beijing, P.R. China, pp. 2183-2188.
- Virkkunen, I., Kemppainen, M. and Hänninen, H., 2000. Residual Stresses Induced by Cyclic Thermal Loads. *The Sixth International Conference on Residual Stresses ICRS-6*, July 10-12, Oxford, UK, pp. 529-536.
- Waites, C. and Bièth, M., 2002. A Comparison of European Guidelines for Inspection Qualification. *The e-Journal of Nondestructive Testing*, August 2002, Vol 7, No 8. ISSN: 1435-4934 (available online at: <http://www.ndt.net/article/v07n08/waites/waites.htm>)
- Waites, C. and Whittle, J., 1998. The Status of Performance Demonstration and Evaluation Developments. *Insight*, Vol 40, No 12, December 1998, pp. 810-813.
- Watson, P. and Edwards, R.L., 1996. Fabrication of Test Specimens Simulating IGSCC for Demonstration and Inspection Technology Evaluation. *Proceedings of the 14th International Conference on NDE in the Nuclear and Pressure Vessel Industries*, 24-26 September 1996, Stockholm, Sweden, pp. 165-168.
- Weronski, A. and Hejwowski, T., 1991. *Thermal Fatigue of Metals*. Marcel Dekker Inc., New York, USA, 1991. 366 p. ISBN 0-8247-7726-3
- Wesseling, U. and Kilian, R., 1999. Schadensbeispiel der interkristallinen Spannungsrisskorrosion austenitischer Stähle in Hochtemperaturwasser. *VDI Berichte 1484*, Verein Deutscher Ingenieure, VDI-Gesellschaft Werkstofftechnik, Korrosion in Kraftwerken, 11. VDI-Jahrestagung Schadensanalyse, 12 p.
- Wirdelius, H. and Österberg, E., 2000. Study of Defect Characteristics Essential for NDT Testing Methods ET, UT and RT. *SKI Project Number 98267*, SKI Report 00:42, October 2000, Sweden, 50 p.
- Wirdelius, H., 1992. Probe Model Implementation in the Null Field Approach to Crack Scattering. *Journal of Nondestructive Evaluation*, Vol 11, No 1, pp. 29-39.

Wüstenberg, H. and Erhard, A., 1994. Problems with Artificial Test Reflectors at the Performance Demonstration of Ultrasonic Inspections. Proceedings of 6th European Conference on Non Destructive Testing, Nice, pp. 741-746.

Wåle, J. and Ekström, P., 1995. Crack Characterisation for In-service Inspection Planning, SKI Projekt 14.4-940389, 94164 SAQ/FoU-Rapport 95/70, SAQ Kontroll AB, Stockholm, Sweden, 1995, 84 p.

Yoneyama, H., Senoo, M., Miharada, H. and Uesugi, N., 2000. Comparison of Echo Heights between Fatigue Crack and EDM Notch. Proceedings of 2nd International Conference on NDE in Relation to Structural Integrity for Nuclear and Pressurized Components, 24-26 May, 2000, New Orleans, Louisiana, U.S.A., 8 p.

Zinn, S. and Semiatin, S.L., 1988. Elements of Induction Heating, Design, Control and Applications. ASM International, Metals Park, Ohio, USA, 355 p.



ISBN 951-22-8262-3
ISBN 951-22-8263-1 (PDF)
ISSN 1795-2239
ISSN 1795-4584 (PDF)